

A microscopic analysis of *Arabidopsis* chromatin

Joost Willemsen

Promoter: Prof. Dr. A.H.J. Bisseling
Hoogleraar in de Moleculaire Biologie
Wageningen Universiteit

Co-promoters: Dr. J.H.S.G.M. de Jong
Universitair docent
Laboratorium voor Erfelijkheidsleer
Wageningen Universiteit

Dr. Ir. J. Wellink
Universitair docent
Laboratorium voor Moleculaire biologie
Wageningen Universiteit

Promotiecommissie:
Prof. Dr. R. van Driel (Universiteit van Amsterdam)
Prof. Dr. W.J. Stiekema (Wageningen Universiteit)
Prof. Dr. A.J.G.W. Visser (Wageningen Universiteit)
Prof. Dr. S.C. de Vries (Wageningen Universiteit)

Dit onderzoek is uitgevoerd binnen de onderzoeksschool Experimentele
Plantenwetenschappen

A microscopic analysis of *Arabidopsis* chromatin

Joost (Jacobus Joseph) Willemse

Proefschrift

Ter verkrijging van de graad van doctor

op gezag van de rector magnificus

van Wageningen Universiteit

Prof. Dr. M.J. Kropff

in het openbaar te verdedigen

op vrijdag 2 maart 2007

des namiddags te half twee in de Aula.

A microscopic analysis of *Arabidopsis* chromatin

Willemse, Joost

Thesis Wageningen University, The Netherlands

With references - with summary in Dutch

ISBN:90-8504-596-7

Table of contents

Table of contents.....	5
Chapter 1: General Introduction	7
Outline of the thesis	23
Chapter 2: Quantification of nuclear DNA in whole mount <i>Arabidopsis</i> roots.....	25
Chapter 3: Histone 2B exchange in <i>Arabidopsis</i>	45
Chapter 4: AtLHP1 forms chromatin complexes at trimethylated histones.....	61
Chapter 5: AtLHP1 mutants in <i>Arabidopsis thaliana</i>	82
Chapter 6: General Discussion	94
Summary.....	109
Nederl andse Samenvatting	111
Dankwoord	113
Curriculum Vitae.....	115
Publication List.....	119

Chapter 1: General Introduction

Nuclear DNA of eukaryotic organisms is associated with several proteins, which together form chromatin. The most abundant chromatin proteins are histones. In all eukaryotes DNA is folded around a core of histones (H) by which the so-called nucleosomes are formed. (Kornberg 1974); 146 base pairs of DNA are wrapped around an octamer containing two copies of each of the four core histones. During replication DNA is first wrapped around H3-H4 tetramers before two H2A-H2B dimers assemble into the nucleosome complex (Ridgway and G. 2000). These nucleosomes are positioned every 200bp on a DNA strand, and can be linked together by H1. H1 and other proteins are believed to stabilize this 10 nm fiber and other more compact nucleosome structures involved in the higher order organization of the nucleus.

Chromatin is roughly divided in heterochromatin and euchromatin. Euchromatin is less compacted and gene rich, whereas heterochromatin is more compact and mainly consists of repetitive DNA (Heitz 1928; Fransz *et al.* 2003). In many organisms heterochromatic DNA is hypermethylated and this is used as an additional mechanism to regulate transcription (Finnegan and Kovac 2000). Between 5% and 40% of the cytosines in an organism can be modified into 5-methylcytosine by DNA-methyltransferases, either after DNA replication during maintenance of methylation, or through *de novo* methylation at specific sites. Three classes of cytosine modifications can be distinguished, CpG, CpNpG, and asymmetric Cytosine methylation respectively. (Cao and Jacobsen 2002; Vanyushin 2005)

Besides DNA also histones can be covalently modified, by for example acetylation, phosphorylation, methylation, and ubiquitination, and this provides signals to which other factors can bind and additionally alters the biochemical properties of chromatin (i.e., 'histone code' (Jenuwein and Allis 2001; Berger 2002; Turner 2002)). In general acetylation of histones is correlated with active genes, whereas methylation of histones at different positions result in different effects; methylation of lysine 9 of H3 (H3K9) is associated with heterochromatin formation while H3K4 methylation is related to gene activation and positioned in euchromatin (Rice and Allis 2001). In recent years the number of modifications, both positional as well as structural, that have been identified on histones has increased. Over 50 different amino acids in the histones (mainly in the histone tails) have the potential to be modified in this manner. (Figure 1- 1). In addition to the modifications shown in Figure 1- 1 also glycosylation (exclusively on histone 1), ADP-ribosylation, carbonylation (exclusively on histone 1) and sumoylation and several other

modifications of specific amino acid residues have been identified. An additional degree of complexity is added by the fact that multiple modifications (methylation, phosphorylation and acetylation) can be added to a single amino acid in the histone tail (Zhang *et al.* 2004). Some histone binding proteins recognize multiple forms of modification with different binding affinity (Badugu *et al.* 2005). Assuming that the various forms of modifications are not linked this creates a huge amount of regulatory possibilities (Over 230 options, Maher 2006). This amount of possibilities immediately rules out that there is a simple code in which each modification has a unique effect. Probably the recognition of specific combinations of histone modifications will be required for certain effects. Additionally different histone modifications could result in similar effects.

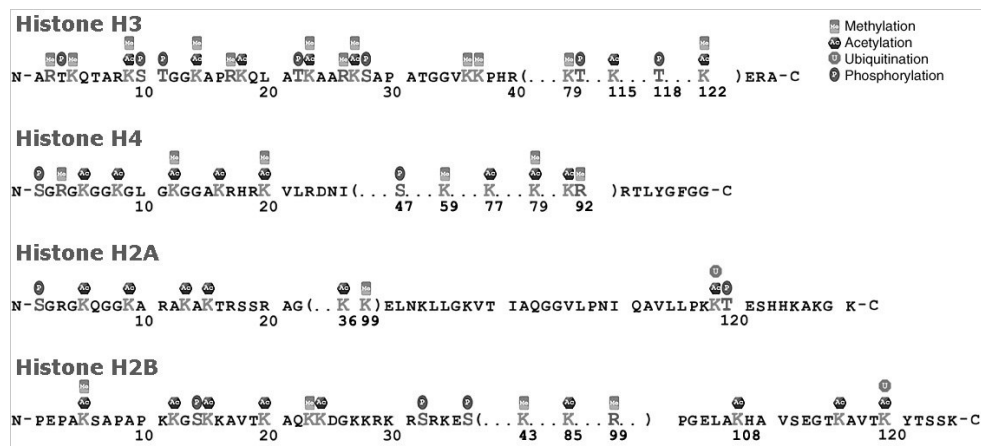


Figure 1- 1

Modification sites on the core histones H3,H4 H2A and H2B respectively , adapted from (Histone.com 2006)

Several proteins are able to specifically recognize modified histones. Many of these proteins recognize the modified histones using conserved protein domains, while their other domains exert a variety of regulatory functions. For example, the polycomb group proteins (PcG), which recognize specific histone modifications using their chromodomain (Min *et al.* 2003), play a central role in maintaining epigenetic patterns of gene expression (Bantignies and Cavalli 2006; Buszczak and Spradling 2006).

One of the most studied histone binding proteins is HP1, which is also a subject of the research described in this thesis (Lorvellec *et al.* Chapter 4; Willemse *et al.* Chapter 5). HP1 is known to bind to H3K9me3 (Bannister *et al.* 2001; Lachner *et al.* 2001; Lorvellec *et al.* Chapter 4), and was identified in drosophila as a protein localized in heterochromatic areas of the nucleus (James and Elgin 1986; James *et al.* 1989). HP1 proteins contain three conserved domains. The most N-terminal is the Chromo Domain (CD), which is needed for binding to H3K9me3. The CD also binds, albeit with a lower affinity, to H3K9me2 and H3K9me (Fischle *et al.* 2003). The hinge is a more variable domain, both in sequence as in length, which is used for DNA binding (Sugimoto *et al.* 1996; Meehan *et al.* 2003). The most C-terminal domain is the Chromo Shadow Domain (CSD), this domain is used for dimerization as well as binding to other proteins (Le Douarin *et al.* 1996). This multi-partite organization of HP1 allows several proteins to bind simultaneously, suggesting that HP1 proteins are needed for macromolecular complex formation. HP1 probably serves as a bridging protein, connecting histones through interactions with the CD to non-histone proteins via the CSD. This explains why there is a long list of HP1 binding proteins (Li *et al.* 2002). The initial function appointed to HP1 was the formation of heterochromatin and silencing of genes.

Most organisms have several variants of this protein (named HP1 α , HP1 β and HP1 γ), and these HP1 variants do not all localize exclusively in heterochromatin. In mice HP1 β has been reported to localize both in chromocenters as well as euchromatic areas (Minc *et al.* 2000; Nielsen *et al.* 2001), whereas HP1 γ locates exclusively in euchromatin (Volpe *et al.* 2002). Despite its (putative) role as bridging protein, FRAP studies revealed that HP1 is still highly mobile (Cheutin *et al.* 2003; Festenstein *et al.* 2003; Schmiedeberg *et al.* 2004; Zemach *et al.* 2006).

Besides proteins modifying or binding to histones or DNA, another group of chromatin remodelling proteins act on nucleosomes. Nucleosome assembly factors for

example are involved in the deposition of histones on the DNA strand after DNA replication. Furthermore, ATP dependent nucleosome remodelling proteins are involved in sliding of nucleosomes to allow controlled access to DNA sequences during transcription initiation (Saha *et al.* 2006). Many chromatin proteins seem to form multimeric complexes that exhibit the capacity to introduce histone and/or DNA modifications as well as remodel chromatin. A striking example is the chromatin remodeling ATPase DDM1, which is required for methylation of DNA and is likely to function in multi-protein complexes (Finnegan and Kovac 2000).

By their capability of altering chromatin modifications and chromatin structure chromatin remodelling proteins control an additional step in gene expression, on top of transcription factors and DNA based promoter elements. Through this role they are essential in several developmental processes such as leaf morphology, stem cell maintenance, cell cycle control, and seed development (Habu *et al.* 2001; Muller and Leutz 2001; Berger and Gaudin 2003; Sharma *et al.* 2003; Guyomarc'h *et al.* 2005). For example FAS1, a subunit of a chromatin assembly factor (Exner *et al.* 2006), regulates the expression of WUS in the shoot meristem, and of SCR in the root meristem, which both are essential for maintenance of meristem identity (Guyomarc'h *et al.* 2005). And AtLHP1 is involved in flowering time control by repressing *FT*, a gene involved in the conversion of the shoot meristem to a floral meristem (Pineiro and Coupland 1998). The capability of altering chromatin modifications or chromatin structure requires flexibility to be able to adapt to changes in the environment or during various stages of differentiation.

Arabidopsis is well suited to be used as a model organism to study nuclear organisation and dynamics. The *Arabidopsis* genome is small (~150 Mb) and consists of five chromosomes. Chromosomes 1, 3, and 5 only contain only one heterochromatic region around the centromere, and chromosomes 2 and 4 also have a heterochromatic Nucleolar Organizer Region (NOR). This limited amount of heterochromatin can be easily distinguished from the euchromatin in interphase nuclei using light microscopy. On average ~ 7% of the DNA is heterochromatic in *Arabidopsis* pachytene nuclei, which is less than most other plants (15% in *Medicago*, 24% in *Lycopersicum* (Fransz *et al.* 1998)), or mammals (46% in Human, 38% in mouse (Holmquist and Ashley 2006)). Not all plants with small genomes are suitable for chromatin organization studies. Whereas the heterochromatin of *Arabidopsis* is concentrated around the chromocenters, in rice for example the heterochromatin is spread all over the chromosomes.

In *Arabidopsis* interphase nuclei the small number of heterochromatic areas are easily visualized with fluorescence microscopy as distinct areas (chromocenters). *Arabidopsis* chromocenters consists of centromeric and pericentromeric regions mostly the NORs are co-localize with the chromocenters (Fransz *et al.* 1998). The centromere core, consists mainly of a 180-bp tandem repeat and spans between 1.4 and 2.2 Mbp (Haupt *et al.* 2001). Surprisingly the length of the repeat is conserved in most eukaryotic organisms although the sequence is not. It has also been shown that at least 0.5 Mb of the repeat is essential for functioning of the centromere. Two heterochromatic pericentromere domains, containing transposons and other repeats, flank the centromeric region, (Fransz *et al.* 2003). The centromeric regions and the NOR contain all major tandem repeats of *Arabidopsis* (Heslop-Harrison *et al.* 2003).

The chromocenters are possibly involved in controlling the expression of euchromatic sequences. The current model of nuclear organization states that euchromatic gene rich regions are organized into loops that are between 200kb and almost entire chromosome arms in length, which are attached to the chromocenter (Fransz *et al.* 2003). These euchromatic sequences that are selectively organized into the chromocenters might be silenced euchromatic sequences.

The *Arabidopsis* root is a thin organ (~150 μm) allowing it to be captured within a single confocal stack of images, also there is hardly any autofluorescence in the tissue. Both characteristics allow *in vivo* nuclear imaging of an intact organ. Another advantage of the *Arabidopsis* root is that it divides in a fixed pattern (Figure 1- 2) allowing measurements on specific cell types in chronological developmental stages (van den Berg *et al.* 1997). The root meristem regulates the cell fate of all surrounding cells, the cells that are in control of regulating this organ process are called quiescent centre (QC) cells. These do not normally divide (Clowes 1954), and act by suppressing differentiation of the surrounding initials (Dolan *et al.* 1993; Doerner 1998). Each group of cells, consisting of one or more cell types, is maintained by its own specific initial (Figure 1- 2). Behind these initials is a file of daughter cells (Figure 1- 2) that undergo a small number of cell divisions and then start to differentiate and elongate.

Since chromatin organization has an important role in controlling nuclear processes involved in development it is useful to understand the principles underlying these

rearrangements. Modelling how chromatin (re)organisation is related to gene activity is therefore essential. These models should contain all biologically relevant information, for example how much time it takes to modify a histone tail, which proteins can bind to it, for how long do they bind, and how efficiently they are targeted. These parameters can be studied using several techniques.

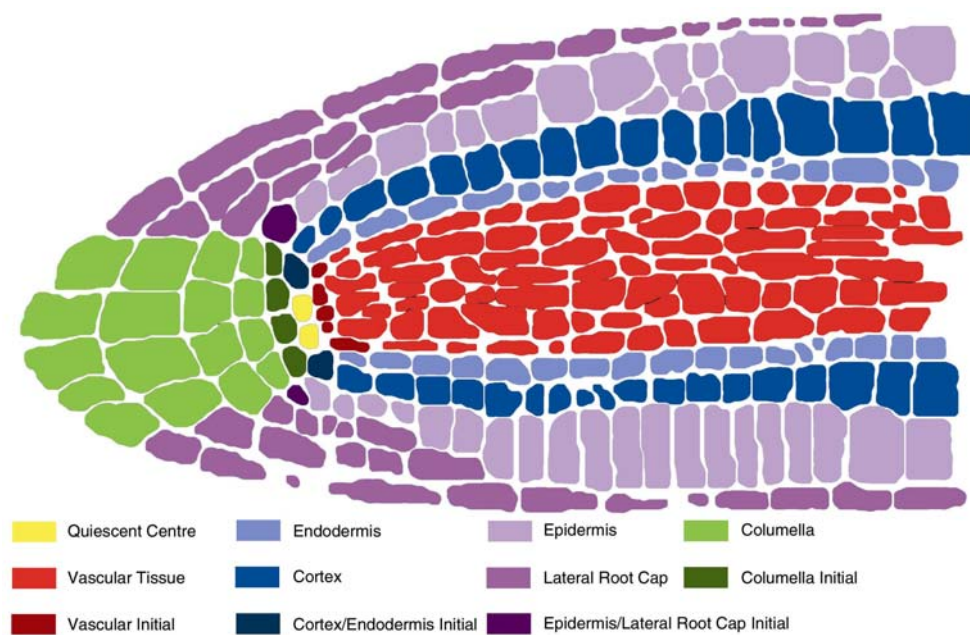


Figure 1- 2

The *Arabidopsis* root tip can be divided in 5 groups of cells. Besides the yellow QC cells there are four groups of cells arising from their unique initials. In green the columella cells are shown, a group of non-dividing fully differentiated cells. Purple marks the lateral root cap (LRC) and the epidermal tissue. The ground tissue, consisting of cortical and endodermal cells, is depicted in blue, whereas the vascular cells in the centre of the root are shown in red.

Microscopic techniques requires visualization of the cellular component that need to be imaged, for fluorescence microscopy this can be done in three manners; by direct staining, by detection with fluorescent antibodies, or by tagging with a fluorescent protein. This last solution is widely applied to monitor proteins in living tissue.

Protein mobility in living cells can be studied using Fluorescence Correlation Spectroscopy (FCS) or Fluorescence Recovery After Photobleaching (FRAP), which each have their specific advantages and disadvantages. FCS can be used to determine the diffusion constant of a protein (as well as to determine absolute protein concentrations). In a FCS experiment the fluctuations in fluorescence intensity within the observation volume (~ one femtoliter) of a confocal microscope is determined. The fluctuations are caused by fluorescent molecules moving into and out of the observation volume. The amplitude of the autocorrelation function is inversely proportional to the concentration of fluorescent molecules (Cluzel *et al.* 2000). When only a few molecules are present in the observation volume, the fluctuations in fluorescence intensity due to for example diffusion are relatively high. At a concentration of 10 nM on average 1 molecule is present in a femtoliter. Therefore FCS is powerful for example to study molecules involved in signal transduction. However chromatin (remodelling) proteins are present at relatively high concentrations. For example the average concentration of a histone protein in an *Arabidopsis* nucleus is ~100 μ M (~15000 histone molecules in one focal volume). Therefore FCS is not suitable to study the dynamics of chromatin remodelling proteins that are present at relatively high concentration. Additionally slow moving molecules will likely be photobleached while diffusing in the focal volume since FCS makes use of continues excitation of the fluorophore, resulting in an overestimation of mobility. Since the majority of the chromatin remodelling proteins interact with chromatin their mobility is relatively slow.

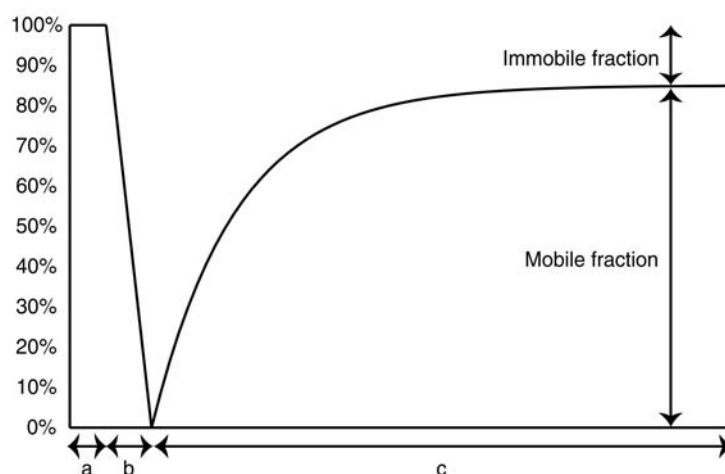


Figure 1- 3

A typical FRAP curve, with the relative fluorescence intensity on the y-axis and time on the x-axis. a) The initial phase before the bleach to determine the original fluorescence intensity. b) The bleaching phase of a FRAP experiment. c) The final recovery phase of a FRAP experiment from which the mobility is determined.

Another technique that can be used to determine protein mobility is FRAP. A typical FRAP experiment consists of three phases. During the first phase the initial fluorescence intensity is measured, after which a high power laser pulse photobleaches the fluorophores in a small region of interest (ROI), and finally the recovery of the fluorescent intensity is monitored (Figure 1- 3). The diffusion of the remaining fluorescent proteins into the ROI causes the recovery of fluorescent intensity. One can also monitor the depletion of fluorescence outside the region of interest to determine protein mobility; this technique is called FLIP (Fluorescence Loss In Photobleaching). FRAP is applicable on proteins present in higher concentrations as it requires a substantial amount of fluorescence to be present after photobleaching.

Therefore, FRAP was the preferred method to investigate the kinetic parameters of chromatin remodelling proteins. Two parameters can be determined with FRAP, namely the diffusion constant (D) and the mobile fraction. The diffusion constant reflects the area a protein explores by Brownian motion per time unit (related to its size and its cellular environment). A fast diffusion of free molecules is often used as the means for protein

distribution within cellular compartments. However, processes such as active transport or transient binding will influence the mobility, thereby creating an apparent diffusion constant (Wachsmuth *et al.* 2003). The affinity of chromatin remodelling proteins for chromatin indicates that simple diffusion is unlikely for these proteins. If a shouldered curve is observed this model likely represents “slow” and “fast” components.

Although it is difficult with FRAP to extract multi-component data from the obtained recovery curve, based on theoretical considerations three different models are available for fitting the measured recovery curve (Carrero *et al.* 2004; Sprague *et al.* 2004; Sprague and McNally 2005); a simple diffusion model, a model in which diffusion and binding/rebinding occur at similar timescales, and an apparent diffusion model. The latter model assumes that free diffusion is fast in comparison to binding and rebinding that it can be ignored in the curve fitting process. Information about the diffusion constant alone is not always sufficient for informative data and changes in mobility related to changes in environment or protein structure can be as informative (White and Stelzer 1999). The mobile fraction reflects the percentage of the protein population undertaking this exploration (Lippincott-Schwartz *et al.* 2001).

FRAP measurements make use of the bleaching capacity of the excitation light. In FRAP experiments a high intensity light pulse bleaches the fluorophore in a specific region of interest (ROI), resulting in a chemically irreversible change in the fluorophore, and a loss of fluorescence. Since the surrounding fluorophores are not affected, diffusion of these fluorophores into the bleached ROI can be monitored over time resulting in a fluorescence intensity recovery curve. From a typical FRAP curve the diffusion constant and mobile fraction can be determined by curve fitting.

Intermolecular interactions can be studied with several techniques; FRET-FLIM is one of the few techniques applicable in living cells. Direct interactions of fluorescent proteins with other molecules can be determined quantified by Förster Resonance Energy Transfer (FRET) efficiency. FRET can be observed between a donor and acceptor pair of fluorophores when they are in close proximity (in general between 1 and 10 nm (Peter and Ameer-Beg 2004)). When the spectral overlap of the donor-acceptor pair, the relative dipole orientation, the excitation wavelength, refractive index of the medium, and the quantum yield of the donor are known the R_0 (distance of 50% FRET) can be calculated (Elangovan *et al.* 2002). The knowledge of R_0 transforms the FRET efficiency into a sub

micrometer measurement bar, allowing distance measurements between interaction molecules (Elangovan *et al.* 2002).

Fluorescence Lifetime Imaging (FLIM) can be used as a measure for FRET efficiency as fluorescence lifetime is reduced upon occurrence of FRET (Bacsikai *et al.* 2003). Fluorescence lifetime can be determined using Time Correlated Single Photon Counting (TCSPC), meaning that for each excitation pulse the time between excitation and detection is registered, resulting in a fluorescence intensity histogram plotted against time. TCSPC is the most straightforward way to determine fluorescence lifetime resulting in one lifetime per detected photon (Becker *et al.* 2004). Field modulated lifetime imaging results in two lifetime values, a phase modulated lifetime and a frequency modulated lifetime which makes this detection method harder to interpret but potentially also contains more information (Jares-Erijman and Jovin 2003; Breusegem *et al.* 2006). However due to availability TCSPC was chosen. Making use of the techniques described we are aiming for a better understanding of dynamic chromatin organisation.

References

- Bacsikai, B. J., J. Skoch, G. A. Hickey, R. Allen and B. T. Hyman** (2003). "Fluorescence resonance energy transfer determinations using multiphoton fluorescence lifetime imaging microscopy to characterize amyloid-beta plaques." J Biomed Opt **8**(3): 368-75.
- Badugu, R., Y. Yoo, P. B. Singh and R. Kellum** (2005). "Mutations in the heterochromatin protein 1 (HP1) hinge domain affect HP1 protein interactions and chromosomal distribution." Chromosoma **113**(7): 370-84.
- Bannister, A. J., P. Zegerman, J. F. Partridge, E. A. Miska, J. O. Thomas, R. C. Allshire and T. Kouzarides** (2001). "Selective recognition of methylated lysine 9 on histone H3 by the HP1 chromo domain." Nature **410**(6824): 120-4.
- Bantignies, F. and G. Cavalli** (2006). "Cellular memory and dynamic regulation of polycomb group proteins." Curr Opin Cell Biol **18**(3): 275-83.
- Becker, W., A. Bergmann, M. A. Hink, K. Konig, K. Benndorf and C. Biskup** (2004). "Fluorescence lifetime imaging by time-correlated single-photon counting." Microsc Res Tech **63**(1): 58-66.
- Berger, F. and V. Gaudin** (2003). "Chromatin dynamics and Arabidopsis development." Chromosome Res **11**(3): 277-304.
- Berger, S. L.** (2002). "Histone modifications in transcriptional regulation." Curr Opin Genet Dev **12**(2): 142-8.
- Breusegem, S. Y., M. Levi and N. P. Barry** (2006). "Fluorescence correlation spectroscopy and fluorescence lifetime imaging microscopy." Nephron Exp Nephrol **103**(2): e41-9.
- Busczak, M. and A. C. Spradling** (2006). "Searching chromatin for stem cell identity." Cell **125**(2): 233-6.
- Cao, X. and S. E. Jacobsen** (2002). "Locus-specific control of asymmetric and CpNpG methylation by the DRM and CMT3 methyltransferase genes." Proc Natl Acad Sci U S A **99** Suppl 4: 16491-8.
- Carrero, G., E. Crawford, M. J. Hendzel and G. de Vries** (2004). "Characterizing fluorescence recovery curves for nuclear proteins undergoing binding events." Bull Math Biol **66**(6): 1515-45.
- Cheutin, T., A. J. McNairn, T. Jenuwein, D. M. Gilbert, P. B. Singh and T. Misteli** (2003). "Maintenance of stable heterochromatin domains by dynamic HP1 binding." Science **299**(5607): 721-5.
- Clowes, F. A. L.** (1954). "The Promeristem and the Minimal constructional Centre in Grass Root Apices." New Phytol **53**: 108:116.
- Cluzel, P., M. Surette and S. Leibler** (2000). "An ultrasensitive bacterial motor revealed by monitoring signaling proteins in single cells." Science **287**(5458): 1652-5.

- Doerner, P.** (1998). "Root development: quiescent center not so mute after all." Curr Biol **8**(2): R42-4.
- Dolan, L., K. Janmaat, V. Willemsen, P. Linstead, S. Poethig, K. Roberts and B. Scheres** (1993). "Cellular organisation of the Arabidopsis thaliana root." Development **119**(1): 71-84.
- Elangovan, M., R. N. Day and A. Periasamy** (2002). "Nanosecond fluorescence resonance energy transfer-fluorescence lifetime imaging microscopy to localize the protein interactions in a single living cell." J Microsc **205**(Pt 1): 3-14.
- Exner, V., P. Taranto, N. Schonrock, W. Grüsssem and L. Hennig** (2006). "Chromatin assembly factor CAF-1 is required for cellular differentiation during plant development." Development **133**(21): 4163-72.
- Festenstein, R., S. N. Pagakis, K. Hiragami, D. Lyon, A. Verreault, B. Sekkali and D. Kioussis** (2003). "Modulation of heterochromatin protein 1 dynamics in primary Mammalian cells." Science **299**(5607): 719-21.
- Finnegan, E. J. and K. A. Kovac** (2000). "Plant DNA methyltransferases." Plant Mol Biol **43**(2-3): 189-201.
- Fischle, W., Y. Wang, S. A. Jacobs, Y. Kim, C. D. Allis and S. Khorasanizadeh** (2003). "Molecular basis for the discrimination of repressive methyl-lysine marks in histone H3 by Polycomb and HP1 chromodomains." Genes Dev **17**(15): 1870-81.
- Fransz, P., S. Armstrong, C. Alonso-Blanco, T. C. Fischer, R. A. Torres-Ruiz and G. Jones** (1998). "Cytogenetics for the model system Arabidopsis thaliana." Plant J **13**(6): 867-76.
- Fransz, P., W. Soppe and I. Schubert** (2003). "Heterochromatin in interphase nuclei of Arabidopsis thaliana." Chromosome Res **11**(3): 227-40.
- Guyomarc'h, S., C. Bertrand, M. Delarue and D. X. Zhou** (2005). "Regulation of meristem activity by chromatin remodelling." Trends Plant Sci **10**(7): 332-8.
- Habu, Y., T. Kakutani and J. Paszkowski** (2001). "Epigenetic developmental mechanisms in plants: molecules and targets of plant epigenetic regulation." Curr Opin Genet Dev **11**(2): 215-20.
- Haupt, W., T. C. Fischer, S. Winderl, P. Fransz and R. A. Torres-Ruiz** (2001). "The centromere 1 (CEN1) region of Arabidopsis thaliana: architecture and functional impact of chromatin." Plant J **27**(4): 285-96.
- Heitz, E.** (1928). "Das Heterochromatin der Moose." Jahrb Wiss Botanik **69**: 762-818.
- Heslop-Harrison, J. S., A. Brandes and T. Schwarzacher** (2003). "Tandemly repeated DNA sequences and centromeric chromosomal regions of Arabidopsis species." Chromosome Res **11**(3): 241-53.
- Histone.com (2006). Histone.com
- Holmquist, G. P. and T. Ashley** (2006). "Chromosome organization and chromatin modification: influence on genome function and evolution." Cytogenet Genome Res **114**(2): 96-125.

- James, T. C., J. C. Eissenberg, C. Craig, V. Dietrich, A. Hobson and S. C. Elgin** (1989). "Distribution patterns of HP1, a heterochromatin-associated nonhistone chromosomal protein of *Drosophila*." Eur J Cell Biol **50**(1): 170-80.
- James, T. C. and S. C. Elgin** (1986). "Identification of a nonhistone chromosomal protein associated with heterochromatin in *Drosophila melanogaster* and its gene." Mol Cell Biol **6**(11): 3862-72.
- Jares-Erijman, E. A. and T. M. Jovin** (2003). "FRET imaging." Nat Biotechnol **21**(11): 1387-95.
- Jenuwein, T. and C. D. Allis** (2001). "Translating the histone code." Science **293**(5532): 1074-80.
- Kornberg, R. D.** (1974). "Chromatin structure: a repeating unit of histones and DNA." Science **184**(439): 868-71.
- Lachner, M., D. O'Carroll, S. Rea, K. Mechtler and T. Jenuwein** (2001). "Methylation of histone H3 lysine9 creates a binding site for HP1 proteins." Nature **410**(6824): 116-20.
- Le Douarin, B., A. L. Nilsen, J. M. Garnier, H. Ichinose, F. Jeanmougin, R. Losson and P. Chambon** (1996). "A possible involvement of TIF1 alpha and TIF1 beta in the epigenetic control of transcription by nuclear receptors." Embo J **15**(23): 6701-15.
- Li, Y., D. A. Kirschmann and L. L. Wallrath** (2002). "Does heterochromatin protein 1 always follow code?" Proc Natl Acad Sci U S A **99** Suppl 4: 16462-9.
- Lippincott-Schwartz, J., E. Snapp and A. Kenworthy** (2001). "Studying protein dynamics in living cells." Nat Rev Mol Cell Biol **2**(6): 444-56.
- Lorvellec, M., J. Willemse, O. Kulikova, J. Verver and T. Bisseling** (Chapter 4). "LHP1 forms chromatin complexes at trimethylated histones."
- Maher, B.** (2006). "The Nucleosome Untangled." The Scientist **20**(5): 34-41.
- Meehan, R. R., C. F. Kao and S. Penning** (2003). "HP1 binding to native chromatin in vitro is determined by the hinge region and not by the chromodomain." Embo J **22**(12): 3164-74.
- Min, J., Y. Zhang and R. M. Xu** (2003). "Structural basis for specific binding of Polycomb chromodomain to histone H3 methylated at Lys 27." Genes Dev **17**(15): 1823-8.
- Minc, E., J. C. Courvalin and B. Buendia** (2000). "HP1gamma associates with euchromatin and heterochromatin in mammalian nuclei and chromosomes." Cytogenet Cell Genet **90**(3-4): 279-84.
- Muller, C. and A. Leutz** (2001). "Chromatin remodeling in development and differentiation." Curr Opin Genet Dev **11**(2): 167-74.
- Nilsen, A. L., M. Oulad-Abdelghani, J. A. Ortiz, E. Remboutsika, P. Chambon and R. Losson** (2001). "Heterochromatin formation in mammalian cells: interaction between histones and HP1 proteins." Mol Cell **7**(4): 729-39.
- Peter, M. and S. M. Ameer-Beg** (2004). "Imaging molecular interactions by multiphoton FLIM." Biol Cell **96**(3): 231-6.
- Pineiro, M. and G. Coupland** (1998). "The control of flowering time and floral identity in *Arabidopsis*." Plant Physiol **117**(1): 1-8.

- Rice, J. C. and C. D. Allis** (2001). "Histone methylation versus histone acetylation: new insights into epigenetic regulation." Curr Opin Cell Biol **13**(3): 263-73.
- Ridgway, P. and A. G.** (2000). "CAF-1 and the inheritance of chromatin states: at the crossroads of DNA replication and repair." Journal of cell science **113**: 2647-2658.
- Saha, A., J. Wittmeyer and B. R. Cairns** (2006). "Chromatin remodelling: the industrial revolution of DNA around histones." Nat Rev Mol Cell Biol **7**(6): 437-47.
- Schmiedeberg, L., K. Weisshart, S. Diekmann, G. Meyer Zu Hoerste and P. Hemmerich** (2004). "High- and low-mobility populations of HP1 in heterochromatin of mammalian cells." Mol Biol Cell **15**(6): 2819-33.
- Sharma, V. K., C. Carles and J. C. Fletcher** (2003). "Maintenance of stem cell populations in plants." Proc Natl Acad Sci U S A **100 Suppl 1**: 11823-9.
- Sprague, B. L. and J. G. McNally** (2005). "FRAP analysis of binding: proper and fitting." Trends Cell Biol **15**(2): 84-91.
- Sprague, B. L., R. L. Pego, D. A. Stavreva and J. G. McNally** (2004). "Analysis of binding reactions by fluorescence recovery after photobleaching." Biophys J **86**(6): 3473-95.
- Sugimoto, K., T. Yamada, Y. Muro and M. Himeno** (1996). "Human homolog of Drosophila heterochromatin-associated protein 1 (HP1) is a DNA-binding protein which possesses a DNA-binding motif with weak similarity to that of human centromere protein C (CENP-C)." J Biochem (Tokyo) **120**(1): 153-9.
- Turner, B. M.** (2002). "Cellular memory and the histone code." Cell **111**(3): 285-91.
- van den Berg, C., V. Willemsen, G. Hendriks, P. Weisbeek and B. Scheres** (1997). "Short-range control of cell differentiation in the Arabidopsis root meristem." Nature **390**(6657): 287-9.
- Vanyushin, B. F.** (2005). "Enzymatic DNA methylation is an epigenetic control for genetic functions of the cell." Biochemistry (Mosc) **70**(5): 488-99.
- Volpe, T. A., C. Kidner, I. M. Hall, G. Teng, S. I. Grewal and R. A. Martienssen** (2002). "Regulation of heterochromatic silencing and histone H3 lysine-9 methylation by RNAi." Science **297**(5588): 1833-7.
- Wachsmuth, M., T. Weidemann, G. Muller, U. W. Hoffmann-Rohrer, T. A. Knoch, W. Waldeck and J. Langowski** (2003). "Analyzing intracellular binding and diffusion with continuous fluorescence photobleaching." Biophys J **84**(5): 3353-63.
- White, J. and E. Stelzer** (1999). "Photobleaching GFP reveals protein dynamics inside live cells." Trends Cell Biol **9**(2): 61-5.
- Willemse, J., M. Lorvellec, O. Kulikova, J. Verver, J. Wellink and T. Bisseling** (Chapter 5). "LHP1 mutants in *Arabidopsis thaliana*."

Zemach, A., Y. Li, H. Ben-Meir, M. Oliva, A. Mosquna, V. Kiss, Y. Avivi, N. Ohad and G. Grafi (2006). "Different domains control the localization and mobility of LIKE HETEROCHROMATIN PROTEIN1 in Arabidopsis nuclei." Plant Cell **18**(1): 133-45.

Zhang, K., J. S. Siino, P. R. Jones, P. M. Yau and E. M. Bradbury (2004). "A mass spectrometric "Western blot" to evaluate the correlations between histone methylation and histone acetylation." Proteomics **4**(12): 3765-75.

Outline of the thesis

Genetic information of eukaryotic organisms is stored in the nuclei of their cells. The amount of data stored in each nucleus is enormous and only by compaction of the genetic material it is possible to maintain all information in each cell. In this thesis we are interested in how an organism is able to organize its DNA in such a way that it is still able to access the DNA whenever that is needed. In chapter 1 an introduction of what is known about chromatin organization and a brief description of *Arabidopsis thaliana*, the research model used in this thesis, is given. *Arabidopsis* has a small genome of 150 Mb which is split over 5 chromosomes. Each of these chromosomes contains one centromeric region that is cytogenetically visible as heterochromatin, while the remainder of the DNA is euchromatic. This simple organization makes *Arabidopsis* ideally suited for chromatin organization studies. *Arabidopsis* also has a fixed cell division pattern in the root, which allowed us, with the aid of a DNA quantification program described in the first experimental chapter, to examine the DNA content of nuclei of all different cell layers within the root (Chapter 2).

In recent years it has been shown that chromatin is quite dynamic, and even histones can be rapidly exchanged. Eukaryotic gene expression is also partially regulated by histone modifications such as acetylation, methylation, phosphorylation, and ubiquitination (i.e., 'histone code'). Furthermore several histone variants exist that can be build into a nucleosome with for example altered binding affinity for DNA. In chapter 3 we have examined the mobility of the core histone H2B, which has been proposed to be relatively mobile due to the activity of RNA polymerase II, in intact root tissue. By making use of the DNA methylation mutant *ddm1* we were able to measure the mobility of H2B in euchromatin, heterochromatin as well as centromeric heterochromatin (Chapter 3). One of the observations described in chapter 3 is that H2B is immobile in centromeric regions.

This immobility triggered us to examine the properties of AtLHP1, the *Arabidopsis* homologue of a chromatin remodeling protein which has initially been characterized in *Drosophila* as a heterochromatic protein. This would allow us to test whether the observed immobility of H2B in centromeric regions is a general property of chromatin proteins in this region. In transgenic plants expressing a functional AtLHP1-GFP fusion protein, AtLHP1 was found to form numerous foci inside the nucleus and seems to be excluded from heterochromatin (Chapter 4). These foci are not artifacts since FRET-

FLIM studies show that they maintain an interaction with chromatin, and FRAP shows that the proteins are not freely mobile (Chapter 4). In chapter 5 the roles of the various domains of AtLHP1 in foci formation, mobility and interaction with chromatin are determined using confocal microscopy in combination with FRAP and FRET-FLIM methods. A mutational analysis of AtLHP1, which lacks either one or two domains, allowed us to investigate the properties of the domains. The results obtained, combined with previous results by others, lead to a hypothetical model of how AtLHP1 functions in the nucleus.

The final chapter discusses the results described in this thesis, and evaluates the microscopic and other techniques that are currently used in studies on chromatin organization and dynamics.

**Chapter 2: Quantification of nuclear DNA in
whole mount *Arabidopsis* roots**

Joost Willemse, Hans de Jong and Ton Bisseling

Introduction

One of the most challenging questions in developmental biology is how somatic nuclei of a multicellular eukaryote regulate gene expression and cellular function. These processes may coincide with large scale, microscopically detectable changes in the patterns of nuclear chromatin condensation. One of the phenomena involved in such nuclear changes that can be directly quantified is endoreduplication, which occurs in specialized highly differentiated cells (Nagl 1978). Endoreduplication give rise to endopolyploidy, which can amount up to 80% of all plant tissue (Butterfass 1966; Sugimoto-Shirasu *et al.* 2005). DNA Quantification of nuclei in such tissues is essential for elucidating the endoreduplication status of their cells.

Various methods have been developed to establish DNA amounts in nuclei and chromosomes. The first one is microdensitometry of Feulgen stained cell spread preparations, which allows accurate measurements of nuclear DNA amounts, but its technology is very time consuming and error prone (Hardie *et al.* 2002). More recently, flow cytometric analysis of large numbers of cells, nuclei or chromosomes in aqueous media became possible using DNA-specific fluorophores such as DAPI, Propidium Iodide, Ethidium Bromide, Sytox dyes to quantify DNA amounts (Hulett *et al.* 1969; Fried *et al.* 1976). The GC-specific Propidium Iodide (PI) has the advantage that its fluorescence intensity is linearly correlated with nucleic acid amounts and therefore is very suitable for quantitative analyses (Dean *et al.* 1982; van den Engh *et al.* 1986).

Although flow cytometry is eminent for demonstrating gross variation in DNA amounts, the technology is not suited for measuring DNA amounts of specific cells inside tissue or organs. To allow quantification of individual cellular DNA amounts we choose digital analysis of microscopic images to allow spatial identification. Comparative studies have shown that digital image quantifications and flow cytometry are equally accurate (Rigaut *et al.* 1991). We therefore developed a novel confocal microscopic method for measuring total DNA amounts of spatially reconstructed nuclei with known cell identity by merging subsequent optical slices into a 3D image of the complete tissue and called this *averaging 3D method*. We compared the accuracy of our method (an adapted computerized variant of the so-called *2½D method* of (Ji and Tucker 1997)), with that of *3D method (REF)*. Essentially these methods differ in the way that total DNA amounts were measured in a 3D stack of consecutive optical sections. Whereas the absence of a single nuclear section in the 3D method will result in the exclusion of the entire nucleus from the data, the

2½D method and our averaging 3D method are able to compensate for such lacking data by interpolating missing sections (Ji and Tucker 1997).

Here we report the testing and refining of DNA quantification in *Arabidopsis* nuclei in root tips using the 3D methods. We choose the root as this organ can be imaged as a whole in a single z-stack, whereas its lack of chlorophyll and transparent cell walls allow imaging with little background fluorescence and simple quantification. Roots contain fully differentiated cells as well as cells that are actively dividing, which provides the opportunity to develop a semi-automated DNA quantification method and also to test it on tissues with various properties. Additionally the stereotypic tissue patterning of *Arabidopsis* roots provides important developmental information of every cell (Figure 2- 1e).

The most basal part of the root contains the columella cells (green in Figure 2- 1e), which develop from a single layer of columella stem cells. Directly adjacent to the columella stem cells are the four mitotically inactive quiescent centre cells (yellow in Figure 2- 1e) surrounded by the stem cells for the different cell types (Dolan *et al.* 1993). These stem cells keep dividing while adding mitotically active daughter cells to the different cell type files like cortex (dark blue in Figure 2- 1e), endodermis (light blue in Figure 2- 1e), and vascular bundle (red in Figure 2- 1e). The DNA quantification in the entire root tip is used to develop the averaging 3D method and also to determine the distribution of cell cycle phases along the root as well as the identification of endoreduplicated tissue. To allow this we make use of specific properties of several cell types.

The columella cells do not divide and have a 2C DNA content (Sugimoto-Shirasu *et al.* 2005). Their spherical nuclei and relatively large cells are easily recognizable, which make them ideal to develop a whole mount DNA quantification method. The dividing cells in this meristematic region around the quiescent centre provide the opportunity to test whether nuclei at G1 and G2 phase can efficiently be distinguished. Additionally, their small size allows us to test whether the DNA quantification method is suited for the automated identification of nuclei when they are separated by less than a few micrometers.

After identification of nuclei within image sections the consecutive sections need to be sorted. Sorting of optical sections belonging to one nucleus and separation of sections belonging to other nuclei is based on xy-position, which is similar for each section of a spherical nucleus. This xy-position additionally correlates DNA content with cell type and specific position in the root. Since we do not want to limit the method to only spherical

nuclei, the elongated cells in the differentiated zone are used to test and adapt the method in such a manner that nuclear sections can be sorted when the nucleus does not have the ideal spherical shape. Furthermore, cells in the differentiated zone may undergo endoreduplication. For example endoreduplicated root hairs have an 8C or 16C DNA content, and flow cytometry of isolated root nuclei showed that about 25% of all root cells are endoreduplicated (Wildwater *et al.* 2005). The origin of most of these endoreduplicated nuclei is unknown. Using these properties of the *Arabidopsis* root it can be tested whether the whole mount DNA quantification method allows efficient identification of endoreduplicated cells (like root hairs), and identify other endoreduplicated cell types.

The DNA quantification will be discussed for columella, meristematic tissue and differentiated cells. This will provide insight into the distribution of cell cycle phases in single cell files. Additionally we will determine whether the elongated vascular cells near the QC cells have endoreduplicated to achieve their bigger size. Before being able to discuss these results the averaging 3D method will be tested in three steps; identification of nuclear sections, sorting of the selections into complete nuclei, and finally the quantification.

Results and discussion

Identification of nuclear sections

A method for quantification of nuclear DNA amounts in whole mount preparations was developed and optimized for propidium iodide stained *Arabidopsis* roots. We choose this dye for its specific binding to double-stranded nucleic acids and linear fluorescence intensity with DNA content. Images were captured under a confocal microscope clearly displaying a pattern of brightly fluorescing nuclei in a weakly fluorescing background of cytoplasm and clearly distinguishable, non-fluorescing cell walls (Figure 2- 1a). Roots measure less than 150 μm in width and demonstrate a distinct cell pattern allowing full identification of all cell types in a single z-stack of a root segment (Dolan *et al.* 1993).

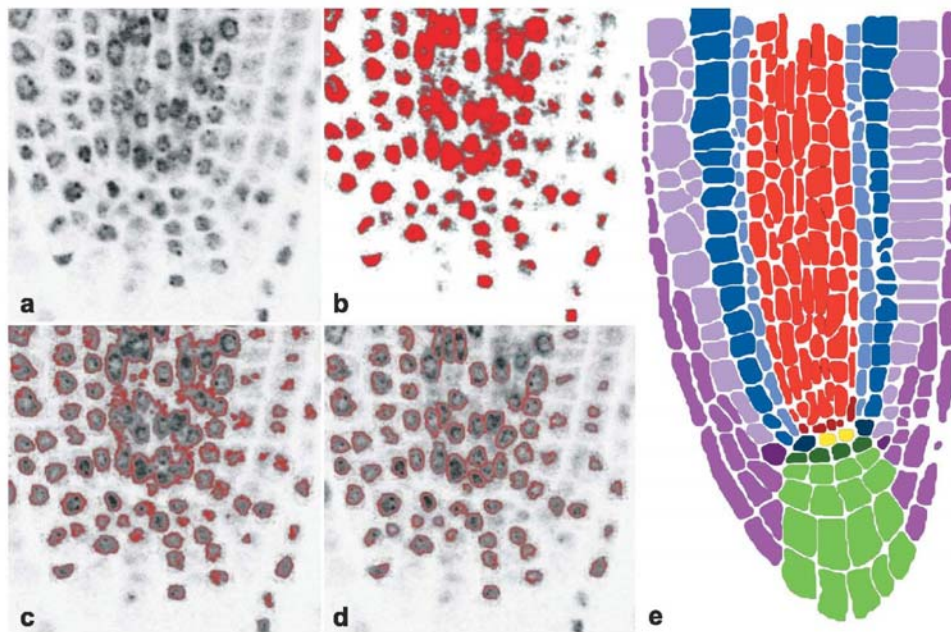


Figure 2- 1

Single z-slice of the stack of images as captured by Lasersharp 2000TM (a). The initial selection based on propidium iodide staining intensity where the red parts show the detected objects (b). Based on image 1b lines are drawn at the edges of the object and the edges are smoothed (c). The image is filtered; all objects smaller than 1.5 μm^2 are removed, as well as all objects only partially present in the image and all objects with a roundness value above 10, ending with the detected nuclei (d). A schematic overview of all cell types; yellow cells are the quiescent centre (QC) cells. Initials are depicted as dark coloured variants of the tissue they maintain. Vascular tissue is shown in red, ground tissue in blue (the cortex being dark blue, and endodermis light) Epidermal and lateral rootcap are shown in purple (light and dark respectively) and finally columella cells are shown in green.

We first identified the nuclear sections in the confocal images on the basis of fluorescence intensity. Pixel size in the confocal microscope was kept at 0.15 μm in all analyses. In Figure 2- 1b we show the selected objects at a given fluorescence threshold just above the background level of the cytoplasm. To further distinguish genuine nuclear fluorescent objects from background we used the morphometric parameters “area” and “roundness” for selecting the spherical nuclear bodies with smooth edges. The area parameter set at 2.25 μm^2 (1.5 μm diameter) allowed distinction of most nuclear sections

from small debris. The few small nuclear sections undeservedly discarded at this level will theoretically lead to less than 0.3% underestimation of the total DNA value.

The *roundness* parameter is the ratio of perimeter and area and can be used to distinguish ragged background objects from regularly shaped nuclei. We considered an object smooth if its perimeter is less than five times the expected value for a spherical body with the same area. Setting the parameter at an even lower (more stringent) value we noticed that objects containing merged nuclear sections were discarded (see identification of nuclear sections in meristem).

The columella cells have spherical nuclei with a diameter of 2.8 μm . These cells are non-dividing and have a 2C ploidy (Sugimoto-Shirasu *et al.* 2005). Their nuclei are spatially separated from their neighbours by at least 1.2 μm . We choose this homogeneous population of nuclei to test the power of our method. The analysis was based on confocal images of six roots, each of them consisting of ~150 sections. Comparing the extracted data with the confocal sections we observed that 99.3% of the nuclear sections (n=823) were identified properly (Figure 2- 1b and c). Only three sections from the middle of nuclei with fluorescence intensity close to the background, and another three sections at the nuclear periphery with a diameter of less than 1.5 μm remained undetectable.

To further evaluate the robustness of the method we assessed the efficiency of nuclear section identification in the vascular tissue, and the remaining tissues in both the meristem and elongation zone. Like in the columella zone meristematic nuclei are also spherical, but measure 3.3 μm across and are separated from their neighbours by a minimum of 0.9 μm . The separation distance is large enough to allow as efficient identification of the sections compared to columella. Vascular tissue nuclei are sometimes separated by less than 0.2 μm hindering the detection as individual sections. In one of the root meristems, which contains 5092 nuclear sections, we identified 99% (n=2833) of the epidermis and cortex nuclei as individual objects (Figure 2- 1b and c). Concerning the nuclei in the vascular tissue that were closer than 0.2 μm 9% of the nuclear sections (n=2259) remained unseparated and could therefore not be identified as individual objects (Figure 2- 1b and c).

Separation of adjacent or nearby nuclear sections such as in the vascular tissue required a border finding tool with manual correction. An example is given in Figure 2- 1d. For attempts to automate this procedure we further tested the autosplit and watershed split functions, but found that such functions interpret the dark areas of the unstained nucleoli

often as gaps between nuclei, and hence are not suitable for this procedure. Notwithstanding the manual procedure of the vascular tissue, we were able to detect 98 % nuclei correctly.

Nuclei of the elongation zone are oval and can measure up to 25 μm in length. Proper distinction of the nuclei from the ragged and fragmented cell walls could be achieved by increasing the value for minimum area for objects from 2.5 μm^2 to 5 μm^2 . Since the roundness limit was not set stringently to prevent removal of clustered vascular nuclei this parameter was not changed. (Figure 2- 1c). Accordingly, the program identified more than 99% of the nuclei in the elongation zone and vascular tissue properly (n=2033), which corresponds well with the success rate for the total analysis of all 7142 nuclear sections.

Establishing complete nuclei from consecutive optical sections

The next step of the procedure involves identification of complete nuclei from consecutive focal sections in the 3D stack. We first established x and y coordinates for the centre of every nuclear section and sorted them in a spreadsheet on the basis of most similar x*y and x/y values (see Material and Methods for details), which is easy and straightforward for the spherical nuclear sections in the radial symmetrical nuclei of columella and meristematic tissues. The pinhole setting was such that nuclear sections are $\sim 1 \mu\text{m}$ thick, since meristematic nuclei are often separated by less than 1 μm these nuclei will be sorted together. These nuclei on top of each other had to be separated manually. Sorting of the nuclear sections of the columella from the six roots led to full identification of all 104 nuclei, whereas of the meristematic region excluding vascular cells only 12 out of 315 nuclei (4%) were not sorted properly. Of the vascular cells in the meristem 7% (19 out of 268) were not properly sorted.

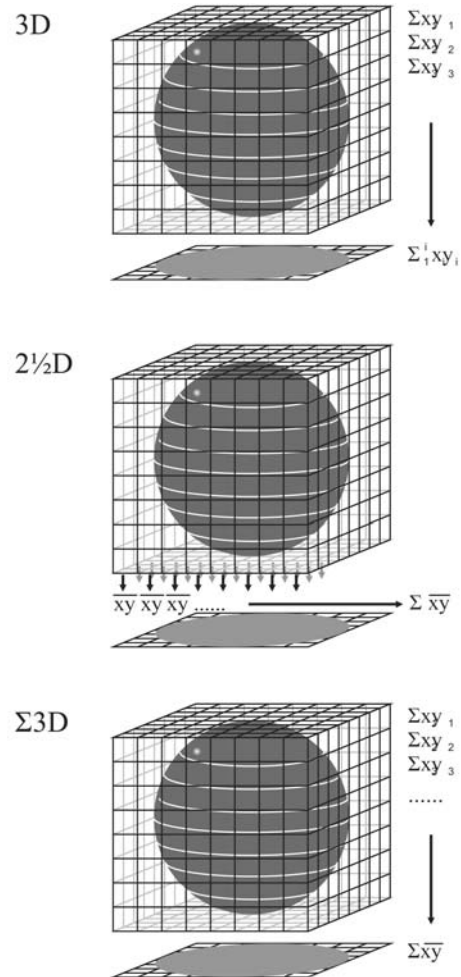


Figure 2- 2

The three different methods for DNA quantification. a) The 3D method uses the sum of all detected nuclear sections. b) The 2½D method uses a projection to average the intensity after which the sum of the pixels within the nucleus is measured. c) The averaging 3D method averages the sums of the intensity of each nuclear section.

For the more difficult sorting of the ellipsoid nuclear sections in the elongation zone of the root we had to slightly adapt the procedure. Firstly, we always rotate the root in the confocal microscope with the nuclei of the elongation zone parallel to the y-axis. As these nuclei are not always perfectly perpendicular to the xy-plane the larger variation of size, shape and nuclear position required that the upper limit of acceptable variation between the sorted xy-values had to be changed. This upper limit is automatically determined by the average difference between xy positions of consecutively sorted sections. After sorting nuclei at a higher automatically determined level of maximum variation we obtained a success rate of properly sorted nuclei of 92% (n=213). However, 99% of correct identification of nuclear sections (7077 out of 7142), and 98 % proper sorting (6988 out of 7142) would, since the average thickness of a nucleus of 9 sections, result in complete identification of only 76% of the nuclei.

DNA quantification

After selection of all nuclear sections of a nucleus its DNA content can be quantified. In the 3D method (Figure 2- 2a) DNA content is quantified by summing the fluorescence intensity of all nuclear sections. A drawback of this method is that the detection of all sections of a nucleus is essential for quantification. Our method succeeds in this in tissues with ideal properties, like the columella. However, for example in the root meristem this is only the case for about 75 % of the nuclei. The 2½D method (Figure 2- 2b) uses the sum of the intensity of a projection of a nucleus, this has the advantage that when nuclear sections are missing still rather accurate DNA quantification data can be obtained. This method uses projections of the images (Figure 2- 2b). Therefore the method does not allow studies on specimen of more than one cell layer thick, since nuclei from different layers can overlap in a projection. Therefore we adapted the 2½D method accordingly, by calculating the summed intensity of every identified nuclear section and subsequently calculating the average intensity of the sections, thereby preserving the spatial location of nuclei (Figure 2- 2c). This method will be named the averaging 3D method. To test whether the averaging 3D method and the 3D method have a similar accuracy, when all nuclear sections are identified, we first studied columella cells, as they are known to be non-dividing cells with a 2C DNA content (Sugimoto-Shirasu *et al.* 2005). We analyzed 6 roots and for each root the average fluorescence intensity of all columella nuclei is set to 2.00. (DNA content of a 2C nucleus), eliminating differences between roots due to variation in staining efficiency.

The variance of the nuclear DNA content indicates the accuracy of the method as all nuclei of the columella have a 2C content. The variances obtained with the 2 methods are 2.00 ± 0.05 (3D) and 2.00 ± 0.03 (averaging 3D showing that there is no significant difference in variance between the averaging 3D and 3D method (F-test = 0.96) and also not between roots. So the 3D and the averaging 3D method show a similar accuracy when analyzing ideal tissues. To test whether the averaging 3D method provides better data than the 3D method when data sets are incomplete we used the columella nuclei data set and from this we generated a new data set in which 3% of the nuclear sections were eliminated. A simulation on ideal spherical nuclei of which 3% of the nuclear sections were eliminated showed that the missing data would result in a deviation from the expected values of 0.34% with the averaging 3D method and an underestimation of 8.5% with the 3D method. In this way at least one section was eliminated from about 20% of the nuclei. From these nuclei the original data sets as well as the incomplete sets were quantified with both the averaging 3D and 3D method. These data were normalized using the average DNA value of all columella nuclei

As expected the DNA values and variance of the original data sets with the 3D method (1.97 ± 0.10) and the averaging 3D method (1.93 ± 0.07), do not differ significantly (F-test 0.96). In contrast, the data obtained with the 3D method and the averaging 3D method, in the modified data set are 1.76 ± 0.10 and 1.97 ± 0.10 respectively. This shows that the averaging 3D method is better suited for determining DNA content in less than ideal data since the nuclei missing nuclear sections are determined to have similar DNA content compared to the complete nuclei (average deviation from complete data is 0.5%, no significant difference $p=0.5$), whereas the 3D method underestimates the DNA content by 10.5% on average (significantly lower $p<0.001$). As the averaging 3D method allows for absence of nuclear sections, we used this method for quantifying DNA content of nuclei in whole mount preparations.

(The distribution of DNA content in columella cells does not deviate significantly from a normal distribution (Kolmogorov Smirnov). We then focused on several biological questions.

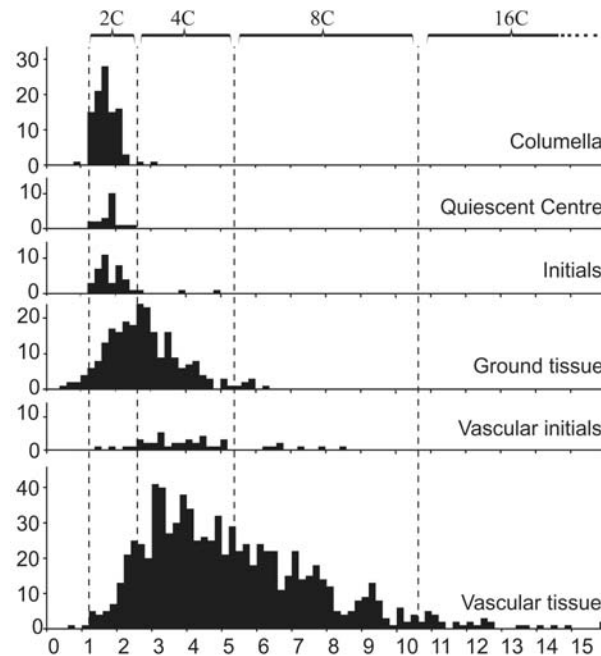


Figure 2- 3

The distribution of fluorescence intensity of the different ploidy groups detected in all roots. 2C, 4C and 8C peaks can be observed which correspond to the different cell cycle phases observed in the root tip.

Quiescent Centre cells

The strength of the whole mount procedure, compared to flow cytometry, is that DNA content of cells with a specific localization can be determined, even when they represent a small minority within an organ or tissue. A typical example in the *Arabidopsis* root, are the Quiescent Centre (QC) cells in the heart of the root meristem, these 4 non-dividing cells (Clowes 1954) are essential to maintain the stem cell identity of the surrounding initials (van den Berg *et al.* 1997). We analyzed the 4 QC nuclei of 6 roots, and the DNA content of these were normalized against the corresponding average DNA content of columella nuclei. The average DNA content of the 24 QC nuclei is $2.08 \pm 0.08C$. So the average DNA content and variance of QC nuclei is similar to that of columella nuclei $2.00 \pm 0.08C$ (T-test: $p=0.32$, and F-test: $p=0.61$). This is also clear from the similar distribution of nuclear DNA values in QC and columella as depicted in the histogram shown in Fig 2. So all tested QC nuclei have 2C DNA content, which is consistent with their non-dividing nature.

Initials

The root meristem is composed of initials and files of cells. Within these files cells remain mitotically active until cell elongation is activated. The frequency of division within these files is markedly higher than that of the initials and varies based on the cells distance from the initial (Fiorani and Beemster 2006). The relatively slow cell cycle progression of the initials suggest that G1 and/or G2 phase are markedly longer than in the other meristematic cells. To determine whether the initials are primarily maintained in G1 or in G2 of the cell cycle we analyzed their DNA content. 82 initials from three roots were analyzed; the distribution of the DNA content of cortex/endodermis, epidermis/lateral root cap and columella initials is shown in Figure 2- 3B. The nuclei have an average DNA content of $2.17 \pm 0.11C$ (40 nuclei). Based on the distribution of DNA values it is clear that two nuclei have a DNA content that is close to 4C (Figure 2- 3). Since stem cells are dividing cells these nuclei are most likely at G2.

Vascular tissue endopolyploidy

In contrast with the cortex/endodermis, epidermis/lateral root cap and columella initials vascular initials have an average DNA content of $4.42 \pm 0.24C$ (42 nuclei). This indicates that either the vascular initials are maintained in G2 of the cell cycle, or they are in G1 and are endotetraploid. We can distinguish between the two options by quantifying the DNA content of the daughter cells of these vascular initials. Their nuclear DNA content is $\sim 4C$ as well ($5.5 \pm 2.2C$) Therefore, the vascular initials must be maintained in G1 and thereby are similar to the other initials, with the exception that they are endotetraploid. (The vascular tissue nuclei are much larger than the nuclei of surrounding ground tissue. (Melaragno *et al.* 1993; Traas *et al.* 1998; Sugimoto-Shirasu and Roberts 2003) reported a strong correlation between cell nuclear size and endopolyploidy).

Examining the distribution of DNA content in the meristem, without the ground tissue nuclei, shows a shifted distribution compared to columella cells. Many cells have an amount of DNA in between 2C and 4C showing that the meristematic zone contains many cells in S-phase (Figure 2- 3). Based on the assumption that all 2.0C ploidy cells are actually G1 cells and that all 4.0C cells are in G2 we find that 50% of the cells are in S-phase, 30% in G1 and 20% in G2. The DNA-content of the S-phase nuclei is 3.0 ± 0.04 , and is normally distributed (Kolmogorov-Smirnov).

The DNA content of the vascular cells is on average 5.5 ± 0.1 (Figure 2- 3, 846 nuclei), again confirming one round of endoreduplication has occurred in the vascular tissue. The distribution of the DNA content observed shows us that only 7% of the cells is 2C in ploidy and the vast majority 89% is 4C, 8C or in between. The vascular cells maintain their 4C ploidy and in S-phase increase their DNA content to 8C (Figure 2- 3 & Figure 2- 4). After about 20 cell layers the endoreduplicated vascular cells disappear from the tissue, possibly sieve cells that die at the beginning of the elongation zone are responsible for this temporary increase in DNA content.

Cell file

Based on the distribution of DNA content within the complete meristem it seems that most cells are in S-phase or G2. However, in a cell file the DNA content should differ between the cells at various distances from the initial since not all cells are progressing through the cell cycle at similar speed (Fiorani and Beemster 2006). To determine the DNA content distribution of a series of cells, from QC, Initial to 12th daughter cell. We quantified the DNA content of three cell files, Figure 2- 4 shows the ploidy levels of each cell in two endodermis cell files as well as one vascular cell file. The QC and the initial are 2C in ploidy after which a series of cells are at the verge of division; they contain double the amount of DNA. Further in the root the cells have divided and show their 2C ploidy again, another round of cell division is initiated in the end, shown by the fact that cells start to duplicate their DNA once more.

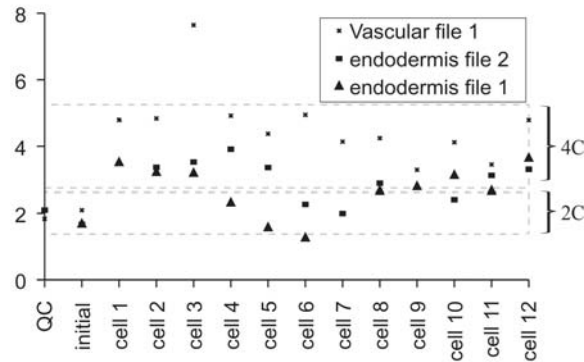


Figure 2- 4

The ploidy of the first 14 cells of two endodermis and one vascular cell file are shown. The graph shows a zone of S-phase cells for the endodermis cell files and an endo-reduplication for the vascular cell file in which the S-phase cells are 8C

Conclusion

The identification and sorting of nuclear sections is properly done for 97% of all visible nuclear sections. Therefore, the chance that a nucleus will not be detected at all is less than 0.01%. Since some of the nuclei are incomplete either due to sorting or detection problems two quantification methods were compared. The comparison of the 3D method, that needs complete nuclei for correct DNA quantification, and the averaging 3D method, that allows for absence of nuclear sections, showed that both methods result in similar mean and variance on ideal tissues. In general DNA measurements are highly variable, with a standard deviation close to half the average measurement. This amount of variation has been observed with several methods (Weigel and Glazebrook 2002), our method allows calculation of DNA intensities with similar variation. In addition it allows the detection of all nuclei within a tissue as well as the estimation of DNA content for partially imaged nuclei. The method is applicable for any fluorescence probe since the fluorescence intensity is measured from 8-bit gray scale images. There are some criteria that need to be fulfilled, background fluorescence has to be low, and the tissue thin enough to image with a fluorescence microscope. Based on these results the method shows similar results as Flow Cytometry with the additional advantage that positional information within tissues is retained.

Arabidopsis root tip contains nuclei with different ploidy levels, the QC and initials are maintained in G1 but their daughter cells progress through the cell cycle much faster, on average 50% of the meristematic cells are in S-phase. It is also shown that vascular tissue is endoreduplicated from the initial onward, the distribution of the vascular meristematic cells is similar to that of the rest of the meristem only with double the ploidy. The quantification of DNA content of single cell files shows us that several cell layers above the QC, the DNA content of the cells is duplicated in all cell types but this is reduced further up the root (Figure 2- 4), this suggest that this is a phase of the root where most cells are in S or G2-phase. A similar result is observed in a vascular cell file with double the DNA content of the endodermal cell file.

Experimental procedures

Arabidopsis growth conditions

Arabidopsis seeds were spread on 0.5 MS plates (2.2 g Murashige and Skoog medium with vitamins, 10 g sucrose and 8 g Diashin agarose per liter) and left at 4 °C for 2-4 days. Seeds were germinated in a growth chamber at 20 °C.

Root fixation

Five-days-old *Arabidopsis* Columbia seedlings were fixed in a vial containing 5 ml fixation buffer (1% formaldehyde and 10% DMSO (Dimethyl Sulfoxide in 1 x Phosphate Buffer Saline, pH 7.2), 0.06 M EGTA (Ethylene Glycol-Bis-β-aminoethyl ether (-) N,N,N',N' Tetra Acetic Acid), pH 7.5 adjusted with NaOH). The seedlings were fixed for 30 min at 20 °C during which they were de-aerated twice in a vacuum chamber. After fixation the material was dehydrated in two steps of 100% methanol and four steps of absolute ethanol, each 10 minutes, and stored at -20 °C for 2-4 days. Then, the seedlings were rinsed 2 x 5 min with ethanol, incubated in ethanol: xylene (1:1) for 40 min, rinsed 2 times 5 min with ethanol, 2 times 5 min with methanol, and rinsed with PBS containing 0.1% Tween 20 (PBT) and 1% v/v formaldehyde for 5 min. Seedlings were post-fixed with PBT containing 1% v/v formaldehyde, and rinsed 5 times 5 min with PBT. The seedlings were transferred to Eppendorf tubes and washed in 0.5 ml PBT and 0.5 ml 2x Saline Sodium Citrate (SSC) containing 50% formamide for 10 minutes, washed 2 times in 2x SSC with 50% formamide, boiled for 7 min, and placed on ice for 5 min, and stored at 16 °C overnight.

Finally seedlings were washed 4 times 15 min in freshly prepared PBS, stained with 0.5 µg/ml propidium iodide (PI) in PBS for 30 min at 20°C and mounted in Citifluor™.

Microscopy

PI stained intact roots were studied under a Zeiss LSM 510 and a Biorad Radiance 2100 MP-VIS confocal microscopes. The minimum resolution used was 0.15 µm per pixel, just below the Raleigh limit, which means that image size of the microscope was set at 150 x 150 µm. At the total image size of 1024x1024 pixels it was still possible to capture the entire root tip in one picture. Z-stack setting was adjusted to allow 50% overlapping between consecutive images. Stacks of fluorescence images were captured with Lasersharp 2000™ (Bio-Rad cell science division, Maylands avenue, Hemel Hempstead, UK) and stored for digital processing later.

Image processing and fluorescence quantification

All digital processing was carried out with Image Pro Plus v. 5 (Media Cybernetics Inc., Silver Spring, MD, 20910-5611 USA). A semiautomated script designed for the full procedures of the image analyses and DNA quantification and written in Image Pro Plus macro language can be obtained free of charge from our laboratory (contact Ton.Bisseling@wur.nl), or from the supplementary data. Individual nuclei were identified with the count command in the count/size menu. The size limit and roundness parameters were considered to distinguish nuclei from debris. Detection of putative nuclei was based on objects with a diameter more than 1.5 µm, an area more than 3.5 µm², and the roundness (Eq. 1) less than 10, thereby selecting only spherical and ellipsoid nuclei.

$$Roundness = \frac{Perimeter^2}{4 * \pi * Area} \quad (1)$$

The following parameters of fluorescent nuclear sections present in an image were determined: area, x-position, y-position, pixel intensity, total intensity, average diameter, maximum and minimum diameter and roundness.

Sorting and splitting of nuclei

The data were further processed in an MS Excel spreadsheet by calculating nuclear sections in different layers that together compose a nucleus. For this operation we created two new

variables by multiplying and rounding the corresponding x and y values, and these were subdivided into 21 equal classes, of which the two lowest value classes were split again into six more classes, thus producing a total of 25 different classes. Sorting of the data sets resulted in big groups of complete nuclei. To create smaller groups of sorted objects containing single nuclei the objects sorted in this manner were subsequently sorted according to the number created by dividing the x-position of the object by its y-position. Nuclei that were in a different position but have the same multiplied x and y position could still be distinguished in this way. For example a nucleus with x,y positions 100, 300 has the same $x*y$ variable as nuclei at position 300, 100. When the data were combined with the x/y position these nuclei produced the values 3 and 0.35 respectively). Sorting creates, from an 1024 by 1024 pixels image, 1852 groups with an average size of 15 by 40 pixels. The resolution is smaller in the x-direction because the nuclei are observed in cell files, which have less variation in the x-position. Cell elongation takes place in the y-direction and causes more variation in this direction.

The first and last image in the stack of a nucleus are established by calculating the absolute difference of the x and the y position between each data point obtained which was sorted as described before. The absolute difference between two nuclei in this manner is higher than the standard deviation because on average a nucleus consists of 10 slices with low variation in the x and y position. When the difference is above the standard deviation of all data points, the two data points are determined to be in different nuclei. (This results in the assumption that the two data points in the calculation belong to a different nucleus and copies each object to the next slide and leaves an empty line in between the data points.)

Acknowledgements

We thank Olga Kulikova and Maelle Lorvellec for providing us with some of the analyzed images, as well as valuable discussions about the technique.

References

- Butterfass, T.** (1966). "Neue Aspekte der Polyploidieforschung und Züchtung." Mitt. Max-Planck-Ges 1: 47-58.
- Clowes, F. A. L.** (1954). "The Promeristem and the Minimal constructional Centre in Grass Root Apices." New Phytol 53: 108:116.
- Dean, P. N., J. W. Gray and F. A. Dolbeare** (1982). "The analysis and interpretation of DNA distributions measured by flow cytometry." Cytometry 3(3): 188-95.
- Dolan, L., K. Janmaat, V. Willemsen, P. Linstead, S. Poethig, K. Roberts and B. Scheres** (1993). "Cellular organisation of the *Arabidopsis thaliana* root." Development 119(1): 71-84.
- Fiorani, F. and G. T. Beemster** (2006). "Quantitative analyses of cell division in plants." Plant Mol Biol 60(6): 963-79.
- Fried, J., A. G. Perez and B. D. Clarkson** (1976). "Flow cytofluorometric analysis of cell cycle distributions using propidium iodide. Properties of the method and mathematical analysis of the data." J Cell Biol 71(1): 172-81.
- Hardie, D. C., T. R. Gregory and P. D. Hebert** (2002). "From pixels to picograms: a beginners' guide to genome quantification by Feulgen image analysis densitometry." J Histochem Cytochem 50(6): 735-49.
- Hulett, H. R., W. A. Bonner, J. Barrett and L. A. Herzenberg** (1969). "Cell sorting: automated separation of mammalian cells as a function of intracellular fluorescence." Science 166(906): 747-9.
- Ji, L. and J. Tucker** (1997). "DNA measurement of overlapping cell nuclei in thick tissue sections." Anal Cell Pathol 14(1): 41-9.
- Melaragno, J. E., B. Mehrotra and A. W. Coleman** (1993). "Relationship between Endopolyploidy and Cell Size in Epidermal Tissue of *Arabidopsis*." Plant Cell 5(11): 1661-1668.
- Nagl, W.** (1978). Endopolyploidy and polyteny in differentiation and evolution. Amsterdam, North-Holland Publishing Company.
- Rigaut, J. P., J. Vassy, P. Herlin, F. Duigou, E. Masson, D. Briane, J. Foucrier, S. Carvajal-Gonzalez, A. M. Downs and A. M. Mandard** (1991). "Three-dimensional DNA image cytometry by confocal scanning laser microscopy in thick tissue blocks." Cytometry 12(6): 511-24.
- Sugimoto-Shirasu, K., G. R. Roberts, N. J. Stacey, M. C. McCann, A. Maxwell and K. Roberts** (2005). "RHL1 is an essential component of the plant DNA topoisomerase VI complex and is required for ploidy-dependent cell growth." Proc Natl Acad Sci U S A 102(51): 18736-41.
- Sugimoto-Shirasu, K. and K. Roberts** (2003). "'Big it up': endoreduplication and cell-size control in plants." Curr Opin Plant Biol 6(6): 544-53.
- Traas, J., M. Hulskamp, E. Gendreau and H. Hofte** (1998). "Endoreduplication and development: rule without dividing?" Curr Opin Plant Biol 1(6): 498-503.

van den Berg, C., V. Willemsen, G. Hendriks, P. Weisbeek and B. Scheres (1997). "Short-range control of cell differentiation in the *Arabidopsis* root meristem." Nature 390(6657): 287-9.

van den Engh, G. J., B. J. Trask and J. W. Gray (1986). "The binding kinetics and interaction of DNA fluorochromes used in the analysis of nuclei and chromosomes by flow cytometry." Histochemistry 84(4-6): 501-8.

Weigel, D. and J. Glazebrook (2002). Whole mount DAPI staining and Measurement of DNA content. Arabidopsis, A laboratory manual. S. Curtis. New York, Cold Spring Harbor Laboratory Press: 99.

Wildwater, M., A. Campilho, J. M. Perez-Perez, R. Heidstra, I. Blilou, H. Korthout, J. Chatterjee, L. Mariconi, W. Gruissem and B. Scheres (2005). "The RETINOBLASTOMA-RELATED gene regulates stem cell maintenance in *Arabidopsis* roots." Cell 123(7): 1337-49.

Chapter 3: Histone 2B exchange in *Arabidopsis*.

Joost Willemse, Joan Wellink, and Ton Bisseling

Introduction

Nucleosomes consisting out of H3-H4 tetramers and two H2A-H2B dimers form the basic building block of chromatin in nuclei of eukaryotic cells (van Holde *et al.* 1992; Hamiche *et al.* 1999). The linker histone H1 can be present between the nucleosomes, and together with other proteins is involved in the formation of compact higher order structures of chromatin. Interphase nuclei contain microscopically recognizable less dense euchromatic and dense heterochromatic areas. In an interphase nucleus chromatin turns out to be highly dynamic, and studies on the mobility of histone proteins revealed that the various histones have very different dynamic properties (Vicent *et al.* 2004; Park *et al.* 2005; Wunsch and Jackson 2005) (Kimura and P.R. 2001). However, in none of these studies it was possible to directly distinguish between the behaviour of histones in heterochromatin and euchromatin. Here we exploit the simple architecture of nuclei of the model plant *Arabidopsis* to address this issue.

Histone dynamics has been studied in living stable HeLA cell lines expressing histone proteins fused to a fluorescent protein using fluorescence recovery after photobleaching (FRAP). In cell lines expressing core histon fusion proteins, these tagged molecules were shown to be incorporated into nucleosomes in concentrations up to 10% of that of the unmodified protein without deleterious effect on the viability of the cell (kimura and cook 2001).

These studies revealed that the H1 linker histone positioned outside the nucleosome core, is highly mobile compared to the core histone proteins (Lever *et al.* 2000; Mistelli *et al.* 2000) However whereas more than 80% of the core histones H3 and H4 remain bound permanently, about 50% of the H2B core histone were found to exhibit significant exchange (Kimura and P.R. 2001; Kimura 2005). About 3% of H2B exchanged within minutes, whereas about 40% did so more slowly independent from replication and transcription and with a $t_{1/2}$ of about 130 min. Based on experiments with transcription inhibitors it was proposed that the rapidly exchanging fraction represents the transcriptionally active fraction, while the more slowly exchanging fraction represents the surrounding euchromatin, and the permanently bound fraction the heterochromatin (Kimura and P.R. 2001). However, this has not been tested directly.

In *Arabidopsis*, heterochromatin is confined to the regions around the centromeres of its 5 chromosomes and its 2 nuclear organizers. In contrast the chromosome arms are euchromatic. In interphase nuclei the heterochromatic regions form so-called

chromocenters, that can be clearly distinguished from the euchromatic area. Usually 5-12 chromocenters are visible, as chromocenters have a tendency to cluster (Soppe *et al.* 2002; Fransz *et al.* 2003). (Fransz *et al.* 2003). This simple distribution of euchromatin and heterochromatin makes *Arabidopsis* an ideal organism to address the question whether mobility of histones is different in these two types of chromatin. Further *Arabidopsis* allows studies on living cells while they are part of the intact multicellular organisms. For example the root of *Arabidopsis* is only 100 μ m wide allowing studies on each cell by confocal microscopy. This is of importance as tissue culture conditions could affect chromatin properties.

The central domain of the *Arabidopsis* centromeric heterochromatin has an estimated size of about 0.4-2.9 Mb and consist out of a 180bp long repeat (PAL1) interspersed with *Athila* retrotransposons (106B) (Lippman *et al.* 2004). This is similar to the centromeric repeats in most eukaryotes. This central domain is devoid of (transcribed) genes and is flanked by pericentromeric regions of about 0.5-2 Mb containing many gypsy-class retrotransposons and a low gene density (1 in 100kb). About 200 of these genes are transcribed (Initiative 2000).

Since the heterochromatin is composed of 2 fundamentally different regions it would be attractive to separate these regions. For this we can make use of a *ddm1* mutant. DDM1 is a SWI/SNF-like chromatin remodeling protein. In contrast to animal *ddm1* mutants *Arabidopsis ddm1* knock out mutants are vital, but have a markedly reduced DNA methylation (Vongs *et al.* 1993). Further the pericentromeric heterochromatin obtains a condensation degree similar to euchromatin whereas the central domain repeats remain highly condensed (Mittelsten Scheid *et al.* 2002; Soppe *et al.* 2002). Therefore in nuclei of a *ddm1* mutant the chromocenters are reduced in size and consist only out of the centromeric repeats (Vongs *et al.* 1993; Soppe *et al.* 2002).

Here we report how we have made use of this mutant and FRAP to determine the mobility of H2B in euchromatic, centromeric and heterochromatic regions.

Results

Characterization of H2B:YFP transgenic lines

For our studies we used 2 *Arabidopsis* lines expressing a 35S::H2B:YFP transgene. One line was in accession C24 and was provided by Frederic Berger, the second line was created by transforming accession Columbia with a similar construct, which allowed us to

perform crosses with the *ddm1* mutant, which is in the same accession. A southern analyses of the lines show that they contain 1 insertion of the H2B:YFP construct (data not shown). Selfing of the C24 and Columbia transgenic lines resulted in a 2:1 segregation of YFP fluorescence as well as kanamycine resistance, suggesting that both lines can only be maintained as heterozygotes. This is confirmed by the absence of seeds in 1/4th of the available spaces in the siliques. To be able to distinguish between heterochromatic and centromeric H2B fractions we have crossed the H2B:YFP expressing line was crossed with the *ddm1* mutant.

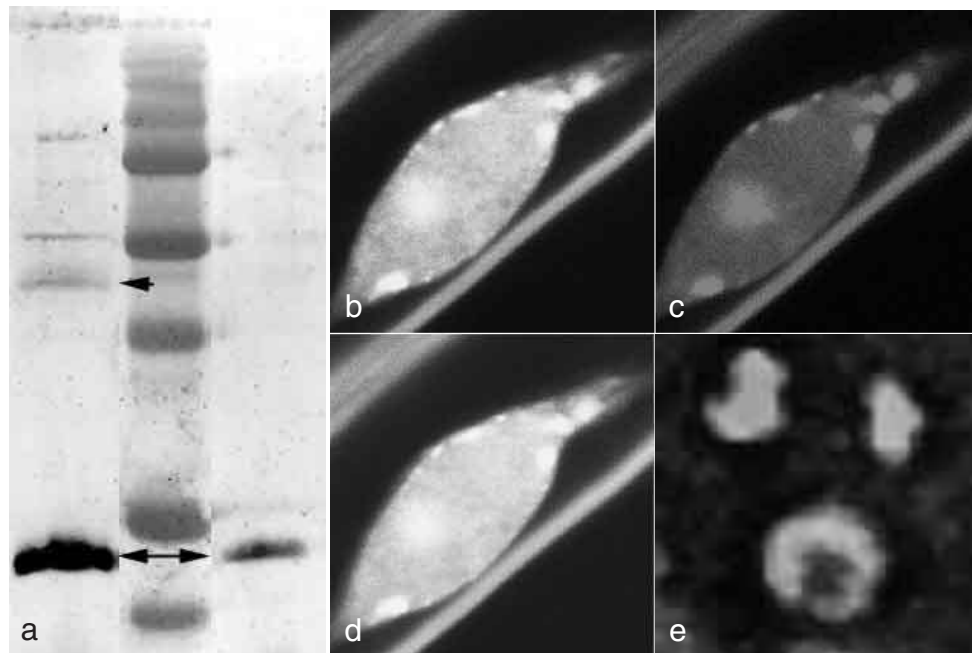


Figure 3- 1

a) Western blot of isolated nuclei from H2B-YFP expressing plants (lane 1), and columbia plants (lane 3), incubated with antibodies against aminoacid 111-125 of humanH2B. Lane 2 shows the size marker (Biorad 161-0310). Arrowheads indicate the position of H2B and the H2B-YFP fusion on the blot. b-e) Confocal sections of a *Arabidopsis* root hair cell. b) Shows the H2B::YFP distribution within the nucleus, c) shows the PI staining pattern and d) an overlay of b and c. e) H2B-YFP is associated with chromatin in interphase as well as anaphase as visualized by the H2B fluorescence co-localizing with the separating chromosomes.

To determine the fraction of H2B proteins present as H2B:YFP fusion protein a protein blot was made of nuclei isolated from leaves of both wt Columbia and transgenic plants. The blot was incubated with a H2B specific antibody and showed a single band at 14 kD (Figure 3- 1a) for the wild type nuclei of accession Columbia, which is at the expected size for H2B. In the sample from the transgenic line an additional band of 41 kD can be observed, which is at the expected position of the H2B:YFP fusion protein. A comparison of the intensities of the bands show that ~10% of the total H2B population is fused to YFP. Within the nuclei regions with higher concentrations of fusion proteins were observed (Figure 3- 1b). Counterstaining nuclei with propidium iodide showed that these regions corresponded to the heterochromatic chromocentres ((Boisnard-Lorig *et al.* 2001), Figure 3- 1c). During cell division, fluorescence exclusively colocalized with the chromosomes, indicating that the majority of the fusion protein remains a part of chromatin throughout the entire cell cycle (Figure 3- 1e). Therefore we conclude that the behaviour of the fluorescent H2B proteins is similar to the native H2B proteins.

The mobility studies were performed on root nuclei, therefore we also tested whether root development was affected. In the transgenic lines in Columbia and C24, neither root hair positioning, nor root tip patterning or growth speed were affected. The obtained H2B:YFP *ddm1* lines showed the *ddm1* phenotype (late flowering, small leaves and reduced fertility (Kakutani *et al.* 1996) as well as H2B:YFP fluorescence, and allowed us to determine the mobility of H2B in the centromeric chromatin.

Relative chromatin fraction measurements of trichoblasts, using the method described by (Soppe *et al.* 2002), in both transgenic lines show that H2B:YFP expression did not have an effect on heterochromatin content (Table 3- 1). Additionally flow cytometry analysis revealed no repartition of cell cycle phases in plants expressing H2B:YFP (Boisnard-Lorig *et al.* 2001), leading us to the conclusion that the H2B expression has no effect on plant development.

H2B Mobility

Plant line	Heterochromatin percentage
H2B-YFP line	16% \pm 6% (n=10)
Columbia Wt	14% \pm 6% (n=11)
H2B-YFP ddm1	9% \pm 3% (n=10)
ddm1	10% \pm 1% ¹

Table 3- 1 : Heterochromatin fractions

No significant difference is observed in heterochromatin content between Wt nuclei and nuclei of the transgenic line expressing H2B-YFP.

¹ as determined by (Soppe *et al.* 2002)

	T _{1/2} (s/ μm^2) in euchromatin	T _{1/2} (s/ μm^2) in heterochromatin
Trichoblasts	80.0 \pm 5.1 (n=16)	421 \pm 76 (n=2)
Atrichoblasts	79.7 \pm 3.6 (n=21)	409 \pm 22 (n=10)

Table 3- 2 : H2B mobility in epidermal cell types

No significant difference can be observed between the recovery times of H2B in trichoblasts and atrichoblasts.

FRAP analyses of H2B in Arabidopsis thaliana.

Initially, FRAP experiments were performed on both root epidermal cell types, trichoblasts and atrichoblasts. Measurements were performed on H2B localized in euchromatin (80.0 \pm 5.1s and 79.7 \pm 3.6s respectively) as well as heterochromatin (421 \pm 76s and 409 \pm 22s respectively). Since no differences in mobility were observed between these two cell types (Table 3- 2), and also between the C24 and the Columbia (data not shown), the data of both ecotypes and both cell types were combined and no further distinction between cell types or ecotypes will be made.

FRAP experiments were done by bleaching $0.81 \mu\text{m}^2$ and monitoring the fluorescence recovery for approximately 30 minutes. Curves were fit with a single exponential and a double exponential recovery formula and the best fits were used in the final analysis. In our experiments all curves fitted best with a single exponential curve. For wt euchromatic regions (n=39) the observed half time per square micron was 79.9 seconds. The diffusion coefficient, for H2B:YFP, that can be calculated from these values is $7.8 \cdot 10^{-4} \mu\text{m}^2/\text{s}$ (Table 3- 3). The immobile fraction was on average 49%. In the ddm1 mutant the immobile fraction in euchromatin remained the same as in wt, while the half time of recovery decreased from 79.9 s/ μm^2 to 47.3 s/ μm^2 (Table 3- 3).

Protein	<i>H2B-YFP plants</i>		
	$T_{1/2}/\mu\text{m}^2$ in s	D in $\mu\text{m}^2/\text{s}$ (n)	Immobile fraction (n)
Histone 2B (euchromatin)	79.9 ± 3.3	$7.8 \cdot 10^{-4} \pm 0.4 \cdot 10^{-4}$ (39)	$49 \pm 3\%$ (50)
Histone 2B (heterochromatin)	411 ± 22	$1.6 \cdot 10^{-4} \pm 0.1 \cdot 10^{-4}$ (13)	$36 \pm 6\%$ (14)
G/YFP	0.014 ± 0.004	5.9 ± 1.9 (4)	$7.1 \pm 6.2\%$ (4)
	<i>H2B-YFP ddm1 plants</i>		
	$T_{1/2}/\mu\text{m}^2$ in s	D in $\mu\text{m}^2/\text{s}$ (n)	Immobile fraction (n)
Histone 2B (euchromatin)	47.3 ± 8.5	$15.9 \cdot 10^{-4} \pm 3 \cdot 10^{-4}$ (6)	42 ± 7 (10)
Histone 2B (heterochromatin)	38.8 ± 6.7	$19.7 \cdot 10^{-4} \pm 2 \cdot 10^{-4}$ (8)	72 ± 2 (10) 95 ± 3 (10) ¹

Table 3- 3 : FRAP measurements of H2B-YFP

results of mobility measurements in H2B-YFP plants, and H2B-YFP ddm1 plants respectively. From the half times ($T_{1/2}$) in column 2 the diffusion constant (D) in column 3 is calculated. The final column shows the percentage of fluorescent protein that was displaced during the measurement. N is the number of measurements used to calculate the different values and their standard error. For ¹ the measured area is set to $0.3 \mu\text{m}^2$.

FRAP experiments (n=13) on wt heterochromatic chromocentres resulted in a half time of recovery of H2B:YFP fluorescence of 411 seconds, which gives a diffusion coefficient of $1.6 \cdot 10^{-4} \mu\text{m}^2/\text{s}$, which is about 5 times slower than the diffusion constant observed in wt euchromatin (Table 3- 3). The immobile fraction was on average 36%. Due to the smaller chromocentre size in the ddm1 mutant the bleached area, which was set at $0.81 \mu\text{m}^2$ as in previous experiments, will also contain parts of the chromatin surrounding the centromeric sequences. To determine the mobile fraction inside the centromere itself the recovery of H2B:YFP fluorescence was measured in a smaller region selected inside the bleached area. This revealed that 95% of the H2B:YFP fraction in the centromere of the ddm1 mutant is immobile in the timescale of this experiment (30 min). Consequently the mobility of H2B:YFP that has been measured in the entire bleach area containing the heterochromatic chromocenters of the ddm1 mutant has to be attributed to H2B:YFP present in the surrounding pericentromeric and euchromatic regions. The observed half time of recovery in the region surrounding the centromeres is similar to the rest of the euchromatin in the nucleus (47 and 39 $\text{s}/\mu\text{m}^2$, Table 3- 3).

Discussion

In both wt and the ddm1 mutant the heterochromatic sequences appear, in the majority of the nuclei, as distinct spots which allowed the analysis of mobility of H2B in euchromatic, heterochromatic, and centromeric regions. We have measured the mobility of H2B on a time scale of about half an hour in living plant root cells and found three distinguishable fractions of H2B; a euchromatic mobile fraction, a less mobile heterochromatic fraction and an immobile fraction.

Euchromatic mobile fraction

Euchromatic mobility measurements revealed the presence of only a single exponential recovering H2B population, indicating that the mobility of a putative second population would differ less than fivefold from the detected population. In wt plants the diffusion coefficient of mobile euchromatic H2B is $7.8 \cdot 10^{-4} \pm 0.4 \cdot 10^{-4} \mu\text{m}^2/\text{s}$, which is calculated from a half time of $79.9 \pm 3.3 \text{ s}/\mu\text{m}^2$, and is comparable to the most mobile fraction with a half time of recovery of $80.5 \text{ s}/\mu\text{m}^2$ found in HeLa cells (Kimura 2001). The fitting of the recovery curve reveals the dissociation constant (k_{off}) is $8.6 \cdot 10^{-3}$, and this can be

recalculated to a residence time of 116 seconds. Transcription probably contributes to this exchange of H2B by two means. Active RNA polII complexes are known to translocate nucleosomes along the DNA strand. Additionally when a RNA polymerase complex passes a nucleosome a H2A/H2B dimer is displaced from that nucleosome (Kireeva 2002).

Heterochromatic mobile fraction

A second population of histones consists of slower moving H2B in the heterochromatin. To our surprise the H2B proteins here are still quite mobile, with a half time of recovery of ~400 s, which is fivefold slower compared to the euchromatic mobile fraction. This is recalculated to a residence time of 10 minutes. For *Arabidopsis* it has recently been shown that a substantial part of the (peri)centromeric regions are still transcribed (Yamada *et al.* 2003; Hall *et al.* 2006), which will very probably contribute to the observed movement of H2B in the heterochromatin. The lower mobility of H2B in heterochromatin might be explained by the higher packaging ratio of the DNA and the nucleosomes, resulting in less active RNA polymerases per transcription unit, or a lower speed of transcription compared to gene rich euchromatic regions (Workman and Kingston 1998).

To determine how much transcription contributed to H2B mobility roots were treated with RNA polII inhibitors α -amanitin or actinomycin D. This indeed caused a marked (2 fold) reduction in H2B mobility in the euchromatin (data not shown). Since at the same time we observed a marked increase (7 fold) in mobility of H2B in heterochromatin, which we cannot explain at the moment, as well as the concern expressed by some authors about the actual relevance of *in vivo* experiments in the presence of these inhibitors we did not pursue this approach any further (Kimura 2001).

Immobile fraction

By using the ddm1xH2B:YFP line, we have shown that H2B present in the nucleosomes at the centromeric repeat sequence is completely immobile over a time period of at least an hour (Immobile fraction of 95%). This shows that *Arabidopsis* centromeric chromatin is rarely transcribed and complies with the original static idea of heterochromatin.

A highly variable immobile fraction is observed in euchromatin, 49% with a standard deviation of 21%. This immobile fraction probably represents regions within the euchromatin that are not transcribed. The variation in the amount of immobile fraction between the different measurements could be explained by a non-random distribution of

actively transcribed genes in the nucleus. Other processes are expected to be distributed more equal over the nucleus and therefore should not contribute to the observed variation. The immobile fraction in the euchromatin is only immobile at the timescale used for these experiments and by measuring for a longer time it may be possible to determine the presence of another population of histones with a much slower mobility.

The $36 \pm 22\%$ immobile fraction observed in the heterochromatin of wt plants is not significantly different from the immobile fraction observed in the euchromatin.

Ddm1 mobile fraction(s)

The *ddm1*xH2B:YFP cross allowed us to measure the H2B:YFP mobility in a changed nuclear environment. The mobility of H2b:YFP in the euchromatin and in the pericentromeric heterochromatin of the *ddm1* mutant is increased by a factor 2 reducing the residence time of H2B in nucleosomes to 70s, whereas the immobile fraction slightly decreased compared to wt H2B:YFP expressing plants. Both observations could be explained by the assumption that transcription contributes to H2B mobility. In the *ddm1* mutant, due to a decrease in DNA methylation, several genes that are silent in wt are transcribed which could explain the slight decrease in the immobile fraction (Vielle-Calzada *et al.* 1999). The increase in exchange rate of H2B can be explained, by an increase in the amount of RNA polymerases active at each transcription unit and/or by an increase in the transcription speed of RNA polII due to the decrease in DNA methylation.

Materials and methods

Plant lines

The transgenic H2B-YFP C24 plant line was a gift from Frederique Berger. This line was already tested for viability and no phenotype due to possible over expression of the fusion protein was observed (Boisnard-Lorig *et al.* 2001). The H2B:YFP Columbia plant line was constructed as follows. A PCR was performed on *Arabidopsis* ecotype Columbia with specific primers constructed for the H2B sequence that is in the GenBank database under accession number Y07745. The obtained H2B gene was fused at the C terminus to YFP, and expressed under the control of the cauliflower mosaic virus (CaMV) 35S promoter. The fusion protein is 43.3 kD and has a 7 amino acids linker. Transformation of *Arabidopsis* ecotype Columbia was performed according to (Clough and Bent 1998). Crossing the *ddm1.2* mutant with the H2B:YFP expressing line resulted in a H2B expressing plant with

the ddm1 phenotype, 4th generation plants of this line were used for the FRAP experiments. The plants were genotyped by examining size differences of PCR fragments (Bartee and Bender 2001).

Microscopy

Transgenic *Arabidopsis* roots were cut from the plant and put on a slide with water. The cover slips were glued to the slides with nail polish. Half of the experiments were done on a LSM 510 confocal microscope using a 40x plan neofluor, 1.3 NA lens with a 20x digital zoom. On the LSM 510, FRAP was done with the 25 mW Ar laser with 25% power output and 1% intensity. Photobleaching was performed by scanning 2 to 10 times using 50 to 75% laser intensity. The other experiments were performed on a Biorad confocal microscope using a 60x 1.3 NA lens with a 10x digital zoom. The imaging was done with 2-5% laser intensity and bleaching with 10% laser intensity. Histone 2b fluorescent fusion protein was observed each 5 seconds for a hundred images in euchromatin and each 20 seconds for 100-200 images in heterochromatin.

To measure centromeric mobility of H2B in the ddm1 line a spot size of $0.30 \mu\text{m}^2$ was used, whereas in the measurements in euchromatin and wt heterochromatin the spot size was $0.81 \mu\text{m}^2$. Using smaller spots results in a noisier signal, however the diffusion constant is not affected (Starr and Thompson 2002), data not shown. The confocal pinhole determines the thickness of the slice, which in this study was set to $1 \mu\text{m}$. In Wt most heterochromatic spots are bigger than $1 \mu\text{m}$ in diameter and euchromatic H2B will not interfere in these measurements. However in the ddm1 mutant in which the size of the chromocentres is decreased these optical sections will contain euchromatic, pericentromeric and centromeric localized proteins.

The intensity values observed were corrected for background intensity ($I_{\text{roi cl}} = I_{\text{roi}} - I_{\text{background}}$), scanning bleach ($I_{\text{roi c2}} = I_{\text{roi cl}} / (I_{\text{total nucleus}} / I_{\text{total nucleus just after bleach}})$), and the decrease in total fluorescence by the bleach pulse. Curves were analyzed with Slide Write plus for windows, version 5.01 (32-bit edition) or KaleidaGraph, version 3.5b5. The formula the corrected data was fitted to is shown below.

$$I_{\text{roi c2}} = I_{\text{afterbleach}} + (I_{\text{after recovery}} - I_{\text{afterbleach}})(1 - e^{-(kt)}) \quad (\text{Salmon } et al. 1984)$$

From the obtained k value the half time of recovery can be calculated.

$$T_{1/2} = \ln(2)/k \quad (\text{Salmon } et al. 1984)$$

And with the aid of this $T_{1/2}$ the diffusion coefficient can be calculated. In which ω represents the diameter of the bleached region.

$$D = \omega^2 / 4 * T_{1/2} \quad (\text{Salmon } et al. 1984)$$

Several criteria are used to determine whether the obtained data can be used for the calculation of a diffusion coefficient. First, the bleach pulse was not allowed to bleach more than 25% of the total intensity of the nucleus. Second, the bleaching during the scanning phase should not be above 25%. Third the reliability of the curve fitting should be at least 75%. Finally the bleaching pulse should bleach at least 15% of the original intensity on the bleached spot to be used for calculation. For the mobile and immobile fraction determination the measurements in which no recovery is observed were discarded. Measurements that showing more than 100% recovery after fitting are assumed to have no immobile population. The calculation of immobile fractions was done after fitting. The immobile fractions observed in this way are highly variable, and no clear differences between experiments can be detected.

Western Blots

Nuclei were isolated from leaves of transgenic H2b lines. The proteins were isolated according to (Liu and Whittier 1994), after which 1/5th volume of protein sample buffer (PSB, 50% glycerol, 10% SDS, 50 mM Tris-HCL pH 6.8, 0.05% Brome Phenol Blue) was added and the sample was boiled for 5 minutes. A 15% polyacrylamide protein gel was electroblotted overnight and incubated with primary antibody for one hour after blocking with TBST (TRIS buffered saline with Tween) containing 5% skim milk. The blot was washed three times with TBST before incubating with the secondary antibody. After the second incubation the blot is washed twice with TBST, once with TBS, and once with AP buffer. The coloring reaction is done in AP buffer with NBT and BCIP solution. The H2B antibody was obtained from Abcam and was raised against a peptide consisting of amino acids 111-125 of human H2B (AB1790), which is highly conserved between mammals and plants.

Acknowledgements

We thank Frederic Berg r for the kind donation of his H2B-YFP transgenic plants in accession C24 and Jeroen Strating for the creation of such a fusion in the Columbia accession.

References

- Bartee, L. and J. Bender** (2001). "Two Arabidopsis methylation-deficiency mutations confer only partial effects on a methylated endogenous gene family." Nucleic Acids Res **29**(10): 2127-34.
- Boisnard-Lorig, C., A. Colon-Cammona, M. Bauch, S. Hodge, P. Doerner, E. Banchard, C. Dumas, J. Haseloff and F. Berger** (2001). "Dynamic analyses of the expression of the HISTONE:YFP fusion protein in arabidopsis show that syncytial endosperm is divided in mitotic domains." Plant Cell **13**(3): 495-509.
- Clough, S. J. and A. F. Bent** (1998). "Floral dip: a simplified method for Agrobacterium-mediated transformation of Arabidopsis thaliana." Plant J **16**(6): 735-43.
- Fransz, P., W. Soppe and I. Schubert** (2003). "Heterochromatin in interphase nuclei of Arabidopsis thaliana." Chromosome Res **11**(3): 227-40.
- Hall, A. E., G. C. Kettler and D. Preuss** (2006). "Dynamic evolution at pericentromeres." Genome Res **16**(3): 355-64.
- Hamiche, A., R. Sandaltzopoulos, D. A. Gdula and C. Wu** (1999). "ATP-dependent histone octamer sliding mediated by the chromatin remodeling complex NURF." Cell **97**(7): 833-42.
- Initiative, T. A. G.** (2000). "Analysis of the genome sequence of the flowering plant Arabidopsis thaliana." Nature **408**(6814): 796-815.
- Kakutani, T., J. A. Jeddeloh, S. K. Flowers, K. Munakata and E. J. Richards** (1996). "Developmental abnormalities and epimutations associated with DNA hypomethylation mutations." Proc Natl Acad Sci U S A **93**(22): 12406-11.
- Kimura, H.** (2005). "Histone dynamics in living cells revealed by photobleaching." DNA Repair (Amst) **4**(8): 939-50.
- Kimura, H. and C. P.R.** (2001). "kinetics of core histones in living human cells: little exchange of h3 and h4 and some rapid exchange of h2b." the journal of cell biology **153**(7): 1341-1353.
- Kireeva, L., Walter W., Tchernajenko V., Bondarenko V., Kashlev M. and S. V.M.** (2002). "Nucleosome Remodeling Induced by RNA Polymerase II: Loss of the H2A/H2B Dimer during Transcription." Molecular Cell **9**: 541-552.
- Lever, A. M., Th'ng J.P.H., Sun X. and H. M.J.** (2000). "Rapid exchange of histone H1.1 on chromatin in living human cells." Nature **408**(14-december 2000): 873-876.
- Lippman, Z., A. V. Gendrel, M. Black, M. W. Vaughn, N. Dedhia, W. R. McCombie, K. Lavine, V. Mittal, B. May, K. D. Kasschau, J. C. Carrington, R. W. Doerge, V. Colot and R. Martienssen** (2004). "Role of transposable elements in heterochromatin and epigenetic control." Nature **430**(6998): 471-6.
- Liu, Y. G. and R. F. Whittier** (1994). "Rapid preparation of megabase plant DNA from nuclei in agarose plugs and microbeads." Nucleic Acids Res **22**(11): 2168-9.

- Mistelli, T., G. A., B. M. and B. D.T.** (2000). "Dynamic binding of histone H1 to chromatin in living cells." Nature **408**(14 december 2000): 877-881.
- Mittelsten Scheid, O., A. V. Probst, K. Afsar and J. Paszkowski** (2002). "Two regulatory levels of transcriptional gene silencing in Arabidopsis." Proc Natl Acad Sci U S A **99**(21): 13659-62.
- Park, Y. J., J. V. Chodaparambil, Y. Bao, S. J. McBryant and K. Luger** (2005). "Nucleosome assembly protein 1 exchanges histone H2A-H2B dimers and assists nucleosome sliding." J Biol Chem **280**(3): 1817-25.
- Salmon, E. D., W. M. Saxton, R. J. Leslie, M. L. Karow and J. R. McIntosh** (1984). "Diffusion coefficient of fluorescein-labeled tubulin in the cytoplasm of embryonic cells of a sea urchin: video image analysis of fluorescence redistribution after photobleaching." J Cell Biol **99**(6): 2157-64.
- Soppe, W. J., Z. Jasencakova, A. Houben, T. Kakutani, A. Meister, M. S. Huang, S. E. Jacobsen, I. Schubert and P. F. Fransz** (2002). "DNA methylation controls histone H3 lysine 9 methylation and heterochromatin assembly in Arabidopsis." Embo J **21**(23): 6549-59.
- Starr, T. E. and N. L. Thompson** (2002). "Fluorescence pattern photobleaching recovery for samples with multi-component diffusion." Biophys Chem **97**(1): 29-44.
- van Holde, K. E., D. E. Lohr and C. Robert** (1992). "What happens to nucleosomes during transcription?" J Biol Chem **267**(5): 2837-40.
- Vicent, G. P., A. S. Nacht, C. L. Smith, C. L. Peterson, S. Dimitrov and M. Beato** (2004). "DNA instructed displacement of histones H2A and H2B at an inducible promoter." Mol Cell **16**(3): 439-52.
- Vielle-Calzada, J. P., J. Thomas, C. Spillane, A. Coluccio, M. A. Hoeppner and U. Grossniklaus** (1999). "Maintenance of genomic imprinting at the Arabidopsis *medea* locus requires zygotic DDM1 activity." Genes Dev **13**(22): 2971-82.
- Vongs, A., T. Kakutani, R. A. Martienssen and E. J. Richards** (1993). "Arabidopsis thaliana DNA methylation mutants." Science **260**(5116): 1926-8.
- Workman, J. L. and R. E. Kingston** (1998). "Alteration of nucleosome structure as a mechanism of transcriptional regulation." Annu Rev Biochem **67**: 545-79.
- Wunsch, A. and V. Jackson** (2005). "Histone release during transcription: acetylation stabilizes the interaction of the H2A-H2B dimer with the H3-H4 tetramer in nucleosomes that are on highly positively coiled DNA." Biochemistry **44**(49): 16351-64.
- Yamada, K., J. Lim, J. M. Dale, H. Chen, P. Shinn, C. J. Palm, A. M. Southwick, H. C. Wu, C. Kim, M. Nguyen, P. Pham, R. Cheuk, G. Karlin-Newmann, S. X. Liu, B. Lam, H. Sakano, T. Wu, G. Yu, M. Miranda, H. L. Quach, M. Tripp, C. H. Chang, J. M. Lee, M. Toriumi, M. M. Chan, C. C. Tang, C. S. Onodera, J. M. Deng, K. Akiyama, Y. Ansari, T. Arakawa, J. Banh, F. Banno, L. Bowser, S. Brooks, P. Carninci, Q. Chao, N. Choy, A. Enju, A. D. Goldsmith, M. Gurjal, N. F. Hansen, Y. Hayashizaki, C. Johnson-Hopson, V. W. Hsuan, K. Iida, M. Karnes, S. Khan, E. Koesema, J. Ishida, P. X. Jiang, T. Jones, J. Kawai, A. Kamiya, C. Meyers, M.**

Nakajima, M. Narusaka, M. Seki, T. Sakurai, M. Satou, R. Tamse, M. Vaysberg, E. K. Wallender, C. Wong, Y. Yamamura, S. Yuan, K. Shinozaki, R. W. Davis, A. Theologis and J. R. Ecker (2003). "Empirical analysis of transcriptional activity in the Arabidopsis genome." Science **302**(5646): 842-6.

Chapter 4: AtLHP1 forms chromatin complexes at trimethylated histones

Maëlle Lorvellec, Joost Willemsse, Olga Kulikova, Jan Verver, and Ton Bisseling

Introduction

Structural and functional changes in the organization and dynamics of the chromatin state are keys to control genome function and are performed by chromatin regulators like chromodomain proteins. The chromodomain proteins are non-histone chromosomal proteins and include Polycomb group and HP1 proteins.

Heterochromatin Protein 1 (HP1), was discovered as a protein associated with heterochromatin in *Drosophila melanogaster* (James and Elgin 1986). Since its discovery, several homologues of HP1 have been identified, from fission yeast (Swi6) to human, showing that HP1 is a highly conserved protein, and several isoforms were discovered as well, each with its own subnuclear location: in heterochromatin and/or in euchromatin. HP1 proteins possess three distinct domains: an amino-terminal chromodomain (CD) a more flexible intervening region (the hinge region) and a specific carboxyl-terminal chromoshadow domain (CSD). The CD was shown in several systems (fission yeast (Nakayama et al. 2000), *Drosophila* (Bannister et al. 2001; Jacobs and Khorasani-zadeh 2002), mammals (Aagaard et al. 1999; Rea et al. 2000)) to bind to methylated histone 3 Lysine 9 (H3K9) and with a highest affinity for trimethylated H3K9 (Fischle et al. 2005). The hinge region would be involved in binding of RNA, DNA and chromatin, and the CSD in protein-protein interaction. Currently HP1 is thought to serve as a bridging protein, connecting histones and non histone chromosomal proteins (Li et al. 2002). In animals and yeast, HP1 was shown to be involved in chromatin structural organization, maintenance of heterochromatin and gene regulation (Hiragami and Festenstein 2005; Hediger and Gasser 2006).

In *Arabidopsis thaliana*, a unique homologue of HP1 was discovered named Like Heterochromatin Protein 1 (Gaudin et al. 2001). Like HP1, AtLHP1 contains a CD, a hinge region and a CSD (Gaudin et al. 2001). AtLHP1 was shown to be located in the euchromatin and to be present in many foci (Kotake et al. 2003; Libault et al. 2005; Nakahigashi et al. 2005). However, whether these foci represent functional chromatin-complexes is unclear as these foci could also be artificial aggregates of transgenic AtLHP1-GFP proteins (Waldo et al. 1999) or interchromatin nuclear bodies like nucleoli, or Cajal bodies (Shaw and Brown 2004). In case AtLHP1 is part of a chromatin complex it most likely interacts with a specific histone modification as has been described for animal/yeast. Therefore we tested whether AtLHP1 is in close vicinity of histone/DNA. In fission yeast,

AtLHP1 was shown to complement the *swi6-* mutant of the HP1 yeast homolog (Kotake et al. 2003) suggesting that AtLHP1 can bind (tri)methylated H3K9 in yeast.

AtLHP1 has been described as having a diffuse pattern in dividing meristematic cells and a speckled-like pattern (foci) in differentiated cells of *Arabidopsis* roots. These foci are located in the euchromatic area of the *Arabidopsis* nuclei (Libault et al. 2005). *Arabidopsis* interphase nuclei have a simple organization with only 10 to 12 heterochromatic chromocenters and so the AtLHP1 foci can easily be distinguished from heterochromatic chromocenters (see figure 2). The region with differentiated cells can be easily identified in roots and all nuclei within a whole mount preparation can be analyzed by CLSM. For these reasons we used the differentiated zone of *Arabidopsis*' roots to study whether AtLHP1 foci represent chromatin complexes.

We showed that like HP1 in animals, AtLHP1 binds to chromatin and that its chromo domain is involved in this binding through its interaction with H3K9m3. AtLHP1 partially colocalizes with H3K9m3 as observed in animals as well as H3K27m3. Furthermore AtLHP1 seems to form chromatin complexes with similar dynamics as its animal counterpart. It is a highly dynamic protein with a slightly slower mobility in the intrafoci region compared to the interfoci region. Our study points to a similar role for AtLHP1 as the animal euchromatic HP1 variants, possibly in gene regulation (Hiragami and Festenstein 2005; Hediger and Gasser 2006).

Results

Subnuclear localization of AtLHP1

Several studies have shown that in *Arabidopsis* nuclei AtLHP1 is localized in euchromatic area and is present in many foci (Kotake et al. 2003; Libault et al. 2005; Nakahigashi et al. 2005). Whether these foci represent functional chromatin complexes, or for example interchromatin nuclear bodies (Shaw and Brown 2004) or even artifacts is unclear. To address this question, AtLHP1-GFP fusion constructs driven by its own promoter (pLHP1::LHP1-GFP) or by the ubiquitously expressed 35S promoter (35S::LHP1-GFP), respectively, were introduced into *lhp1* mutants. These are *Arabidopsis lhp1* knockout mutants, which show pleiotropic phenotypes such as early flowering and reduced growth (Kotake et al. 2003). In case of pLHP1::LHP1-GFP, stable transformants were obtained and these have a restored wild-type phenotype, showing that the fusion protein is biologically active. Despite numerous attempts, no transformants expressing 35S::LHP1-GFP were

obtained. Therefore to obtain 35S::LHP1-GFP expressing plant material, we used the *Agrobacterium rhizogenes* hairy root transformation system on wild-type (accession Columbia) roots. *A. rhizogenes* can generate many transformed roots on one seedling within 8 to 10 days, making this transformation system a fast method to generate genetically transformed roots. (Limpens et al. 2004)

The fluorescence intensity of AtLHP1-GFP in plants expressing pLHP1::LHP1-GFP confirmed that AtLHP1 is higher expressed in the root meristem than in the differentiated zone of the root (Kotake et al. 2003). Furthermore, two different subnuclear localization patterns of AtLHP1-GFP were observed depending on the differentiation state of the cell. In the root meristem, AtLHP1 shows a diffuse distribution throughout the nucleus with sometimes 1 or 2 foci with a diameter of about 0.4 μm and is excluded from the nucleolus (Figure 1.a). In the differentiated zone of the root, AtLHP1 formed numerous foci ($\sim 0.4 \mu\text{m}$) and was also present in a diffuse manner in the interfoci region albeit at a lower level (Figure 1.b). It was absent from the nucleolus.

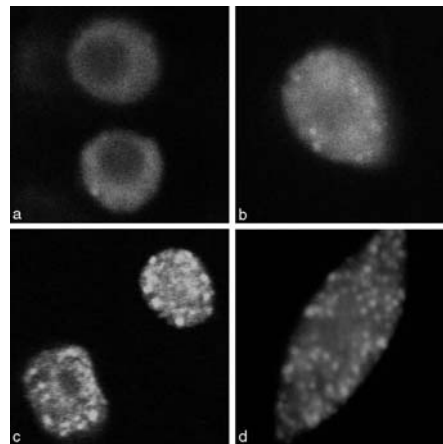


Figure 4- 1

Subnuclear localisation of AtLHP1-GFP in *Arabidopsis* roots. a, b. Roots expressing pLHP1::LHP1-GFP. c, d. Roots expressing 35S::LHP1-GFP. a, c. Meristematic nuclei. b, d. Differentiated nuclei.

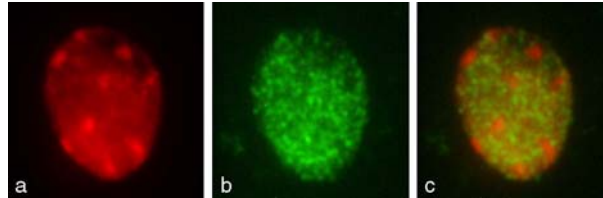


Figure 4- 2

Immunodetection of AtLHP1-GFP in interphase nucleus of *Arabidopsis* plants expressing plhp1::LHP1-eGFP. a. Propidium Iodide staining of the DNA. b. Immunodetection of AtLHP1-GFP with GFP antibody. c. Merged picture of a and b.

In 35S::LHP1-GFP roots, AtLHP1-GFP was present in all nuclei of the root (including meristem) forming numerous foci of about 0.4 μm and show as well a diffuse distribution in the interfoci region (Figure 4- 1. c+d) (Kotake et al. 2003). So ectopic and higher expression with the 35S promoter causes an increase in foci formation.

To investigate if AtLHP1 was associated with heterochromatin, AtLHP1-GFP was detected with rabbit anti-GFP polyclonal antibody (Molecular Probes) and the DNA was stained with propidium iodide in roots expressing pLHP1::LHP1-GFP. In Figure 4- 2, the merged picture (Figure 4- 2.c) clearly shows that AtLHP1-GFP (green signal) is excluded from the chromocenters (bright red spots) and localizes nearly exclusively in the euchromatic regions (Figure 4- 2) as observed by Libault and Nakahigashi (Libault et al. 2005; Nakahigashi et al. 2005). This is the case in meristematic as well as differentiated cells. Similar results were obtained for 35S::LHP1-GFP expressing roots.

LHP1 is present in chromatin complexes

In case the AtLHP1 foci represent chromatin complexes AtLHP1 molecules will be in close vicinity to DNA, especially when they interact with a specific histone modification. In contrast, when they are present in interchromatin nuclear bodies or are artifacts, AtLHP1 proteins will not be in such close vicinity to DNA. FRET (Förster Resonance Energy Transfer) microscopy is a sensitive method to test whether molecules are in close vicinity. FRET is a non-radiative, dipole-dipole coupling process, whereby energy from an excited donor fluorophore is transferred to an acceptor fluorophore (Förster, 1948). FRET causes a decrease of fluorescence intensity as well as the fluorescence lifetime of the donor. Therefore both can be used to quantify the efficiency of FRET. FRET is highly dependent

on the distance between donor and acceptor and in general it is only detectable when this distance is $< 10\text{nm}$. FRET has been successfully used to study interactions of chromatin proteins and DNA. For example, HP1 α and HP1 β were shown by FRET to be in close vicinity to DNA in Hela cells. (Cremazy et al. 2005)

To determine whether FRET occurs between AtLHP1-GFP and DNA in *Arabidopsis* nuclei we made use of the method developed by Cremazy *et al.* (Cremazy et al. 2005), they showed that DNA can efficiently be stained with Sytox orange and this fluorescent dye can be used as acceptor fluorophore in FRET experiments when GFP is used as the donor fluorophore.

As described above, AtLHP1 is not present at an equal concentration throughout the nucleus. Therefore we used Fluorescence Lifetime IMaging (FLIM) to quantify FRET efficiency, as fluorescence lifetime of the fluorophore is independent of its concentration, whereas fluorescence intensity is not. When FRET occurs, the fluorescence lifetime of the donor decreases, because energy transfer to the acceptor provides an additional decay pathway for the donor. The fluorescence lifetime was measured by using two-photon excitation Time Correlated Single Photon Counting (TCSPC) instrumentation to obtain a detailed FLIM image with voxel specific lifetime values.

The staining of DNA with Sytox orange requires that cells are first fixed. However, due to this fixation procedure, the fluorescence intensity of GFP is reduced. Therefore, *Arabidopsis* roots transformed with 35S::LHP1-GFP were studied as they have a higher expression level and numerous foci containing AtLHP1-GFP are formed. 35S::GFP expressing plants were used as a control to determine the fluorescence lifetime of GFP in the absence of FRET.

The fluorescence lifetime of GFP and AtLHP1-GFP, respectively, were measured in root nuclei in the absence of Sytox Orange to test whether AtLHP1 affects the fluorescence lifetime of GFP. Since DNA can only be stained by Sytox orange in fixed cells, we tested as well whether the fixation procedure (see materials and methods) affected the fluorescence lifetime of GFP. The fluorescence lifetime of each voxel is quantified and the average fluorescence lifetime is similar in all cases. In fixed roots, the average fluorescence lifetime of AtLHP1-GFP and GFP are 2.20 ± 0.06 and 2.32 ± 0.05 nanoseconds (ns) (voxels of 10 nuclei) respectively, which is similar to values reported for GFP fusion proteins in Hela Cells (Cremazy et al. 2005). Lifetime values are represented by pseudocolors for each voxel of the FLIM images. Lifetime values of GFP in the absence of

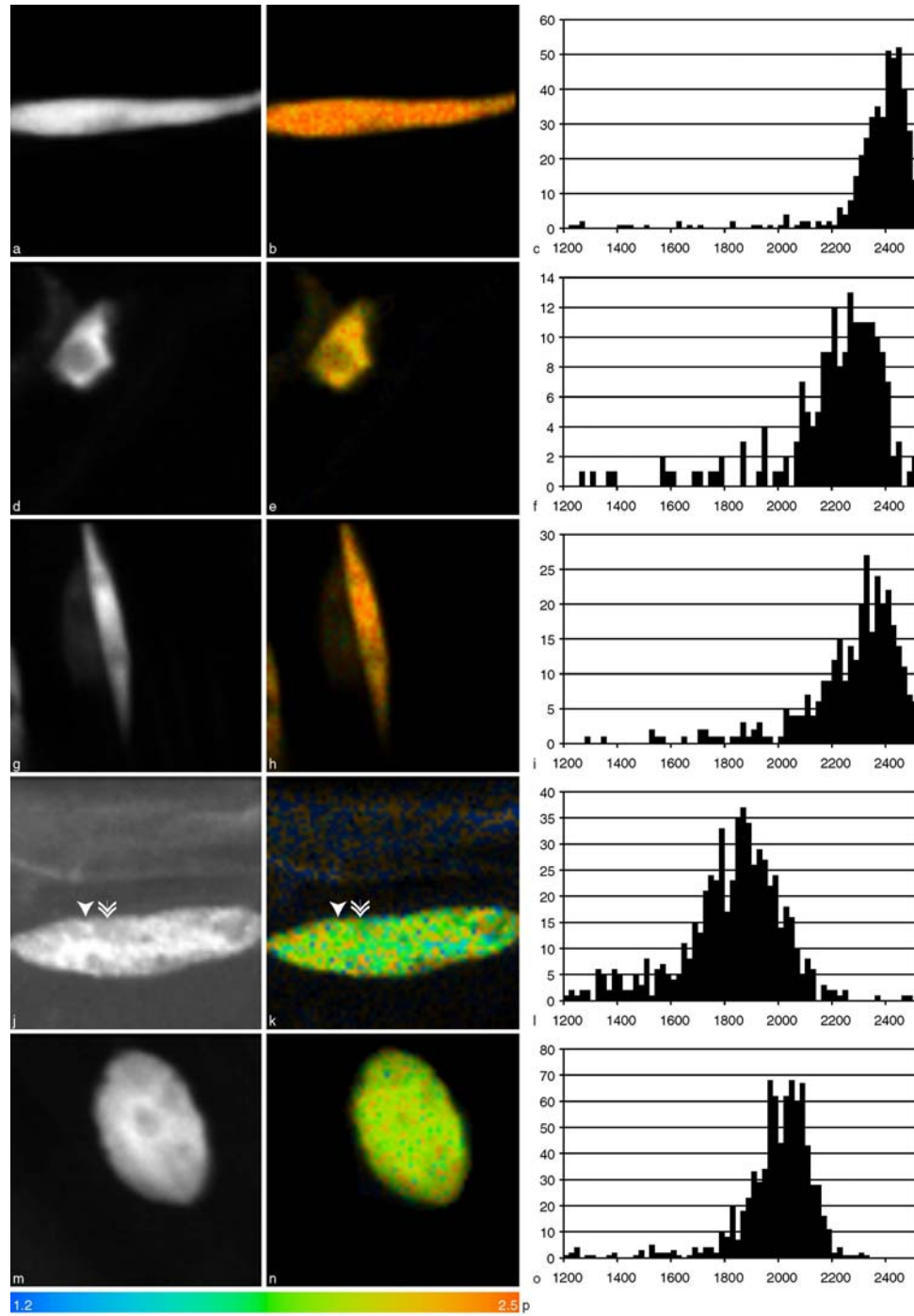
FRET values are pseudocolored in red; shorter lifetime values are pseudocolored in blue indicating FRET (Figure 4- 3). Figure 4- 3 shows that the fluorescence lifetimes of GFP as well as LHP1-GFP are equal throughout the nucleus (Figure 4- 3 a-f).

When DNA of 35S::GFP expressing plants was stained with Sytox Orange, the measured lifetime of GFP was 2.32 ± 0.05 ns (Figure 4- 3 g-i). So the lifetime of GFP is not affected by the Sytox dye implying that FRET does not take place between DNA and a freely mobile GFP. Similar data were obtained with GFP transfected in Hela cells (Cremazy et al. 2005). When DNA of 35S::LHP1-GFP roots were stained with Sytox-orange, the average lifetime of AtLHP1-GFP is 1.85 ± 0.17 ns and the FLIM image showed uniform shorter lifetime values over the nucleus indicated by the blue-green color. (Figure j-l). The distribution histograms of fluorescence lifetimes of LHP1-GFP with or without Sytox show both one uniformly distributed population of the fluorescence lifetimes (Figure 4- 3 c and l). This marked reduction of the lifetime of the donor shows that FRET occurs between DNA and AtLHP1-GFP.

The lifetime values of AtLHP1-GFP are similar in foci and interfoci region (Figure 4- 3.j-k). Therefore within foci as well as in interfoci region, AtLHP1 is in close vicinity to the DNA and seems to be part of chromatin. The reduction in lifetime values of 16% obtained for AtLHP1 in our system is in the same range than the 20% reduction observed in Hela cells for HP1 α -GFP and HP1 β -GFP (Cremazy et al. 2005).

Figure 4- 3

FRET-FLIM study on *Arabidopsis* nuclei in differentiated root cells. a,d,g,j,m. Fluorescence intensity pictures. b,e,h,k,n. FLIM pictures. p. scale of fluorescence lifetimes of the FLIM pictures. c,f,i,l,o. Distribution Histogram of Fluorescence Lifetimes. a - c. 35S::LHP1-GFP without Sytox. d - f. 35S::GFP without Sytox. g - i. 35S::GFP with Sytox. j - l. 35S::LHP1-GFP with Sytox, ► arrow represent foci, » arrow interfoci region. m - o. 35S::LHP1 Δ CD-GFP with Sytox.



The chromodomain of AtLHP1 is necessary for foci formation

The FRET-FLIM studies strongly suggest that AtLHP1 is present in chromatin complexes. This could mean that AtLHP1 interacts with a specific histone modification. The sequence of the CD of AtLHP1 is homologous to the one of HP1/SWI6 and AtLHP1 was shown to complement a *swi6*-mutant in fission yeast (Kotake et al. 2003) suggesting that AtLHP1 can bind trimethylated H3K9 in yeast (Shilatifard 2006). If this is also the case in *Arabidopsis* a deletion of the CD might result in a free mobile protein. To test whether the CD was essential for the association with DNA a mutant AtLHP1 protein was constructed, lacking the CD. This construct was introduced by *A. rhizogenes* transformation in wild-type *Arabidopsis* roots. In none of the cells of these transgenic roots, foci were present in the nuclei and instead AtLHP1 $_{\Delta CD}$ -GFP is present in a diffuse manner throughout the nucleus (see Figure 3 m). By staining these roots with sytox orange and FLIM analysis it was tested whether AtLHP1 $_{\Delta CD}$ is no longer closely associated with DNA. Surprisingly, the average fluorescence lifetime of this AtLHP1 $_{\Delta CD}$ -GFP was 1.89 ± 0.21 ns showing that AtLHP1 lacking the CD is still in close vicinity to DNA (Figure 3 m-o). Collectively these data show that the CD is essential for the formation of the chromatin complexes that are visible as foci and probably during the formation of these foci the CD of AtLHP1 interacts with a histone modification. The close association of AtLHP1 and DNA in the interfoci region does not require the CD and so the association with DNA in these regions must depend on another domain (e.g. the hinge region) and is less likely to depend on a specific histone modification.

LHP1 colocalizes with H3K9m3 and H3K27m3

LHP1 CD could bind to H3K9m3 as shown for HP1/SWI6 in other systems. However, recently Turck et al (submitted) showed by ChIP-chip experiments that AtLHP1 target genes are enriched in H3K27m3 (Turck). Therefore we tested whether AtLHP1 foci colocalize with H3K9m3 or H3K27m3. In roots of *Arabidopsis* plants expressing pLHP1::LHP1-GFP, AtLHP1-GFP was detected with a rabbit anti-GFP polyclonal antibody (Molecular Probes) H3K9m3 with a mouse anti-H3K9m3 monoclonal antibody (Abcam) and H3K27m3 with a mouse anti-H3K27m3 monoclonal antibody (Abcam). Therefore colocalization of AtLHP1 with these histone modifications was studied in separate experiments. Root nuclei from the differentiated zone were imaged with a confocal laser scanning microscope. AtLHP1-GFP (green signal, Figure 4- 4 a+d), H3K9m3 (red

signal, Figure 4- 4 b) and H3K27m3 (red signal, Figure 4- 4 e) are all present in multiple foci located in the euchromatin (Figure 4- 4). AtLHP1 and H3K9m3 appear to overlap as well as AtLHP1 and H3K27m3 as shown by the yellow signal in the merged pictures. However, not all AtLHP1 colocalizes with H3K9m3 and vice versa as shown by the regions indicated by arrows on Figure 4- 4 c and the same is true for AtLHP1 and H3K27m3 (Figure 4- 4 f).

The Pearson's correlation coefficient, R , was calculated. The Pearson's correlation coefficient shows how well 2 signals relate by a linear equation. R ranges from -1 to 1 in which 1 reflects a perfect positive linear correlation, whereas -1 shows a perfect mutual exclusion. Furthermore, to eliminate the possibility that the observed colocalization was due to chance only or to a too low resolution of the microscope, we compared the Pearson correlation coefficient with the one generated by a randomly generated picture (the green or red signal is scrambled whereas the other signal is kept intact (see M&M)). Root nuclei from the differentiated zone were imaged with a confocal laser scanning microscope and the middle section of a Z-stack of a nucleus was analyzed.

The average Pearson's correlation coefficient for AtLHP1 with H3K9m3 and H3K27m3 is 0.720 (19 nuclei) and 0.686 (39 nuclei), respectively, which corresponds to a marked degree of correlation between AtLHP1 and both H3 modifications. (The R values for nuclei in which one of the 2 signals is scrambled are about 0.17 and 0.0) The R values are lower than 1 because not all AtLHP1 foci (but at least more than 50% do) colocalize with one of these H3 marks and further a perfect linearity of the AtLHP1 and H3K9m3/H3K27m3 signal is not expected as the ratio of AtLHP1 molecules and H3 marks is not known to be constant on all their DNA targets.

LHP1 is present in dynamic complexes

To test whether the interaction of AtLHP1 and DNA/histone is dynamic as in animals, Fluorescence Recovery After Photobleaching experiments were performed. FRAP makes use of the photobleaching properties of the excitation laser to selectively destroy the fluorescence of GFP in a region within the cell, after which the fluorescence intensity of the bleached region is monitored. The speed of fluorescence recovery after photobleaching provides insight in the dynamics of the molecule and the ultimate percentage of recovery shows which fraction of the molecules is dynamic.

FRAP has been used to study the dynamics of AtLHP1 in foci as well as in the interfoci regions in transgenic *Arabidopsis* roots expressing 35S::LHP1-GFP. As reference for a freely mobile protein we used transgenic plants expressing 35S::GFP. All experiments used a bleach region of $1 \mu\text{m}^2$. As a control, the half time of recovery for free GFP was measured in 10 nuclei and is about 0.02 s (Table 4- 1).

The mobility of AtLHP1 was measured in 200 nuclei. In foci the half time of recovery is about 1 s whereas in the interfoci regions this is about 0,6 s (Table 4- 1). The difference between these mobilities is significant (T Student test $p = 0.0005$) underlining that the chromatin interaction of AtLHP1 in foci and interfoci regions is different.

35S::LHP1-eGFP(200 nuclei)				35S::eGFP(10 nuclei)	
Interfoci		foci		$t_{1/2}$ (s/ μm^2)	Mobile fraction (%)
$t_{1/2}$ (s/ μm^2)	Mobile fraction (%)	$t_{1/2}$ (s/ μm^2)	Mobile fraction (%)		
0.66 \pm 0.44	62 \pm 20	0.96 \pm 0.37	71 \pm 13	0.018 \pm 0.003	79 \pm 5

Table 4- 1 : FRAP data of AtLHP1

FRAP analysis of AtLHP1-GFP in *Arabidopsis* roots. Half time recovery and mobile fraction with their standard deviation for differentiated nuclei in interfoci regions and in foci.

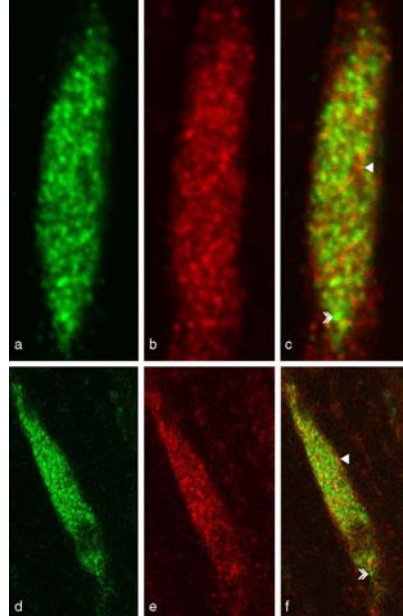


Figure 4- 4

Whole mount immunodetection of AtLHP1-GFP and H3 marks on interphase root nuclei of *Arabidopsis*. a-c. Immunodetection of AtLHP1-GFP(a), H3K9m3 (b) and merged picture (c). ▶ region with H3K9m3 only, » region with AtLHP1-GFP only. d-f. Immunodetection of AtLHP1-GFP (d), H3K27m3 (e) and merged picture (f). ▶ region with H3K27m3 only, » region with AtLHP1-GFP only.

To estimate the degree of colocalization of AtLHP1 and with H3K9m3 and H3K27m3, statistical analysis was performed using ImageJ (v.1.37, National Institutes of Health, USA. <http://rsb.info.nih.gov/ij>).

So the mobility of AtLHP1 is 30-50 times slower than that of a free mobile (GFP) protein. This confirms the FRET-FLIM experiments that showed that AtLHP1 is not a freely mobile protein in the regions between foci as well as in foci. In contrast, Histone 2B has a half time of recovery of $\sim 80 \text{ s}/\mu\text{m}^2$. (Chapter 3) showing that AtLHP1 complexes are markedly more dynamic than histones in nucleosomes.

Values observed for the mobility of AtLHP1 are in the same range as those of HP1 in mammalian cells, which are about 1 s in the euchromatin for the isoform HP1 γ (80% mobile) (Schmiedeberg et al. 2004)

Discussion

Here we showed that AtLHP1 foci that are located in euchromatic area of interphase nuclei are highly dynamic chromatin complexes in which relatively high levels of H3K9m3 and/or H3K27m3 occur. These AtLHP1 foci most likely represent chromatin complexes controlling the expression of genes. The conclusion that AtLHP1 foci represent chromatin complexes is supported by the FRET-FLIM studies demonstrating that AtLHP1 is in close vicinity to DNA as well as the colocalization of AtLHP1 with the histone modification H3K9m3 and/or H3K27m3. The partial colocalization of AtLHP1 and H3K27m3 is well in line with the submitted ChIP-chip studies of Turck *et al.* Since H3K9m3 as well as H3K27m3 were visualised with a mouse monoclonal antibody our studies could not reveal whether both epigenetic modifications are present in foci or whether they occur in different subsets of foci.

The chromodomain is essential for foci formation as was previously shown in *Arabidopsis* protoplasts (Libault *et al.* 2005; Nakahigashi *et al.* 2005). However, since major chromatin reorganisation is induced by protoplast formation (Tessadori *et al.* Submitted) this had to be confirmed in plants. It seems probable that the CD of AtLHP1 recognises H3K9m3 and/or H3K27m3. Turck *et al.* indeed demonstrated that AtLHP1 binds H3K27m3 *in vitro* as well as H3K9m3. Whether AtLHP1 efficiently binds H3K9m3 *in vivo*, remains to be demonstrated. However, since AtLHP1 can complement a yeast swi6 mutant it is probable it will (Kotake *et al.* 2003).

AtLHP1 was shown to affect the expression of genes situated in the euchromatin but not in the heterochromatin (Nakahigashi *et al.* 2005). Furthermore ChIP-chip experiment shows as well that AtLHP1 interacts with chromatin and that its chromodomain is involved in this binding. ChIP experiments performed by Turck demonstrated that AtLHP1 was not found in heterochromatic sequences. Therefore it seems probable that the AtLHP1 foci represent chromatin complexes where target genes are regulated. The euchromatic localization of AtLHP1 is in agreement with most other studies done in *Arabidopsis* (Libault *et al.* 2005; Nakahigashi *et al.* 2005) except one study involving *Arabidopsis* protoplasts where AtLHP1 was shown to be located in the heterochromatin (Zemach *et al.* 2006). The latter might be due to the major global chromatin reorganisation that occurs in *Arabidopsis* protoplasts (Tessadori *et al.* Submitted). We showed that the CD is essential for foci formation but not for the close association with DNA in the regions in between foci. The foci could be the sites where genes are regulated, whereas in the interfoci

region AtLHP1 could be scanning the DNA searching for its target genes. The localisation of AtLHP1 resembles that of HP1 γ in mammals or HP1c in *Drosophila* that can be located in euchromatic areas and these isoforms of HP1 have been demonstrated to be involved in gene regulation (Ogawa *et al.* 2002; Piacentini *et al.* 2003).

Our FRAP studies showed that AtLHP1 forms similar dynamic complexes as the animal isoform HP1 γ (80% mobile) (Schmiedeberg *et al.* 2004) and this supports the conclusion that AtLHP1 and the “euchromatic” HP1 isoforms could fulfill a similar function in gene regulation in chromatin complexes.

Material and methods

Plant material and growth conditions

The *Arabidopsis* Columbia ecotype was used as wild-type. For all experiments, plants were grown vertically for 4-5 days post-germination on 0.8% agar plates containing 2.2g Murashige and Skoog 10 salts with vitamins (Duchefa) plus 1% sucrose at pH 5.8 in LD (16h light/ 8h dark) conditions at 23-24 °C.

Construction of AtLHP1 fusion genes

35S::LHP1-GFP and pLHP1::LHP1-GFP:

LHP1 cDNA was amplified with cLHP1-SalI-F (5' GTCGACCAGGAAATGAAAGGGGC AAGTGG3') and cLHP1-XbaI-R (5' TCTAGATAAGGCGTTCGATTGTAC3') on cDNA of Columbia and introduced into pGEMT (Promega). EGFP from pEGFP-C1 (Clontech) was digested by NheI and SacI and cloned into the XbaI and SacI sites of pGEMT-cLHP1. EGFP was in this way cloned after the C terminal part of AtLHP1 creating a linker of 8 amino acids between the two proteins. After digestion of the pGEMT-cLHP1-eGFP with SalI and SacI, the cLHP1-eGFP fragment was introduced into a modified pBINPLUS binary vector (van Engelen *et al.* 1995) containing two times the constitutive 35S CaMV promoter and the NOS terminator creating pBIN35SLG plasmid. AtLHP1 promoter was amplified with pLHP1-ClaI-2F (5' ATCGATATGGGTGCAGCATGG3') and pLHP1-SalI-R (5' CTGGTC GACAGTATTCGAGCCTCC3') on the Col-0 genomic P1 clone MIVA3 (81701 bp, accession number AB006706) giving a fragment of 2435 bp corresponding to the 11772-14230 MIVA3 region. After digestion with ClaI and SalI, the promoter was

introduced into ClaI and SalI sites of pBIN35SLG, removing in this way the 35S CaMV promoter and creating the pBINILG plasmid.

pBIN35SLG and pBINILG were introduced into *Agrobacterium Rhizogenus* (strain msu440) for hairy root transformation. For stable transformation pLHP1::cLHP1-eGFP was introduced into a pFluar 101 vector (Stuitje et al. 2003) with a modified MCS called pFluar101(+2) using ClaI and PacI sites creating pFluILG which was then introduced into *Agrobacterium tumefaciens* (strain C58).

LHP1_{ΔCD}-GFP

The fragment cLHP1-eGFP was introduced into pBSK (Stratagene) by digestion with XbaI and SalI. The CD deletion was constructed with the aid of the PCR based Quicksite's mutagenesis kit hereby creating a HindIII site at the end of the CD. The CD was deleted in pBSK by a HindIII digestion of a natural occurring site at positions 304-309 in combination with the newly created HindIII site. The primers used to create this mutation were 5' GCCTTTGAGGGAAGTTTGAAGCTTGGAAAGCCTGGTAGGAAACGG3' and 5' CCGTTTCCTACCAGGCTTTCCAAGCTTCAAACCTCCCTCAAAGGC3', the bold letters indicating the mutation sites. The AtLHP1_{ΔCD}-GFP fragment was introduced into a pFluar101(+2) vector containing a 35S promoter using AgeI and SalI digestion sites in pBSK as well as pFluar. The resulting vector 35S::LHP1_{ΔCD}-GFP was introduced into

Agrobacterium Rhizogenus (strain msu440) for hairy root transformation

4-5 dpv old *Arabidopsis* seedlings (accession Columbia) were transformed as described (Limpens et al. 2004) using Färhaeus and Emergence medium instead of ½ MS.

Agrobacterium-mediated vacuum transformation

4-6 weeks old plants of *lhp1* mutants (tfl2-1 and tfl2-3 in Columbia background, Kotake) were transformed as described (Bechtold et al. 1993). The aerial part of the plants was dipped into a solution of *Agrobacterium tumefaciens* (strain C58) carrying the appropriate construct in infiltration medium (Murashige and Skoog + vitamins 2.3 g/l, sucrose (5%) 50 g/l, MES 0.5 g/l pH = 5.8 with KOH, autoclave and add 200 µl/l Silvet L77) under vacuum for 5-10 min

Localization

All confocal images were acquired on a Zeiss 510 inverted microscope using a 40x/1.3 oil immersion objective. Image resolution was always higher than the theoretical limit for light microscopy to insure no data was missed.

FRAP

All FRAP studies were performed with similar settings as described for the imaging. The ROI was kept at approximately $1\ \mu\text{m}^2$ allowing direct comparison between half-times of recovery. Recovery of fluorescence intensity was monitored in such manner that at least 10% of the obtained images were obtained before the half time of recovery. For focal measurements a ROI the size of the focal was set.

FRET-FLIM

Two-photon microscopy was performed on a biorad 1600 using a 60x/1.2 water immersion objective. Fixation procedures and imaging settings were identical to Cremazy et al. Two-photon excitation was used instead of single photon excitation (870 nm). FLIM images were obtained using a 75 Mhz modulated two-photon laser after which Time Correlated Single Photon Counting (TCSPC) was used to determine the fluorescence lifetime.

Immunolocalization

4-5 dpg old seedling roots were immunolabeled as described (Talbert et al. 2002; Jasencakova et al. 2003). Roots were fixed in 4% paraformaldehyde in PBS pH 7.3 0.2% Triton for 1h with 20 min vacuum at room temperature. They were washed 2x 10 min with 1x PBS and transfer to small baskets with filters. They were digested for 40 min at 37°C with a mixture of 2.5% pectinase from *Aspergillus niger* (Sigma) and 2.5% cellulase Onozuka RS (Yakult Honsha Co., Tokyo, Japan) dissolved in PBS. Roots were washed in PBS and squashed onto slides. Slides were immersed in liquid nitrogen, the cover slips were removed, and roots were postfixed in 4% paraformaldehyde in PBS for 20 min at room temperature. After washing with 3x 5 min PBS, slides were incubated in a moist chamber at room temperature with blocking solution (3% BSA, 10% sheep serum) for 1h at 37°C. After cover slips were removed, slides were incubated with rabbit anti-GFP polyclonal antibody (1:200, A11122 Molecular Probes) in labeling solution (1% BSA, 10% sheep serum, 0.1% Tween 20) for detection of AtLHP1-GFP overnight at 4°C. Cover slips

were removed, and the slides were washed twice with PBS. The antibody was detected by applying Alexa 488–conjugated goat anti-rabbit secondary antibody (A11070, Molecular Probes) diluted 1:200 in labeling solution and incubated for 1-2 h, followed by two washes in PBS. The slides were stained and mounted with 2 µg/mL Propidium Iodide in Vectashield (Vector Laboratories, Burlingame, CA).

Whole mount coimmunolocalization

Immunolabeling procedure was performed as described (Friml et al. 2003). 4 dpg old *Arabidopsis* seedlings were fixed in 4% paraformaldehyde in MTSB for 1h00 at + 4°C instead of room temperature. From the driselase treatment, seedlings were kept in small baskets with filters to avoid loosing the root tips during the different washing steps. They were incubated overnight at room temperature in a wet chamber with two primary antibodies: a rabbit anti-GFP polyclonal antibody (1:200, A11122 Molecular Probes) for detection of AtLHP1-GFP and a mouse anti-H3K9m3 monoclonal antibody (1:50, 6001 Abcam) or a mouse anti-H3K27m3 monoclonal antibody (1:50, 6002 Abcam). The seedlings after washing were incubated with two secondary antibodies a Alexa 488 conjugated goat anti-rabbit antibody (1:200, A11070 Molecular Probes) and a Cy3 conjugated donkey anti-mouse antibody (1:100, Jackson ImmunoResearch Laboratories, West Grove, PA) overnight at room temperature. Finally the seedlings were mounted on microscopic slides in citifluor, an antifading mounting medium.

Colocalization analysis

Statistical analysis was performed using ImageJ (v.1.37, Rasband, W.S, National Institutes of Health, USA. <http://rsb.info.nih.gov/ij/>, 1997-2006) with two specific plugins: Manders' coefficients and the Colocalisation test (Tony Collins, Wayne Rasband, <http://www.uhnresearch.ca/facilities/wcif/imagej/>) Both plugings calculate the Pearson's correlation coefficient, R, one of the standard measures in pattern recognition. The Pearson's correlation coefficient is valid only if a linear relationship exists between the red and green signals. To check this, the Mander's coefficients plugin generate a Red-Green scatter plot, if the points scatter in a more or less linear direction then the relationship can be considered linear. Pearson's correlation coefficient is independent from the image background and the intensities of the signals. The coefficient ranges from -1 to 1. A value

of 1 shows that a linear equation describes the relationship perfectly and positively, with all the data points lying on the same line and with G increasing with R. A value of -1 shows also a linear relationship between G and R but G increases as R decreases. A value of 0 shows that there is no linear relationship between G and R so no colocalization. Furthermore, to eliminate the possibility that the observed colocalization was due to chance only or to a too low resolution of the microscope we compared, thanks to the Colocalisation test plugin, the Pearson correlation coefficient r_p (=R) with the one generated by a randomly generated picture (the green or red signal is scrambled by randomly rearranging blocks of size equal to the point spread function of the microscope, the other signal is kept intact).

$$r_p = \frac{\sum((R_i - R_{avg})(G_i - G_{avg}))}{\sqrt{\sum(R_i - R_{avg})^2 \sum(G_i - G_{avg})^2}}$$

R_i, G_i = intensity values of pixel i , R_{avg} and G_{avg} = average intensity R or G

Acknowledgements

The *tfl2-1*, and *tfl2-3 lhp1* knockout mutants were kindly provided by T. Kotake. Furthermore we thank Jan-Willem Borst for his help with the FRET-FLIM data.

References

- Bannister, A. J., P. Zegerman, J. F. Partridge, E. A. Miska, J. O. Thomas, R. C. Allshire and T. Kouzarides** (2001). "Selective recognition of methylated lysine 9 on histone H3 by the HP1 chromo domain." *Nature* 410(6824): 120-4.
- Brasher, S. V., B. O. Smith, R. H. Fogh, D. Nietispach, A. Thiru, P. R. Nilsen, R. W. Broadhurst, L. J. Ball, N. V. Murzina and E. D. Laue** (2000). "The structure of mouse HP1 suggests a unique mode of single peptide recognition by the shadow chromo domain dimer." *Embo J* 19(7): 1587-97.
- Cheutin, T., A. J. McNairn, T. Jenuwein, D. M. Gilbert, P. B. Singh and T. Misteli** (2003). "Maintenance of stable heterochromatin domains by dynamic HP1 binding." *Science* 299(5607): 721-5.
- Cowieson, N. P., J. F. Partridge, R. C. Allshire and P. J. McLaughlin** (2000). "Dimerisation of a chromo shadow domain and distinctions from the chromodomain as revealed by structural analysis." *Curr Biol* 10(9): 517-25.
- Cremazy, F. G., E. M. Manders, P. I. Bastiaens, G. Kramer, G. L. Hager, E. B. van Munster, P. J. Verschure, T. J. Gadella, Jr. and R. van Driel** (2005). "Imaging in situ protein-DNA interactions in the cell nucleus using FRET-FLIM." *Exp Cell Res* 309(2): 390-6.
- Eissenberg, J. C. and S. C. Elgin** (2000). "The HP1 protein family: getting a grip on chromatin." *Curr Opin Genet Dev* 10(2): 204-10.
- Gaudin, V., M. Libault, S. Pouteau, T. Juul, G. Zhao, D. Lefebvre and O. Grandjean** (2001). "Mutations in LIKE HETEROCHROMATIN PROTEIN 1 affect flowering time and plant architecture in Arabidopsis." *Development* 128(23): 4847-58.
- <http://www.expasy.org/prosite/> (2006). Prosite.
- Jacobs, S. A. and S. Khorasanizadeh** (2002). "Structure of HP1 chromodomain bound to a lysine 9-methylated histone H3 tail." *Science* 295(5562): 2080-3.
- Kotake, T., S. Takada, K. Nakahigashi, M. Ohto and K. Goto** (2003). "Arabidopsis TERMINAL FLOWER 2 gene encodes a heterochromatin protein 1 homolog and represses both FLOWERING LOCUS T to regulate flowering time and several floral homeotic genes." *Plant Cell Physiol* 44(6): 555-64.
- Lachner, M., D. O'Carroll, S. Rea, K. Mechtler and T. Jenuwein** (2001). "Methylation of histone H3 lysine 9 creates a binding site for HP1 proteins." *Nature* 410(6824): 116-20.
- Libault, M., F. Tessadori, S. Germann, B. Snijder, P. Fransz and V. Gaudin** (2005). "The Arabidopsis LHP1 protein is a component of euchromatin." *Planta* 222(5): 910-25.
- Limpens, E., C. Franken, P. Smit, J. Willemsse, T. Bisseling and R. Geurts** (2003). "LysM domain receptor kinases regulating rhizobial Nod factor-induced infection." *Science* 302(5645): 630-3.

- Lorentz, A., K. Ostermann, O. Fleck and H. Schmidt** (1994). "Switching gene swi6, involved in repression of silent mating-type loci in fission yeast, encodes a homologue of chromatin-associated proteins from *Drosophila* and mammals." Gene 143(1): 139-43.
- Lorvellec, M., J. Willemse, O. Kulikova, J. Verver and T. Bisseling** (Chapter 4).
- Meehan, R. R., C. F. Kao and S. Pennings** (2003). "HP1 binding to native chromatin in vitro is determined by the hinge region and not by the chromodomain." Embo J 22(12): 3164-74.
- Nakahigashi, K., Z. Jasencakova, I. Schubert and K. Goto** (2005). "The *Arabidopsis* heterochromatin protein1 homolog (TERMINAL FLOWER2) silences genes within the euchromatic region but not genes positioned in heterochromatin." Plant Cell Physiol 46(11): 1747-56.
- Nielsen, A. L., M. Oulad-Abdelghani, J. A. Ortiz, E. Remboutsika, P. Chambon and R. Losson** (2001). "Heterochromatin formation in mammalian cells: interaction between histones and HP1 proteins." Mol Cell 7(4): 729-39.
- Schmiedeberg, L., K. Weisshart, S. Diekmann, G. Meyer Zu Hoerste and P. Hemmerich** (2004). "High- and low-mobility populations of HP1 in heterochromatin of mammalian cells." Mol Biol Cell 15(6): 2819-33.
- Sprague, B. L. and J. G. McNally** (2005). "FRAP analysis of binding: proper and fitting." Trends Cell Biol 15(2): 84-91.
- Starr, T. E. and N. L. Thompson** (2002). "Fluorescence pattern photobleaching recovery for samples with multi-component diffusion." Biophys Chem 97(1): 29-44.
- Stuitje, A., E. Verbree, K. van der Linden, E. Mietkiewska, J.-P. Nap and T. Kneppers** (2003). "Seed-expressed fluorescent proteins as versatile tools for easy (co)transformation and high-throughput functional genomics in *Arabidopsis*." Plant Biotechnology Journal 1: 301-309.
- Takada, S. and K. Goto** (2003). "Terminal flower2, an *Arabidopsis* homolog of heterochromatin protein1, counteracts the activation of flowering locus T by CONSTANS in the vascular tissues of leaves to regulate flowering time." Plant Cell 15(12): 2856-65.
- Wang, G., A. Ma, C. M. Chow, D. Horsley, N. R. Brown, I. G. Cowell and P. B. Singh** (2000). "Conservation of heterochromatin protein 1 function." Mol Cell Biol 20(18): 6970-83.
- Zemach, A., Y. Li, H. Ben-Meir, M. Oliva, A. Mosquana, V. Kiss, Y. Avivi, N. Ohad and G. Grafi** (2006). "Different domains control the localization and mobility of LIKE HETEROCHROMATIN PROTEIN1 in *Arabidopsis* *nudei*." Plant Cell 18(1): 133-45.

Chapter 5: AtLHP1 mutants in *Arabidopsis thaliana*

Joost Willemse, Maëlle Lorvellec, Olga Kulikova,
Jan Verver, Joan Wellink, and Ton Bisseling

Introduction

HP1 (heterochromatin protein 1) is a component of heterochromatin in most eukaryotes. However, in mouse and human, isoforms of HP1 occur that are located in euchromatin (e.g. HP1 γ) (Nielsen *et al.* 2001), where they are part of chromatin complexes most likely involved in the regulation of gene expression (Libault *et al.* 2005). In *Arabidopsis* only one isoform is present (AtLHP1), which is most similar to HP1 γ (Gaudin *et al.* 2001; Takada and Goto 2003; Libault *et al.* 2005; Nakahigashi *et al.* 2005). It localizes in the euchromatin where foci are formed, that most likely represent chromatin complexes (chapter 4). Like all other HP1 proteins, AtLHP1 has a chromodomain (CD) and a chromoshadow domain (CSD), that are separated by a hinge region (H) (Lorentz *et al.* 1994; Eissenberg and Elgin 2000; Wang *et al.* 2000). Further, it contains an acidic domain (AD) at its N terminus. The CD of AtLHP1 is essential for foci formation; however the functions of the other domains of AtLHP1 have hardly been studied. Therefore we performed a mutational analysis with the aim to clarify the involvement of the domains in different processes

The CD of mammalian and *Drosophila* HP1 has been shown to be involved in binding H3K9me3 (Bannister *et al.* 2001; Lachner *et al.* 2001; Jacobs and Khorasani-zadeh 2002). To investigate the properties of the AtLHP1 CD a deletion mutant was constructed. This revealed that the CD of AtLHP1 is essential for foci formation (Lorvellec *et al.* Chapter 4) and most likely recognizes H3K9me3 and/or H3K27me3. Surprisingly, AtLHP1 $_{\Delta CD}$ remains in close vicinity to DNA (Lorvellec *et al.* Chapter 4) as determined by FRET-FLIM studies (Cremazy *et al.* 2005; Lorvellec *et al.* Chapter 4). This led to the conclusion that AtLHP1 $_{\Delta CD}$ is still part of chromatin. Therefore we hypothesize that the foci likely represent chromatin complexes regulating the expression of target genes, whereas AtLHP1 in the interfoci region is part of chromatin and scans the genome to identify these targets. This hypothesis is supported by Fluorescent Recovery After Photobleaching (FRAP) experiments which showed that AtLHP1 is not a free protein but has an average binding time around one second, similar to what has been observed for HP1 γ in mouse and human (Schmiedeberg *et al.* 2004).

The CSD of all HP1 variants is involved in dimerization and can also interact with other proteins. In mice, for example the CSD domain binds to histone methyltransferase to reinforce the binding of HP1 to its target (Brasher *et al.* 2000; Nielsen *et al.* 2001). Deletion of this domain in HP1 β results in an even distribution of the protein within the nucleus,

whereas it normally localizes to a limited number of targets both in eu- or heterochromatin (Cheutin *et al.* 2003). To study the function of the CSD an AtLHP1_{ΔCSD} construct was made.

The interconnecting hinge region of HP1 α has been identified as a DNA-binding region (Meehan *et al.* 2003), in contrast their data indicate that direct binding of the hinge region to DNA of HP1 γ is unlikely. To clarify the role of the AtLHP1 hinge domain a deletion construct with both the CSD and Hinge removed was studied.

In most (L)HP1s a region of acidic amino acids occurs at the N-terminus. This stretch of acidic amino acids is longer in most plants (*Zea mays*, *Populus trichocarpa*, *Oryza sativa*, *Daucus carota*, *Nicotiana benthamiana*, *Fragaria vesca*, and *Citrus clementina*, and *Arabidopsis* do contain a Acidic Domain (Gaudin *et al.* 2001; <http://www.expasy.org/prosite/> 2006)) compared to isoforms of HP1 of other organisms (*Drosophila*, Human, Mouse, Yeast, and *Lycopersicum esculentum*), where the stretch consists of 5 to 7 glutamic acids. The acidic domain (AD) of AtLHP1 consists of 44 amino acids of which 19 are glutamic acid and 9 are aspartic acid. In general, acidic domains are considered to be involved in DNA binding of the protein, the AD of AtLHP1 could therefore aid DNA binding through the hinge region.

In this chapter the roles of the various domains of AtLHP1 in foci formation, mobility and interaction with chromatin are determined using confocal microscopy in combination with FRAP and FRET-FLIM methods. The construction of mutated variants of AtLHP1, which lacks either one or two domains, allowed us to investigate the properties of the domains. The results obtained here combined with previous results obtained by others lead to a hypothetical model of how AtLHP1 functions in the nucleus.

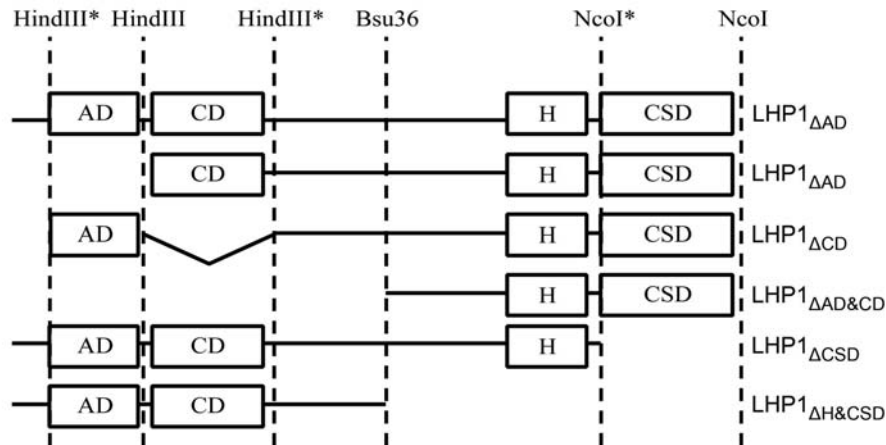


Figure 5- 1

AtLHP1 constructs used in this study. Relevant restriction sites are shown above the picture, stars indicate newly created restriction sites.

Results

The CD and Hinge appear to be important for foci formation

To determine which AtLHP1 domains are essential for foci formation and/or chromatin interaction, several deletion mutations were introduced in AtLHP1 (Figure 5- 1). First, the sub-nuclear localization of all AtLHP1 mutant proteins was examined by introducing the mutated 35S::AtLHP1-GFP fusion constructs in hairy roots of *Arabidopsis*. CLSM imaging of the different transgenic roots showed that AtLHP1 Δ CSD, and the AtLHP1 Δ AD still form foci like the wild type AtLHP1 protein, in contrast Libault et al (Libault *et al.* 2005) have reported that the CSD is essential for foci formation in *Arabidopsis* protoplasts. The other AtLHP1 mutant proteins AtLHP1 Δ CD, AtLHP1 Δ AD&CD, and AtLHP1 Δ H&CSD do no longer form foci and have a more homogeneous distribution in the nucleus (Figure 5- 2). Although AtLHP1 Δ CSD can still form foci, when additionally the conserved part of the hinge is deleted this property is lost (compare Figure 5- 2f with Figure 5- 2g). From this we conclude that the CD is essential for foci formation confirming the results obtained by Libault et al (Libault *et al.* 2005). Further, the hinge region also seems essential. However, it remains to be tested whether a deletion mutant where only the hinge region is deleted also is unable to form foci.

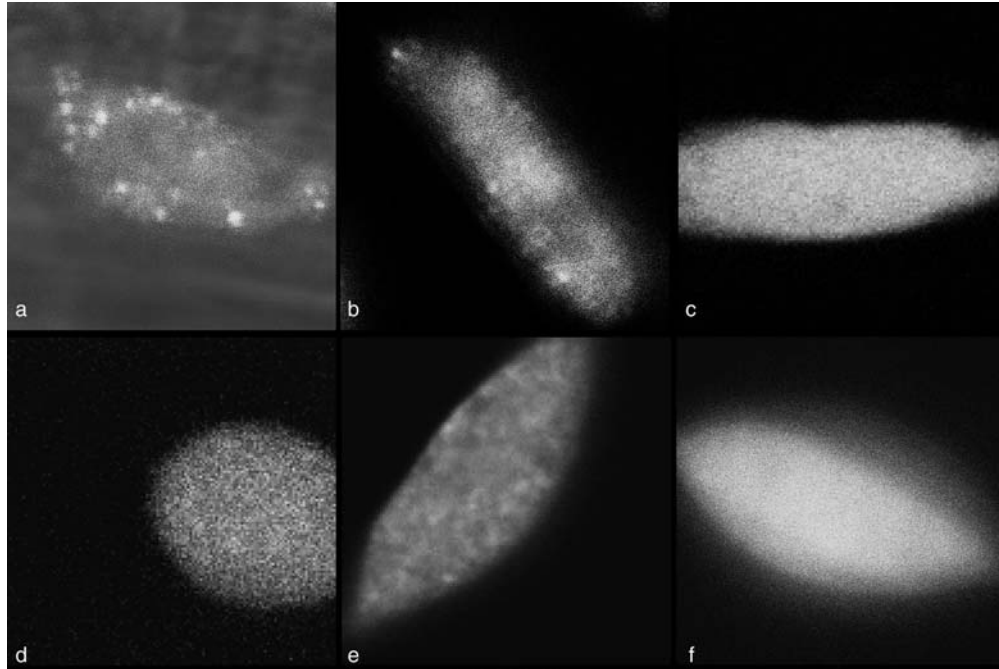


Figure 5- 2

Localization of AtLHP1 (mutant proteins) in nuclei of cells in the differentiation zone of *Arabidopsis* roots. Localization of 35S::AtLHP1-GFP in root nuclei showing foci (a). A similar pattern is observed for 35S::AtLHP1 $_{\Delta AD}$ -GFP (b) and 35S::AtLHP1 $_{\Delta CSD}$ -GFP (e). Other deletion mutants showed a diffuse localization throughout the nucleus; 35S::AtLHP1 $_{\Delta CD}$ -GFP (c), 35S::AtLHP1 $_{\Delta AD \& CD}$ -GFP (d), 35S::AtLHP1 $_{\Delta H \& CSD}$ -GFP (f).

None of the domains (AD, CD, hinge, or CSD) are sufficient for foci formation (Libault *et al.* 2005; Zemach *et al.* 2006), whereas the CD including two nuclear localization signals (NLS) is sufficient (Zemach *et al.* 2006) in *Arabidopsis* protoplasts.

The AD, Hinge and CSD are essential to position AtLHP1 in close vicinity to DNA

Our previous studies on AtLHP1 $_{\Delta CSD}$ showed that the ability of AtLHP1 to form foci is not essential for this protein to be in close vicinity of DNA (Lorvellec *et al.* Chapter 4). Therefore we wondered whether the other mutant proteins that lost the ability to form foci are still in close association with DNA. The association of mutant AtLHP1 protein with DNA was examined by FRET-FLIM, which can reveal whether a (fluorescent) protein is in close proximity (~5-10nm) to DNA if the latter is stained with sytox, (Cremazy *et al.*

2005). Our previous studies show that AtLHP1-GFP has a fluorescent lifetime of 2.3 ns in the absence of an acceptor fluorophore. Upon DNA staining by sytox orange the lifetime is significantly reduced to about 1.8 ns, proving that AtLHP1 is in close vicinity to DNA (table 4-1, Lorvellec *et al.* Chapter 4). When the DNA is not stained with sytox all AtLHP1 derived constructs have a lifetime of about 2.2 ns.

Upon staining with sytox only one mutated protein, namely AtLHP1 Δ CD, had a reduced lifetime (Lorvellec *et al.* Chapter 4) (Ttest:p<0.005) showing that AtLHP1 Δ CD is in close vicinity to DNA. All other mutant proteins show no significant lifetime reduction, indicating that these mutant proteins are no longer in such close proximity to DNA. As wt AtLHP1 all constructs show an equal lifetime throughout the nucleus (data not shown).

So despite the fact that AtLHP1 Δ AD as well as AtLHP1 Δ CSD still form structures resembling the foci formed by wt AtLHP1, the distance between these mutated AtLHP1s and DNA is larger than between wt AtLHP1 and DNA (Table 5- 1). This can imply that the foci formed by these AtLHP1 Δ AD and AtLHP1 Δ CSD are not chromatin complexes. Alternatively, these foci are still chromatin complexes but the distance between the two fluorophores (GFP and Sytox) is larger than normal. A conformational change of AtLHP1 could account for the repositioning of GFP to a distance that can no longer be measured by FRET-FLIM. Since AtLHP1 Δ H&CSD has a diffuse distribution in nuclei and it is no longer in close vicinity to DNA. It is possible that this protein is no longer associated with chromatin.

	Lifetime in ns \pm s.e.		N
AtLHP1 without sytox	2.22	\pm 0.06	6
AtLHP1	1.85	\pm 0.17	12
AtLHP1ΔAD	2.09	\pm 0.11	13
AtLHP1ΔCD	1.89	\pm 0.21	9
AtLHP1ΔCSD	2.11	\pm 0.09	20
AtLHP1ΔAD&CD	2.10	\pm 0.16	19
AtLHP1ΔH&CSD	2.14	\pm 0.03	5

Table 5- 1: Fluorescent lifetime values

FRET-FLIM data of the 35S::AtLHP1-GFP mutant proteins as tested in hairy roots

In case the AtLHP1 $_{\Delta AD}$ and AtLHP1 $_{\Delta CSD}$ foci are not chromatin complexes, but for example artificial aggregates it is probable that the mobility of the mutated proteins would be markedly slower or even immobile. Therefore the mobility of these proteins was studied with FRAP to determine their apparent diffusion within foci.

AtLHP1 $_{\Delta AD}$, has a slower mobility (half time of recovery is $1.46 \pm 0.78s$) than wt AtLHP1 ($0.66 \pm 0.44s$) (Ttest: $p < 0.001$), whereas AtLHP1 $_{\Delta CSD}$ moves faster ($0.13 \pm 0.07s$) but still tenfold slower than free protein ($0.018 \pm 0.003s$). So although the half time of recovery of AtLHP1 $_{\Delta AD}$ is about two times higher than that of AtLHP1, it is still a very mobile protein. Since no immobile fraction was observed it is unlikely that the foci formed by AtLHP1 $_{\Delta AD}$ and AtLHP1 $_{\Delta CSD}$ are artificial aggregates and it is more likely that these foci are chromatin complexes. This indicates that within the foci the interaction of AtLHP1 is directly to histones and not to DNA. The mobility of these mutated proteins was analyzed within foci and in regions between foci, no significant difference was observed between these locations.

Since AtLHP1 $_{\Delta H\&CSD}$ has a diffuse nuclear localization and is no longer in close vicinity to DNA we tested whether its apparent diffusion rate has increased to a similar speed as a freely mobile protein like GFP. These FRAP experiments showed that the apparent diffusion speed of AtLHP1 $_{\Delta H\&CSD}$ ($0.12 \pm 0.06s$) has increased 5 fold compared to wt. However, this is still ~10 fold slower than free GFP. Therefore the theoretical weight of a protein complex with that kind of diffusion speed would be around $3 \cdot 10^4$ kD (Starr and Thompson 2002; Sprague and McNally 2005). It seems unlikely that thousands of proteins operate together as a freely mobile complex, hereby indicating a reduced capacity of complex formation with static nuclear components instead of a complete loss of this interaction (Table 5- 2) (Starr and Thompson 2002; Sprague and McNally 2005).

Half Times of recovery (s/ μm^2)				
Construct	Foci	N	Interfoci	N
AtLHP1	0.96 ± 0.37	51	0.66 ± 0.44	50
AtLHP1 Δ AD	1.40 ± 0.56	51	1.46 ± 0.78	50
AtLHP1 Δ CD			0.19 ± 0.09	59
AtLHP1 Δ CSD	0.20 ± 0.10	49	0.13 ± 0.07	63
AtLHP1 Δ H&CSD			0.12 ± 0.06	54
Free GFP	0.018 ± 0.003			8

Table 5- 2 : Half Times of recovery

FRAP data of the 35S::AtLHP1-GFP mutant proteins as tested in hairy roots

Discussion

Model

Co-localization of AtLHP1 with specific histone modifications within foci indicates that AtLHP1 is part of chromatin complexes regulating specific target genes, which are recognized by specific modifications of H3 (Lorvellec *et al.* Chapter 4). When AtLHP1 has lost the ability to recognize these specific modifications it still remains in close vicinity to DNA. Based on these observations we propose that in the interfoci regions AtLHP1 is scanning the DNA. Scanning of DNA is probably important for AtLHP1 to reach its target sites.

AtLHP1 Δ AD as well as AtLHP1 Δ CSD still form foci, although they are no longer in very close vicinity to DNA (No FRET). So being in close vicinity to DNA does not seem to be essential for the formation of foci. In case scanning is essential for foci formation it might occur without AtLHP1 being in close contact to DNA. Another explanation of the ability to form foci by AtLHP1 Δ AD could be dimerization through the CSD with endogenous wt AtLHP1, which then targets the mutated protein to foci. This can be tested by expressing AtLHP1 Δ AD in a *lhp1* mutant line. However dimerization cannot explain why AtLHP1 Δ CSD still can form foci. Other studies on (L)HP1 have shown that the CSD is essential for foci formation (Cheutin *et al.* 2003; Libault *et al.* 2005) and proper functioning of the protein (Brasher *et al.* 2000; Cowieson *et al.* 2000; Wang *et al.* 2000; Nielsen *et al.* 2001). Moreover our AtLHP1 Δ CSD cannot fully complement the *lhp1* knock out phenotype (data not shown). Therefore the nature of the foci formed by AtLHP1 Δ CSD needs to be analyzed in more detail.

Deletion of CSD and Hinge resulted in the loss of foci and the protein is not in close vicinity to DNA. Therefore the scanning property of the AtLHP1 protein might involve the H region. Further refinement of the AtLHP1 mutational analysis in which H is replaced by a similar sized changed amino acid sequence remains to be done to test this.

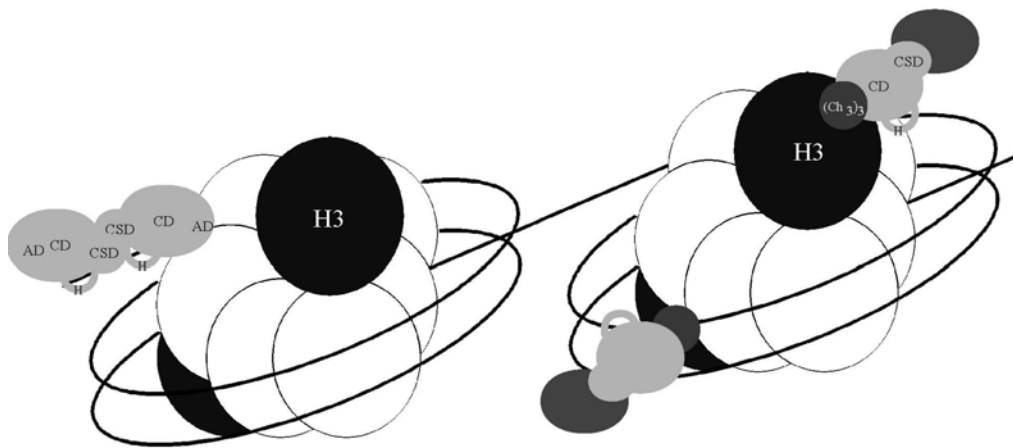


Figure 5- 3

Model of AtLHP1 functioning; the left part showing the scanning phase of the process using the hinge to attach to DNA, and the CSD to dimerize. The right part of the image shows that upon attachment to H3K9me3 (with the CD) AtLHP1 can interact with other proteins using the CSD.

Materials and methods

The AtLHP1_{ΔAD&CD} and AtLHP1_{ΔH&CSD} mutants were constructed by digestion of the AtLHP1 cDNA in pBluescriptSK (pBSK) with Bsu36 which cuts between the CD and the conserved part of the hinge. Afterwards XbaI and SalI digestion was used to put the fragment in pFluar (Stuitje *et al.* 2003). AtLHP1_{ΔCD} was constructed with the aid of the PCR based Quicksite's mutagenesis kit hereby creating a HindIII site at the end of the CD. The CD was deleted in pBSK by a HindIII digestion of a natural occurring site at positions 304-309, in combination with the newly created HindIII site. The primers used to create this mutation were 5' GCC TTT GAG GGA AGT TTG AAG CTT GGA AAG CCT GGT

AGG AAA CGG 3' and 5' CCG TTT CCT ACC AGG CTT TCC **AAG** CTT CAA ACT TCC CTC AAA GGC 3', the bold letters indicating the altered nucleotides.

AtLHP1_{ΔCSD} was created in a similar manner making use of a NcoI site just outside the AtLHP1 protein coding region in the linker between AtLHP1 and GFP, and a NcoI site created at positions 1124-1129. The primers used for this were 5' TTT GTC TCA GAA AAC CAT GGT TGA GGA GTT GGA CAT CAC G 3', and 5' C GAG ATG TCC AAC TCC TCA ACC ATG GTT TTC TGA GAC AAA 3', again the bold letters indicate the modifications.

The AD deletion construct was made using the natural HindIII site (position 304-309), and a StuI site at position 193-198 that was converted to a HindIII. The conversion was established using PCR with 5' CTC GAG GTC GAC CAG GAA ATG 3' (forward) and 5' CCT CCG TAA GCT TAT CAT CAC CAA TCT C 3' (reverse, bold letters indicating modifications) as primers. After digesting the PCR product as well as pBSK containing pAtLHP1::AtLHP1 with HindIII and SalI (a restriction site in the pBlueScript plasmid) the PCR product was ligated into the digested plasmid thereby removing the part between the original StuI and HindIII sites, which contains the coding sequence for 37 of the 44 amino acids in the acidic domain.

All constructs, after confirmation by sequencing, were introduced into pFluar containing a 35S promoter or the AtLHP1 promoter (2.435 bp (Kotake *et al.* 2003)) using AgeI and SalI digestion sites in pBSK as well as pFluar. The resulting vectors (with 35S promoter) were introduced into *Agrobacterium Rhizogenus* (strain msu440) for hairy root transformation (as described in Limpens *et al.*), and into *Agrobacterium Tumefaciens* (strain C58) for stable transformation of *Arabidopsis*. Hairy roots containing the 35S constructs were used for localization, FRAP and FRET-FLIM studies, stable transformants with pAtLHP1 were used for localization studies only.

The methods for localization, FRAP and FRET-FLIM studies are as described in (Lorvellec *et al.* Chapter 4).

Acknowledgements

We thank Maureen Hummel for the studies concerning the AD deletion mutant of AtLHP1, and valuable discussions about the presented model.

References

- Bannister, A. J., P. Zegerman, J. F. Partridge, E. A. Miska, J. O. Thomas, R. C. Allshire and T. Kouzarides** (2001). "Selective recognition of methylated lysine 9 on histone H3 by the HP1 chromo domain." *Nature* 410(6824): 120-4.
- Brasher, S. V., B. O. Smith, R. H. Fogh, D. Nietispach, A. Thiru, P. R. Nilsen, R. W. Broadhurst, L. J. Ball, N. V. Murzina and E. D. Laue** (2000). "The structure of mouse HP1 suggests a unique mode of single peptide recognition by the shadow chromo domain dimer." *Embo J* 19(7): 1587-97.
- Cheutin, T., A. J. McNairn, T. Jenuwein, D. M. Gilbert, P. B. Singh and T. Misteli** (2003). "Maintenance of stable heterochromatin domains by dynamic HP1 binding." *Science* 299(5607): 721-5.
- Cowieson, N. P., J. F. Partridge, R. C. Allshire and P. J. McLaughlin** (2000). "Dimerisation of a chromo shadow domain and distinctions from the chromodomain as revealed by structural analysis." *Curr Biol* 10(9): 517-25.
- Cremazy, F. G., E. M. Manders, P. I. Bastiaens, G. Kramer, G. L. Hager, E. B. van Munster, P. J. Verschure, T. J. Gadella, Jr. and R. van Driel** (2005). "Imaging in situ protein-DNA interactions in the cell nucleus using FRET-FLIM." *Exp Cell Res* 309(2): 390-6.
- Eissenberg, J. C. and S. C. Elgin** (2000). "The HP1 protein family: getting a grip on chromatin." *Curr Opin Genet Dev* 10(2): 204-10.
- Gaudin, V., M. Libault, S. Pouteau, T. Juul, G. Zhao, D. Lefebvre and O. Grandjean** (2001). "Mutations in LIKE HETEROCHROMATIN PROTEIN 1 affect flowering time and plant architecture in *Arabidopsis*." *Development* 128(23): 4847-58.
- <http://www.expasy.org/prosite/> (2006). Prosite.
- Jacobs, S. A. and S. Khorasanizadeh** (2002). "Structure of HP1 chromodomain bound to a lysine 9-methylated histone H3 tail." *Science* 295(5562): 2080-3.
- Kotake, T., S. Takada, K. Nakahigashi, M. Ohto and K. Goto** (2003). "*Arabidopsis* TERMINAL FLOWER 2 gene encodes a heterochromatin protein 1 homolog and represses both FLOWERING LOCUS T to regulate flowering time and several floral homeotic genes." *Plant Cell Physiol* 44(6): 555-64.
- Lachner, M., D. O'Carroll, S. Rea, K. Mechtler and T. Jenuwein** (2001). "Methylation of histone H3 lysine 9 creates a binding site for HP1 proteins." *Nature* 410(6824): 116-20.
- Libault, M., F. Tessadori, S. Germann, B. Snijder, P. Fransz and V. Gaudin** (2005). "The *Arabidopsis* LHP1 protein is a component of euchromatin." *Planta* 222(5): 910-25.
- Limpens, E., C. Franken, P. Smit, J. Willemse, T. Bisseling and R. Geurts** (2003). "LysM domain receptor kinases regulating rhizobial Nod factor-induced infection." *Science* 302(5645): 630-3.

- Lorentz, A., K. Ostermann, O. Fleck and H. Schmidt** (1994). "Switching gene swi6, involved in repression of silent mating-type loci in fission yeast, encodes a homologue of chromatin-associated proteins from *Drosophila* and mammals." Gene 143(1): 139-43.
- Lorvellec, M., J. Willemse, O. Kulikova, J. Verver and T. Bisseling** (Chapter 4).
- Meehan, R. R., C. F. Kao and S. Pennings** (2003). "HP1 binding to native chromatin in vitro is determined by the hinge region and not by the chromodomain." Embo J 22(12): 3164-74.
- Nakahigashi, K., Z. Jasencakova, I. Schubert and K. Goto** (2005). "The *Arabidopsis* heterochromatin protein1 homolog (TERMINAL FLOWER2) silences genes within the euchromatic region but not genes positioned in heterochromatin." Plant Cell Physiol 46(11): 1747-56.
- Nielsen, A. L., M. Oulad-Abdelghani, J. A. Ortiz, E. Remboutsika, P. Chambon and R. Losson** (2001). "Heterochromatin formation in mammalian cells: interaction between histones and HP1 proteins." Mol Cell 7(4): 729-39.
- Schmiedeberg, L., K. Weisshart, S. Diekmann, G. Meyer Zu Hoerste and P. Hemmerich** (2004). "High- and low-mobility populations of HP1 in heterochromatin of mammalian cells." Mol Biol Cell 15(6): 2819-33.
- Sprague, B. L. and J. G. McNally** (2005). "FRAP analysis of binding: proper and fitting." Trends Cell Biol 15(2): 84-91.
- Starr, T. E. and N. L. Thompson** (2002). "Fluorescence pattern photobleaching recovery for samples with multi-component diffusion." Biophys Chem 97(1): 29-44.
- Stuitje, A., E. Verbree, K. van der Linden, E. Mietkiewska, J.-P. Nap and T. Kneppers** (2003). "Seed-expressed fluorescent proteins as versatile tools for easy (co)transformation and high-throughput functional genomics in *Arabidopsis*." Plant Biotechnology Journal 1: 301-309.
- Takada, S. and K. Goto** (2003). "Terminal flower2, an *Arabidopsis* homolog of heterochromatin protein1, counteracts the activation of flowering locus T by CONSTANS in the vascular tissues of leaves to regulate flowering time." Plant Cell 15(12): 2856-65.
- Wang, G., A. Ma, C. M. Chow, D. Horsley, N. R. Brown, I. G. Cowell and P. B. Singh** (2000). "Conservation of heterochromatin protein 1 function." Mol Cell Biol 20(18): 6970-83.
- Zemach, A., Y. Li, H. Ben-Meir, M. Oliva, A. Mosquana, V. Kiss, Y. Avivi, N. Ohad and G. Grafi** (2006). "Different domains control the localization and mobility of LIKE HETEROCHROMATIN PROTEIN1 in *Arabidopsis* *nudei*." Plant Cell 18(1): 133-45.

Chapter 6: General Discussion

Joost Willemse, Joan Wellink and Ton Bisseling

In this chapter I will evaluate microscopic and other techniques that are currently used to study chromatin organization and dynamics.

Chromatin organisation studied by light microscopy

Most eukaryotes have rather large amounts of heterochromatin. This heterochromatin in general occurs in regions around the centromeres, but also in numerous areas along the chromosome arms. Interphase nuclei of such organisms show many heterochromatic regions and their complex organization does not facilitate microscopic analysis. Fortunately, some eukaryotes have rather small genomes and in addition their heterochromatin is primarily localized around the centromeres. Therefore their interphase nuclei only show heterochromatin in a few regions, which are the so-called chromocenters that can be clearly discerned from euchromatin. *Arabidopsis* has such a simple eu-heterochromatin distribution. However, small genomes are no guarantee for a simple chromatin organisation. For example rice, which has a genome size of 430 Mb has a more intermingled eu- and heterochromatin distribution. Especially organisms with such simple eu- and heterochromatin distribution are suitable to study the organization and dynamics of chromatin by microscopy. Furthermore, *Arabidopsis* has a rather thin and translucent root by which nuclei can even be studied in an intact organ.

A more detailed view of the position of DNA sequences within the nucleus can be obtained by Fluorescent In Situ Hybridization (FISH) studies. Such studies have shown that the *Arabidopsis* chromocenters consist of a central region containing the 180 bp centromeric tandem repeat sequence (pal1), and flanking pericentromeric heterochromatin containing numerous transposable elements (e.g. *athila*), and 5S rDNA loci (Fransz *et al.* 1998). Although pericentromeric heterochromatin is sometimes considered to be inert junk DNA, a recent finding of (Tessadori *et al.* Submitted) points to an important function. Upon transition from the vegetative to the reproductive state *Arabidopsis* nuclei reorganize. During this fate shift a loss of 75% of their heterochromatin is observed. Most pericentromeric heterochromatin is decondensed, and even the 180 bp repeat region is more dispersed (Tessadori *et al.* Submitted). After several days the chromocenters are slowly formed again (Tessadori *et al.* Submitted). The chromocenters are also shown to be an “anchor point” of euchromatic loops (Fransz and de Jong 2002). It is possible that these euchromatin- heterochromatin interactions represent a mechanism to control gene expression important for cell fate.

The importance of heterochromatin in controlling cell fate is underlined by the loss of heterochromatin during protoplast formation. When the protoplast forms a new cell wall heterochromatic chromocenters are again formed (Tessadori *et al.* Submitted). Therefore a useful parameter of chromatin organization in *Arabidopsis* interface nuclei is for example the amount of heterochromatin and the sequences that are part of it. Close examination of leaf nuclei showed that the heterochromatin percentage of a nucleus ($15 \pm 4\%$) is highly variable (Soppe *et al.* 2002). This is similar to what was observed for root nuclei (Willemse *et al.* Unpublished data). This indicates that the organization of nuclei within a certain tissue type is variable, although its biological significance is not clear.

FISH studies using sets of BACs that cover chromosomes or large chromosomal regions revealed insight in the organisation of chromosomes. Such studies for example have shown that chromosomes are spatially separated from each other creating distinct chromosome territories (Lysak *et al.* 2001; Pecinka *et al.* 2004). As already mentioned above FISH studies also revealed that the chromocenters are used as anchor points to which euchromatic loops are attached (Fransz and de Jong 2002). Within these loops the positioning of single genes can be determined, however, exact positioning of these genes is not possible due to limits in resolution of light microscopy. Therefore it might be difficult to determine whether a gene in the vicinity of a chromocenter is positioned just in- or outside the heterochromatic region. Furthermore, FISH studies are only possible on fixed material, by which the possibility to examine dynamic organization within the nucleus is eliminated.

A recently developed technique using several copies of a *lac* or *tet* operator sequence allows visualization of this sequence within nuclei of living cells (Belmont 2001; Gasser 2002). Insertion of these operator sequences into the genome creates a binding site, which after binding of a GFP tagged repressor is visible as a bright fluorescent spot within the nuclei. With this tool the organization and dynamics of loci can be studied in two ways. The relative distance to each other in a homozygous diploid plant can be determined, which can reveal the spatial organisation of the two chromosomes. Also the mobility of a locus in relation to for example, expression of nearby genes can be monitored. Further, when multiple repressor binding sites are present on a chromosome arm the distance between the loci can be monitored for example in relation to gene activity.

This kind of studies on *Arabidopsis* have so far shown that nuclear organization varies within nuclei of root cells, as the distance between two sites on the same

chromosome varies between 0.5 to 9 μm . Additionally, it is shown that chromatin is relatively dynamic, allowing localization changes up to 0.2 μm within an hour (Matzke *et al.* 2005). Such experiments are done to obtain insight in the properties of sequences that flank such repressor sites. Therefore the obtained information is indirectly related to the locus of interest. However, insertion of the repetitive operator sequence can lead to local heterochromatin formation, which might also affect the properties of the flanking regions. The potential that the repressor studies introduce artefacts is illustrated by studies with hamster kidney cells. Introduction of the repressor sequence into these cells led to the formation of a promyelocytic (PML) body at the integration site (Tsukamoto *et al.* 2000). In *Arabidopsis* the *lac* operator arrays associate with each other more often than other sequences (Pecinka *et al.* 2004), this also affects the flanking regions (Pecinka *et al.* 2005). Further, the sequences flanking the repressor insert show an increased association with *Arabidopsis* heterochromatin (Pecinka *et al.* 2005). These artifacts create the need for further refinement of this technique.

Additional organizational levels in euchromatin revealed by light microscopy

As discussed above *Arabidopsis* nuclei have a rather a simple organisation of eu- and heterochromatin. The density of euchromatin is rather homogeneous. However, the distribution of histone modifications that are located in euchromatin as well as the subnuclear localization of several chromatin remodelling proteins reveals additional levels of organisation in the euchromatic area. For example, the histone modifications H3K9m3, and H3K27m3 occur in a speckled pattern in the euchromatin and are more or less excluded from the heterochromatic chromocenters (Lorvellec *et al.* Chapter 4). Such a speckled occurrence in the euchromatin has also been observed for chromatin remodelling proteins like AtLHP1 (Gaudin *et al.* 2001; Lorvellec *et al.* Chapter 4), polycomb proteins (Hanson *et al.* 1999), for example VRN2 (Gendall *et al.* 2001) and some of the histone methyl transferases (SuvH) proteins (Kulikova and Lorvellec Personal communication). In case of AtLHP1 it has been shown that part of these speckles co-localise with H3K9m3 and/or H3K27m3 (Lorvellec *et al.* Chapter 4). Therefore it seems probable that these AtLHP1 speckles represent chromatin complexes that are used to regulate gene expression. Possibly the speckles formed by other chromatin remodelling proteins represent chromatin

complexes regulating other genes. Identification of the target genes inside these speckles is essential to understand the function of these complexes.

Quantification of speckle size and number can improve our understanding of these chromatin complexes, for example whether they most likely represent single target genes or multiple genes are regulated in a single speckle. The gene expression pattern is variable between cell types (Birnbaum *et al.* 2003), and probably differences in nuclear organisation will contribute to this. This variation in nuclear organisation between cell types makes it essential that the identity of the cell is known, which makes quantitative microscopy of single nuclei in intact tissue a powerful tool.

In chapter 2, I have described a semi-automated method to quantify the DNA content of single nuclei within roots. This method can be easily used or adapted for any property that can be visualized by fluorescence. For example histone modifications and cytosine methylation, for which antibodies are available which can be used to visualize the global distribution, can thus be quantified. Quantification of parameters (number, size, intensity, nuclear location) of subnuclear structures would require additional programming. Furthermore, the identification of substructures requires a good signal to noise ratio.

ChIP-chip to study chromatin organization

The interaction of chromatin remodeling proteins and genomic DNA has also been studied by ChIP-chip experiments. For example, such a study has confirmed the euchromatic localization of AtLHP1, and additionally has identified ~260 target genes evenly spread on chromosome 4 (Turck *et al.* Submitted). Assuming that putative targets are evenly spread along the *Arabidopsis* genome, this would imply that around 1750 target genes of AtLHP1 exist. The number of speckles in a nucleus (~50) is markedly smaller than the number of target genes. In part this might be explained by cell type or developmental stage specificity of targets. However, it seems unlikely that this can fully account for the large difference. Therefore, it is possible that speckles can contain up to 30 target genes. Since target genes are not clustered on the genome this would involve a specific organisation of the euchromatin, although we cannot exclude the possibility that only a subset of the target genes is bound by sufficient AtLHP1 to visualize them as speckles within the nucleus.

FISH studies could distinguish between these options and could reveal whether multiple targets within a speckle correspond to neighboring targets of a chromosome

region, or originate from different locations of a chromosome. Further, FISH will be powerful to determine to what extent targets are cell type specific. FISH will be powerful to demonstrate that multiple target genes are located within a speckle. However, the resolution obtained with most light microscopic techniques is not sufficient to prove for each identified putative target gene that it really localizes in these speckles. It might be positioned close to a speckle due to being located close to a real target gene.

The use of whole genome ChIP approaches has other limitations, the obtained information only shows the “average” of a large number of cells, whereas microscopy is cell type specific. The isolation of large amounts of cells of a specific cell type is possible, but tedious and labour intensive (Birnbaum *et al.* 2003). In conclusion, both methods have their own advantages and drawbacks; in general the obtained information is complementary and collectively they are most powerful.

Limitations of and new developments in light microscopy for studying chromatin organization

As described above the resolution of light microscopy can be a bottleneck in studies on nuclear organisation. The major limitation of light microscopy is determined by the light optical resolution (Abbe 1873). This determines the minimum distance between objects allowing them to be imaged as two separate objects, instead of one merged object. Fluorescence imaging increased the resolution over normal light microscopy to around 250nm (Malkusch *et al.* 2001), due to the lower wavelength of the light used for excitation of the fluorophores. The Nyquist theorem for defining the maximal axial resolution shows that the axial resolution is much lower than the lateral resolution, globally around 1 μ m. Using water immersion objectives, and low wavelengths to excite the fluorophores can boost this resolution up to 650 nm.

So what is the impact of this resolution limit at a microscopical level for the resolution by which chromatin organisation can be analyzed? The meristematic nuclei of *Arabidopsis* have an average diameter of 3.3 μ m, by which its volume is $\sim 18 \mu\text{m}^3$. The smallest illuminated volume taking into account the resolution limits as described above is $\sim 0.02 \mu\text{m}^3$ ($4/3 \pi * 0.125^2 * 0.325$). The amount of DNA in a diploid *Arabidopsis* nucleus is ~ 300 Mb. Therefore, the smallest illuminated volume will contain on average 330 Kb of DNA. Based on the average gene density of *Arabidopsis* this region (The *Arabidopsis*

Genome Initiative 2000) contains ~75 genes, which illustrates the limits of fluorescence microscopy in identification of target genes.

Currently new advanced microscopy techniques with higher axial and/or lateral resolution are being created. The next steps in improving resolution can be based on mathematics; for example, using deconvolution or innovative background subtraction methods. These advances can enhance the light microscopic resolution around twofold (Heintzmann *et al.* 2003). Another improvement is obtained by the development of several innovative techniques capable of penetrating living tissue. These so-called invasive techniques with improved resolution are multifocal, multiphoton microscopy (MMM-4Pi), and I⁵M that combines incoherent image interference microscopy (I³M) with image interference microscopy (I²M), which can increase the resolution inside living tissue to 100 nm. STimulated Emission Depletion (STED) goes one step further; by adapting the physical properties of the microscopes point spread function a resolution of 30 nm can be obtained (Garini *et al.* 2005). This super resolution would in the case of *Arabidopsis* imply that adjacent genes can be identified as individual objects and so would provide a major improvement in analysing chromatin organisation.

Förster Resonance Energy Transfer (FRET) as a tool to study protein interactions.

In addition to accurate localization data it is important to obtain information on the molecular behavior of chromatin components; for example, their dynamic properties (see following paragraph) and their ability to interact with other components. Protein-protein and protein-DNA interactions can be studied using FRET, acting as a microscopic ruler determining distances between proteins and/or DNA. The technique is useful for determining interactions, but it only reveals interactions when the distance between the molecules is less than 10 nm. Therefore, proteins could have no FRET interaction even when they are present in the same complex. So far FRET studies have provided information about protein-DNA interaction of histones, and HP1 (Cremazy *et al.* 2005; Lorvellec *et al.* Chapter 4). Additionally, they have led to a model of nucleosome stability (Li and Widom 2004). Further, differential effects of H3 acetylation and H4 acetylation on nucleosome DNA interaction have been identified. This kind of characterization of histone modifications will advance the knowledge of the histone code (Toth *et al.* 2006). Although FRET has not yet frequently been applied in chromatin research it is clear it has great potential to provide more insight into *in vivo* complex formation and behavior.

A disadvantage for FRET-FLIM measurements is the temporal resolution for acquiring data; a single FRET measurement takes between 15 and 120 seconds. Since nuclear processes occur at shorter time intervals changes can occur during the acquisition of the image and these will be averaged. A similar problem arises when measuring pools of proteins at one location, especially if not all are involved in identical processes. The measured lifetime will be an average of the two processes, with limited mathematical possibility of extracting two separate interaction processes.

FRAP as a tool to study dynamics and interaction.

A technique to study the dynamics of molecules/proteins within living cells is FRAP. Especially for chromatin proteins, which are present at relatively high concentration and have a slow mobility, FRAP is the preferred technique. Although the technique only measures average properties of a large population of molecules (Anderson *et al.* 1992) it has been successfully applied to for example DNA repair proteins, revealing that the subunits of a repair complex first assemble on the site of DNA damage. The time span DNA repair takes could be quantified (Houtsmuller *et al.* 1999; Essers *et al.* 2006). Furthermore a transient chromatin binding has been observed for several DNA repair proteins (Pryde *et al.* 2005). These studies show the potential that information about the dynamic behaviour of nuclear proteins can provide.

So far the mobility of several histones has been investigated. Acetylation and phosphorylation of H1 increase H1 mobility, indicating a destabilization of chromatin (Lever *et al.* 2000; Mistelli *et al.* 2000). Histone mobility studies performed in HeLa cells have revealed several populations of H2B with different mobilities whereas the mobility of H3 and H4 is rather uniform (Kimura and P.R. 2001; Kimura *et al.* 2004). We used FRAP as a tool to investigate H2B exchange in euchromatin, heterochromatin and centromeric heterochromatin of *Arabidopsis*. The mobility of this histone markedly differs between these chromatin regions, which revealed that the three populations observed in HeLa cells most likely arise from these different forms of chromatin. Additionally we tried to identify the effect of RNA polymerase II activity on histone mobility in the various chromatin regions. Unfortunately, the variability in the RNA polymerase inhibition in our studies was too high to interpret the results. In the following paragraph I will discuss if RNA polymerase II activity could be responsible for all H2B mobility.

The role of transcription in H2B mobility in Arabidopsis

FRAP experiments have shown that about 50% of H2B present in euchromatin is surprisingly mobile, indicating that H2B is replaced in euchromatic nucleosomes every two minutes (Willemse *et al.* Chapter 3), whereas the other 50% is immobile (Willemse *et al.* Chapter 3). Based on the average gene size, gene number and the size of the *Arabidopsis* genome about 50% of the euchromatic part of the *Arabidopsis* genome is transcribed. Therefore, we wondered if transcription could account for the mobile population of H2B in the euchromatic regions of the nucleus. Transcription influences nucleosomes in two manners; when a polII unit passes a nucleosome a H2A/H2B dimer is displaced, furthermore a nucleosome can be repositioned to give access to the underlying DNA. However, the process of nucleosome translocation along the DNA strand will hardly contribute to the observed mobility since the distance at which this movement occurs is small compared to the size of a bleached region in a FRAP study. Therefore H2A/H2B dimer displacement caused by a passing polII complex (Kireeva *et al.* 2002) is the only transcription related process that influences H2B mobility. Based on the assumption that the number of mRNAs in *Arabidopsis* cells is similar to what is observed in rat liver cells a steady state level of ~360.000 mRNA molecules/cell might be present (Kane *et al.* 2000). If we also assume that the average transcript lifetime is ~15 minutes as is the case in yeast (Holstege *et al.* 1998; Cao and Parker 2001), then about 400 mRNA molecules will have to be produced per second to retain the steady state level. Since for *Arabidopsis* the average gene length is ~2000 bp, the transcription machinery in the cell has to transcribe ~800 kb/s. With the average spacing of 1 nucleosome per 200 bp, the transcription machinery will have to pass ~4000 nucleosomes every second. In 2C cells there will be 1.1 million nucleosomes located in euchromatic areas (15% of the DNA is heterochromatic). Each second, 0.4% of the nucleosomes is passed by a RNA polymerase II complex. Since this is reported to displace a H2A/H2B dimer from the nucleosome (Kireeva *et al.* 2002), 0.2% of the H2Bs in a cell will be displaced each second. Assuming an equal distribution of genes within a bleached region, also 0.2% of the H2Bs in a bleach region will be displaced. From this a theoretical recovery curve can be calculated $(1-(1-x)^t)$ which has a $T_{1/2}$ of 378s, which is ~5-fold longer than the $T_{1/2}$ obtained from our FRAP experiments. Therefore it seems unlikely that transcription can fully account for the observed H2B mobility.

Also the number of RNA polymerases and their activity can provide insight in the contribution of transcription to mobility. DNA is transcribed by pol II at a rate of about 20

nt/s, and in HeLa cells on average one pol II is active on a gene (Shermoen and O'Farrell 1991; Jackson *et al.* 1998). It is estimated that the number of active RNA pol II's is about 75000 in tetraploid HeLa cells (Jackson *et al.* 1998). Based on the assumption of a linear relation between ploidy and mRNA level and a comparable number of genes in the human and *Arabidopsis* genome, this should mean that around 37500 polymerase II units are active in a *Arabidopsis* 2C cell. These would displace 3750 H2B/s ($37500 \times 20/200$), which is close to number obtained by the calculation based on the amount of mRNAs/cell (~4000).

Based on the considerations described above transcription probably only contributes a little bit to the observed H2B exchange in the euchromatin. Other processes that could contribute to the observed movement of H2B are DNA replication and repair (Tsukuda *et al.* 2005) and histone exchange to alter histone modifications without the need for enzymes (Davie and Dent 2002). Breathing of nucleosomes will probably involve histone movement as well (Li *et al.* 2005; Tomschik *et al.* 2005). These processes will occur at different time intervals, therefore the observed H2B mobility is probably an interplay of all these processes.

In conclusion the advantage of microscopy is its cell type specificity and the possibility to apply it *in vivo*. Chapter two reports the endoreduplication of the vascular tissue in a very early stage of development. In Chapter 3 I have shown that H2B movement is influenced by chromatin organization and although transcription influences its mobility it cannot fully account for this displacement. These studies show that microscopic tools are useful in investigating chromatin remodelling, especially in combination with data obtained from whole genome studies or *in vitro* studies.

References

- Anderson, C. M., G. N. Georgiou, I. E. Morrison, G. V. Stevenson and R. J. Cherry** (1992). "Tracking of cell surface receptors by fluorescence digital imaging microscopy using a charge-coupled device camera. Low-density lipoprotein and influenza virus receptor mobility at 4 degrees C." *J Cell Sci* **101** (Pt 2): 415-25.
- Beldmont, A. S.** (2001). "Visualizing chromosome dynamics with GFP." *Trends Cell Biol* **11**(6): 250-7.
- Birnbaum, K., D. E. Shasha, J. Y. Wang, J. W. Jung, G. M. Lambert, D. W. Galbraith and P. N. Benfey** (2003). "A gene expression map of the Arabidopsis root." *Science* **302**(5652): 1956-60.
- Cao, D. and R. Parker** (2001). "Computational modeling of eukaryotic mRNA turnover." *Rna* **7**(9): 1192-212.
- Cremazy, F. G., E. M. Manders, P. I. Bastiaens, G. Kramer, G. L. Hager, E. B. van Munster, P. J. Verschure, T. J. Gadella, Jr. and R. van Driel** (2005). "Imaging in situ protein-DNA interactions in the cell nucleus using FRET-FLIM." *Exp Cell Res* **309**(2): 390-6.
- Davie, J. K. and S. Y. R. Dent** (2002). "Translational control: an activating role for arginine methylation." *Current Biology* **12**: r59-61.
- Essers, J., A. B. Houtsmuller and R. Kanaar** (2006). "Analysis of DNA recombination and repair proteins in living cells by photobleaching microscopy." *Methods Enzymol* **408**: 463-85.
- Fransz, P., S. Armstrong, C. Alonso-Blanco, T. C. Fischer, R. A. Torres-Ruiz and G. Jones** (1998). "Cytogenetics for the model system Arabidopsis thaliana." *Plant J* **13**(6): 867-76.
- Fransz, P. F. and J. H. de Jong** (2002). "Chromatin dynamics in plants." *Curr Opin Plant Biol* **5**(6): 560-7.
- Garini, Y., B. J. Vermolen and I. T. Young** (2005). "From micro to nano: recent advances in high-resolution microscopy." *Curr Opin Biotechnol* **16**(1): 3-12.
- Gasser, S. M.** (2002). "Visualizing chromatin dynamics in interphase nuclei." *Science* **296**(5572): 1412-6.
- Gaudin, V., M. Libault, S. Pouteau, T. Juul, G. Zhao, D. Lefebvre and O. Grandjean** (2001). "Mutations in LIKE HETEROCHROMATIN PROTEIN 1 affect flowering time and plant architecture in Arabidopsis." *Development* **128**(23): 4847-58.
- Gendall, A. R., Y. Y. Levy, A. Wilson and C. Dean** (2001). "The VERNALIZATION 2 gene mediates the epigenetic regulation of vernalization in Arabidopsis." *Cell* **107**(4): 525-35.
- Hanson, R. D., J. L. Hess, B. D. Yu, P. Ernst, M. van Lohuizen, A. Berns, N. M. van der Lugt, C. S. Shashikant, F. H. Ruddle, M. Seto and S. J. Korsmeyer** (1999). "Mammalian Trithorax and polycomb-group homologues are antagonistic regulators of homeotic development." *Proc Natl Acad Sci U S A* **96**(25): 14372-7.

- Heintzmann, R., V. Sarafis, P. Munroe, J. Nailon, Q. S. Hanley and T. M. Jovin** (2003). "Resolution enhancement by subtraction of confocal signals taken at different pinhole sizes." Micron **34**(6-7): 293-300.
- Holstege, F. C., E. G. Jennings, J. J. Wyrick, T. I. Lee, C. J. Hengartner, M. R. Green, T. R. Golub, E. S. Lander and R. A. Young** (1998). "Dissecting the regulatory circuitry of a eukaryotic genome." Cell **95**(5): 717-28.
- Houtsmuller, A. B., S. Rademakers, A. L. Nigg, D. Hoogstraten, J. H. Hoeijmakers and W. Vermeulen** (1999). "Action of DNA repair endonuclease ERCC1/XPF in living cells." Science **284**(5416): 958-61.
- Initiative, T. A. G.** (2000). "Analysis of the genome sequence of the flowering plant *Arabidopsis thaliana*." Nature **408**(6814): 796-815.
- Jackson, D. A., F. J. Iborra, E. M. Manders and P. R. Cook** (1998). "Numbers and organization of RNA polymerases, nascent transcripts, and transcription units in HeLa nuclei." Mol Biol Cell **9**(6): 1523-36.
- Kane, M. D., T. A. Jatkoe, C. R. Stumpf, J. Lu, J. D. Thomas and S. J. Madore** (2000). "Assessment of the sensitivity and specificity of oligonucleotide (50mer) microarrays." Nucleic Acids Res **28**(22): 4552-7.
- Kimura, H., M. Hieda and P. R. Cook** (2004). "Measuring histone and polymerase dynamics in living cells." Methods Enzymol **375**: 381-93.
- Kimura, H. and C. P.R.** (2001). "kinetics of core histones in living human cells: little exchange of h3 and h4 and some rapid exchange of h2b." the journal of cell biology **153**(7): 1341-1353.
- Kireeva, L., Walter W., Tchernajenko V., Bondarenko V., Kashlev M. and S. V.M.** (2002). "Nucleosome Remodeling Induced by RNA Polymerase II: Loss of the H2A/H2B Dimer during Transcription." Molecular Cell **9**: 541-552.
- Kulikova, O. and M. Lorvellec** (Personal communication).
- Lever, A. M., Th'ng J.P.H., Sun X. and H. M.J.** (2000). "Rapid exchange of histone H1.1 on chromatin in living human cells." Nature **408**(14-december 2000): 873-876.
- Li, G., M. Levitus, C. Bustamante and J. Widom** (2005). "Rapid spontaneous accessibility of nucleosomal DNA." Nat Struct Mol Biol **12**(1): 46-53.
- Li, G. and J. Widom** (2004). "Nucleosomes facilitate their own invasion." Nat Struct Mol Biol **11**(8): 763-9.
- Lorvellec, M., J. Willemse, O. Kulikova, J. Verver and T. Bisseling** (Chapter 4). "LHP1 forms chromatin complexes at trimethylated histones."
- Lysak, M. A., P. F. Fransz, H. B. Ali and I. Schubert** (2001). "Chromosome painting in *Arabidopsis thaliana*." Plant J **28**(6): 689-97.

- Malkusch, W., H. Bauch and L. Schafer** (2001). "Digital light microscopy: prerequisite for optimum contrast enhancement and increase of resolution." Exp Gerontol **36**(7): 1199-217.
- Matzke, A. J., B. Huettel, J. van der Winden and M. Matzke** (2005). "Use of two-color fluorescence-tagged transgenes to study interphase chromosomes in living plants." Plant Physiol **139**(4): 1586-96.
- Mistelli, T., Gunjan A., Bustin M. and B. D.T.** (2000). "Dynamic binding of histone H1 to chromatin in living cells." Nature **408**(14 december 2000): 877-881.
- Pecinka, A., N. Kato, A. Meister, A. V. Probst, I. Schubert and E. Lam** (2005). "Tandem repetitive transgenes and fluorescent chromatin tags alter local interphase chromosome arrangement in *Arabidopsis thaliana*." J Cell Sci **118**(Pt 16): 3751-8.
- Pecinka, A., V. Schubert, A. Meister, G. Kreth, M. Klatte, M. A. Lysak, J. Fuchs and I. Schubert** (2004). "Chromosome territory arrangement and homologous pairing in nuclei of *Arabidopsis thaliana* are predominantly random except for NOR-bearing chromosomes." Chromosoma **113**(5): 258-69.
- Pryde, F., S. Khalili, K. Robertson, J. Selfridge, A. M. Ritchie, D. W. Melton, D. Jullien and Y. Adachi** (2005). "53BP1 exchanges slowly at the sites of DNA damage and appears to require RNA for its association with chromatin." J Cell Sci **118**(Pt 9): 2043-55.
- Shermoen, A. W. and P. H. O'Farrell** (1991). "Progression of the cell cycle through mitosis leads to abortion of nascent transcripts." Cell **67**(2): 303-10.
- Soppe, W. J., Z. Jasencakova, A. Houben, T. Kakutani, A. Meister, M. S. Huang, S. E. Jacobsen, I. Schubert and P. F. Fransz** (2002). "DNA methylation controls histone H3 lysine 9 methylation and heterochromatin assembly in *Arabidopsis*." Embo J **21**(23): 6549-59.
- Tessadori, F., M.-C. Chupeau, Y. Chupeau, M. Knip, R. v. Driel, P. Fransz and V. Gaudin** (Submitted). "Large-scale chromatin decondensation and recondensation during nuclear reprogramming in *Arabidopsis* protoplasts."
- Tomschik, M., H. Zheng, K. van Holde, J. Zlatanova and S. H. Leuba** (2005). "Fast, long-range, reversible conformational fluctuations in nucleosomes revealed by single-pair fluorescence resonance energy transfer." Proc Natl Acad Sci U S A **102**(9): 3278-83.
- Toth, K., N. Brun and J. Langowski** (2006). "Chromatin compaction at the mononucleosome level." Biochemistry **45**(6): 1591-8.
- Tsukamoto, T., N. Hashiguchi, S. M. Janicki, T. Tumbar, A. S. Belmont and D. L. Spector** (2000). "Visualization of gene activity in living cells." Nat Cell Biol **2**(12): 871-8.
- Tsukuda, T., A. B. Fleming, J. A. Nickoloff and M. A. Osley** (2005). "Chromatin remodelling at a DNA double-strand break site in *Saccharomyces cerevisiae*." Nature **438**(7066): 379-83.

Turck, F., F. Roudier, S. Farrona, E. Guillaume, R. Martienssen, V. Colot and G. Couplang (Submitted). "Arabidopsis TFL2/LHP1 is Polycomb Group Protein that associates with a large set of genes encoding developmental regulators."

Willemse, J., J. Wellink and T. Bisseling (Chapter 3). "Histone 2B exchange in arabidopsis."

Summary

Summary

Genetic information of eukaryotic organisms is stored as DNA in the nuclei of their cells. Nuclear DNA is associated with several proteins, which together form chromatin. The most abundant chromatin proteins are histones, they arrange the initial packaging step of the DNA. DNA staining reveals two cytogenetically different versions of chromatin; lightly stained euchromatin and intensely stained heterochromatin. Heterochromatinization is used to keep DNA elements selectively repressed. Several modifications on histones and/or DNA are used to distinguish eu- from heterochromatin. The histone modifications are collectively called the histone code. HP1 is one of the proteins that can bind histone modifications; it has a bi-partite organization to allow simultaneous binding to histones as well as to other proteins. *Arabidopsis thaliana*, the model plant to investigate chromatin organization, has a small genome and a simple distribution of eu- and heterochromatin allowing an easy distinction between the two forms of chromatin by light microscopy. The fixed division pattern of the Arabidopsis root allows monitoring of the chromatin organization through developmental progression. The dynamic chromatin organization in Arabidopsis is investigated in this thesis.

Chapter 2 describes a semi-automated method to quantify fluorescence intensity in intact organs and tissues, composed of several cell layers. The method has been developed and tested on whole mount preparations of Arabidopsis root tips containing Propidium Iodide stained nuclei. With a diameter of less than 150 μm the root tip is thin enough for standard confocal 3D microscopy, which makes the organ very suitable for whole mount imaging. Advantages of the root as model system for such a study are the lack of chlorophyll and the presence of transparent cell walls with only little background fluorescence. In addition the technique enables structural and quantitative analyses of stereotypic tissue patterns and cell position, thus providing important information about the developmental history of every cell. With our method we now can measure DNA amounts in spatially reconstructed nuclei of a complete root tip. In our novel *averaging 3D method* we calculate the mean of the summed fluorescence intensities of all nuclear sections of one nucleus and interpolate the missing sections, thereby avoiding small detection problems with accuracy comparable with the existing 3D methods. The quantification showed that vascular tissue cells endoreduplicate after the first cell division from the stem cell. Furthermore, cortical and endodermal cells progress through the cell cycle at comparable velocity as mother and daughter cells, as visualized by groups of cells containing increased amounts of DNA. The organizational changes in chromatin during development led us to investigate mobility of principal parts of chromatin like histones and histone binding proteins.

Histones are the proteins organizing the first step of folding DNA into chromatin fibers. These organizing proteins need to be flexibly positioned on the DNA to allow accession to the DNA for several processes. By making use of H2B-YFP expressing plants in a wt and in a DNA methylation mutant (ddm1) background, the mobility of the core histone H2B was analysed using FRAP (Chapter 3). In both transgenic plants the heterochromatic sequences appeared, in the majority of the nuclei, as distinct spots which allowed us to determine the mobility of H2B in euchromatic, heterochromatic, and centromeric regions. The mobility of H2B was measured on a time scale of about half an hour in living cells of intact roots and three distinguishable fractions of H2B were found; a euchromatic mobile fraction, a less mobile heterochromatic fraction and an immobile fraction. The half time of recovery in euchromatin was about 80 seconds, therefore the binding time of a H2B protein inside a nucleosome is around 2 minutes in these regions. Heterochromatic mobility of H2B was slower with a half time of recovery of about 7 minutes. The centromeric H2B was shown not to be mobile at all (immobile fraction 95%). Since histones seem to be reasonably fixed in position especially in heterochromatin we wondered about the dynamics of histone binding proteins.

AtLHP1 the HP1 homologue in Arabidopsis was shown to be located in foci in the euchromatic area of interphase root cell nuclei in which relatively high levels of H3K9m3 and/or H3K27m3 occur (Chapter 4), and by using FRET-FLIM, to closely interact with DNA. The interaction with DNA was quite loose as FRAP data shows an average binding time of 1.2 seconds. The mobility of AtLHP1 did not differ between foci and interfoci, and also no distinction in DNA binding efficiency was observed. The AtLHP1 containing foci most likely represent chromatin complexes controlling the expression of genes present in these foci.

Using mutated versions of AtLHP1 from which the Chromodomain (CD), Chromoshadow domain (CSD), the Acidic domain (AD), or the conserved part of the hinge (H) were deleted we assessed the functions of these separate domains (Chapter 5). Localization studies showed that the CD and H are essential for foci formation, whereas no influence of deletions of the CSD or AD were observed. FRET-FLIM data showed that the CSD and AD are essential for DNA binding anywhere in the nucleus, while deletion of the CD did not have any effect on the DNA binding capacity of AtLHP1. FRAP data indicated that the AD is essential to keep AtLHP1 mobile, whereas the CD, and CSD are essential for binding. Based on these results a hypothetical model of AtLHP1 functioning is presented (Chapter 5).

In Chapter 6 the results obtained in the preceding chapters are discussed. Limits of the microscopical techniques used in this thesis are evaluated. Furthermore the histone displacement caused by transcription is discussed.

Nederlandse Samenvatting

Genetische informatie van eukaryote organismen is opgeslagen in de kernen van de cellen waaruit organismen zijn opgebouwd. Hierbij zijn meerdere eiwitten betrokken, en samen met het DNA wordt dit chromatine genoemd. De meest voorkomende chromatine eiwitten zijn de histonen, die zijn betrokken bij de eerste condensatie stap van het DNA in nucleosomen. Met behulp van DNA kleuring kunnen met behulp van de microscoop twee soorten chromatine onderscheiden worden, licht gekleurd euchromatine en intens gekleurd heterochromatine. Het DNA dat in heterochromatine voorkomt komt niet of nauwelijks tot expressie. Eu- en heterochromatine worden ieder gekenmerkt door specifieke modificaties op histonen en DNA. Alle histon modificaties samen vormen de histone code die een belangrijke rol speelt bij gen expressie en kern organisatie. Heterochromatine proteïne 1 (HP1) is een van de eiwitten die kan binden aan een histon met een specifieke modificatie. *Arabidopsis thaliana*, de model plant die we voor onze studie aan chromatine organisatie hebben gebruikt, heeft een klein genoom waarin het verschil tussen eu- en heterochromatine duidelijk zichtbaar is, wat niet in alle organismen mogelijk is. Het vaste delingspatroon van de wortel maakt het gemakkelijk om de chromatine organisatie gedurende de ontwikkeling te volgen. In dit proefschrift is de dynamische organisatie van chromatine in *Arabidopsis* bestudeerd.

Hoofdstuk 2 beschrijft de ontwikkeling van een nieuwe methode om de hoeveelheid DNA in individuele kernen in de wortel van *Arabidopsis* te bepalen. Deze techniek maakt het mogelijk om de DNA hoeveelheden in alle kernen in een intact weefsel te bepalen terwijl de positie informatie bewaard blijft. Door het vaste delingspatroon van de wortel kon de hoeveelheid DNA daarna gerelateerd worden aan het cel type. De kwantificatie maakte duidelijk dat de cellen in de vaatbundel geëndoredupliceerd zijn na de eerste celdeling gerekend vanaf de stam cel. De cel cyclus progressie in de corticale en endodermale cellen verloopt ongeveer gelijk met de naastliggende cellen, dit is zichtbaar doordat groepen van cellen tegelijkertijd een verhoogde hoeveelheid DNA bevatten. De veranderingen die optreden in de organisatie van het chromatine tijdens de ontwikkeling van de wortel, waren de aanleiding om de mobiliteit van onderdelen van het chromatine, zoals histonen en histon bindende eiwitten, te gaan onderzoeken.

Histonen zijn betrokken bij de eerste condensatie stap van het DNA waarbij een 10 nm chromatine streng gevormd wordt. Deze eiwitten moeten flexibel gepositioneerd zijn in het chromatine zodat verschillende processen toegang hebben tot het onderliggende DNA. Door gebruik te maken van planten waarin functioneel H2B-YFP tot expressie komt in een wild type plant en een DNA methylatie mutant (ddm1) achtergrond is de mobiliteit van Histon 2B bepaald m.b.v. Fluorescentie Recovery After Photo bleaching (FRAP) techniek in euchromatine,

heterochromatine en het centromeer gebied (Hoofdstuk 3). De halfwaarde tijd van het fluorescentie herstel was ongeveer 80 seconden in euchromatine, zodat de bindingstijd van een H2B molecuul binnen een nucleosoom ongeveer 2 minuten is. In het heterochromatine is de mobiliteit lager met een halfwaardetijd van ongeveer 7 minuten. De centromeer gelokaliseerde H2B eiwitten waren helemaal niet mobiel (immobiele fractie 95%). Omdat histonen redelijk vast liggen, zeker in heterochromatine, vroegen we ons af hoe dynamisch histone bindende eiwitten zijn.

Hoofdstuk 4 beschrijft hoe LHP1, de HP1 homolog in Arabidopsis, hiervoor is gebruikt. In de kernen van wortel cellen van transgene planten waarin functioneel LHP1-GFP tot expressie komt werd LHP1 in foci in het euchromatine aangetroffen. In deze foci werden relatief grote hoeveelheden van de H3K9me3 en/of H3K27me3 modificatie gevonden, en gebruik makend van FRET-FLIM werd aangetoond dat LHP1 een interactie heeft met DNA. De interactie met DNA is flexibel, en met behulp van FRAP werd bepaald dat een LHP1 molecuul gemiddeld 1.2 seconden bindt. De mobiliteit van LHP1 verschilt niet tussen de foci en buiten de foci, en ook is er geen verschil in de affiniteit voor DNA gevonden. De foci bestaan waarschijnlijk uit LHP1 bevattende chromatine complexen, die specifieke genen reguleren.

Door gebruik te maken van gemuteerde LHP1 eiwitten, waarvan het Chromodomein (CD), het Chromoshadow domein (CSD), het Zure domein (ZD), of het geconserveerde deel van de hinge (H) waren verwijderd, werden de functies van de verschillende domeinen bepaald (Hoofdstuk 5). De lokalisatie van de deletie mutanten in de kern lieten zien dat het CD en H noodzakelijk zijn om foci te creëren, terwijl de CSD en ZD geen invloed op de foci formatie hebben. FRET-FLIM studies lieten zien dat het CSD en ZD nodig zijn om aan DNA te kunnen binden. Deletie van het CD resulteerde niet in een verminderde affiniteit voor DNA. Uit de FRAP experimenten bleek dat het ZD nodig is om LHP1 mobiel te houden, terwijl het CD en CSD nodig zijn om te binden aan het chromatine. Gebaseerd op deze resultaten, en resultaten van eerdere studies is een model gemaakt dat beschrijft hoe LHP1 functioneert.

Hoofdstuk 6 bevat een algemene discussie over de verkregen resultaten, en een evaluatie van de beperkingen van de microscopische technieken die gebruikt zijn in dit onderzoek. Tevens wordt de mobiliteit van histonen die veroorzaakt wordt door transcriptie bediscussieerd.

Dankwoord

Na een lange tijd in Wageningen is het dan eindelijk zo ver, het proefschrift is af en er rest enkel nog de verdediging voordat ik gepromoveerd ben. Het was een leuke tijd waarbij ik genoten heb van de altijd gezellige sfeer op Molbi en van de gezellige mensen, vaste medewerkers, AIO's en studenten die daar rond neigen te hangen.

Als eerste wil ik mij promotor Ton Bisseling, die ook mijn directe begeleider was bedanken voor de stevige discussies die we hebben gevoerd, en de ideeën die we hebben besproken over de experimenten. Ook vond ik de vrijheid om zelf experimenten te bedenken, te plannen en uit te voeren hier erg fijn. Ook Joan heeft mij veel geholpen tijdens voornamelijk de laatste periode van mijn promotieonderzoek. Het schrijven werd een stuk makkelijker doordat jij al die uren hebt gestopt in het kritisch nakijken van de hoofdstukken. Hans zonder jouw wetenschappelijk inzicht en geduld om een verhaal uit mij te trekken was het eerste hoofdstuk nooit tot stand gekomen, bedankt hiervoor en voor alle andere dingen die je voor me gedaan hebt. Maelle, ook voor jou in het Nederlands, bedankt voor de fijne discussies die we hebben gehad, zowel op werk gerelateerd gebied als daarbuiten. Het is fijn dat je een collega hebt waarbij je je verhaal kwijt kan. Verder wil ik je ook bedanken voor de experimentele ondersteuning en de achtergrondmuziek op onze kamer. Jan Verver, jij hebt me naast de meeste ins en outs van het kloneren ook geleerd dat photoshop je vriend is. Olga your drive to keep doing experiments helped filling in parts of this book as well. Ludmilla, thanks for always thinking about your “neighbours” when stumbling upon a nice article.

Tijdens mijn promotie heb ik een aantal studenten begeleid tijdens hun afstuderen, ook zij hebben veel bijgedragen aan dit boekje en hen wil ik dus ook bedanken voor alle input. Maureen, bedankt voor alle discussies die we gehad hebben over AtLHP1 en het model dat we hiermee hebben samengesteld, ik hoop dat je net zo eigenzinnig door je promotie heenloopt als dat je hier bij je afstudeervak hebt gedaan. Paula, bedankt voor je inzet en je harde werken, ook al was er niet altijd genoeg te doen voor twee personen op mijn project heb je je altijd ingezet om een zo goed mogelijk resultaat te bereiken. Martijn, helaas staat nauwelijks iets van jouw experimenten in dit boekje maar toch nogmaals bedankt voor het complementeren van de FRAP data van sommige AtLHP1 mutanten. Wouter, het was van begin af aan duidelijk dat je al meerdere afstudeervakken gedaan had, je wist hoe alles werkte en een idealere afstudeerstudent kan je niet begeleiden. Bedankt

Dankwoord

voor alle dingen die je gedaan hebt met de cellijnen en ook al kwam er weinig resultaat uit vond ik het erg plezierig samenwerken. Ook de discussies die we gehad hebben over de theoretische verplaatsing van H2B was erg interessant en leerzaam voor ons beide denk ik, succes verder.

Boudewijn, Mark Hink en Jan-Willem, zonder jullie had ik nu nooit zoveel geweten over de technische kant van microscopie, bedankt voor alle uitleg en hulp bij de experimenten. Verder natuurlijk ook een bedankje voor alle andere mensen op het lab die me geholpen hebben met verschillende dingen tijdens mijn promotie. Ook alle mensen van de lunchgroep (Jeroen, Tinri, Stefan, Eric, Pieter, Harm, Gerben, Marjolein, Stefan, Andreas, Sylvester, Diederik, Rianne) van Molbi/Bioinformatica het was altijd een punt van rust tijdens de dag waarbij de discussies altijd uiteenliepen van politiek tot melkbingo.

Buiten het lab wil ik voor de nodige ontspanning iedereen van de AD&D groep bedanken, de WDC en natuurlijk Sandra en Marcel met wie we vele leuke concerten hebben bezocht. Pa en Ma bedankt voor een luisterend oor op de momenten dat ik er behoefte aan had.

Als laatste wil ik Chantal bedanken, voor de support en motivatie die ik vooral aan het einde nodig had om door te zetten. Bedankt voor je geduld met me tijdens de laatste maanden van mijn promotie ik weet dat ik niet helemaal mijzelf was. Ik vind het heel fijn dat je bereid bent met me mee te gaan naar een volgende baan, ik hou van je en ik kijk uit naar onze bruiloft.

Nogmaals bedankt allemaal

Curriculum Vitae

Joost Willemse werd op 29 augustus 1979 te Terheijden geboren. Hij behaalde het VWO diploma aan het Monsigneur Frencken College te Oosterhout (NB) in juni 1997. In september 1997 begon hij met de opleiding Moleculaire Wetenschappen aan de Landbouwwuniversiteit te Wageningen, waar hij zich specialiseerde in de richting moleculaire biologie. Het eerste afstudeervak werd gedaan bij de vakgroep moleculaire biologie (Prof. S.C. de Vries) in Wageningen waar de co-localisatie van AtSerk met KAPP eiwitten werd onderzocht m.b.v. confocale microscopie. Vervolgens is het tweede afstudeervak ook in Wageningen gedaan bij Dr. Ir Geurts, waarbij de infectiedraad formatie van de symbiotische relatie tussen de plant *Medicago truncatula* en de bacterie *Sinorhizobium meliloti* werd onderzocht. Hierna werd de opleiding Moleculaire Wetenschappen afgerond in juni 2002, waarna in juli begonnen werd met het promotieonderzoek aan heterochromatine organisatie in *Arabidopsis* onder begeleiding van Prof. Dr. A.H.J. Bisseling and Dr. J.H.S.G.M. de Jong. De resultaten van dit onderzoek staan beschreven in dit proefschrift. Hierna is begonnen met een post-doc baan op het Gorleaus laboratorium te Leiden in de groep van Dr. Gilles van Wezel, om onderzoek te doen naar de celdeling en ontwikkeling van *Streptomyces Coelicolour*.

Curriculum Vitea

Education Statement of the Graduate School
Experimental Plant Sciences



Issued to: Jacobus Joseph Willemse
Date: 2 March 2007
Group: Molecular Biology, Wageningen University

1) Start-up phase	<i>date</i>
<ul style="list-style-type: none"> ▶ First presentation of your project Localization and mobility of heterochromatin proteins ▶ Writing or rewriting a project proposal ▶ Writing a review or book chapter ▶ MSc courses ▶ Laboratory use of isotopes 	November 2002
<i>Subtotal Start-up Phase</i>	<i>1.5 credits*</i>
2) Scientific Exposure	<i>date</i>
<ul style="list-style-type: none"> ▶ EPS PhD student days <ul style="list-style-type: none"> PhD Student day 2003, Utrecht PhD Student day 2004, Amsterdam PhD Student day 2005, Nijmegen ▶ EPS theme symposia <ul style="list-style-type: none"> Theme symposium IV, 2002, Wageningen Theme symposium IV, 2003, Nijmegen Theme symposium IV, 2004, Wageningen Theme symposium IV, 2005, Wageningen ▶ NWO Lunteren days and other National Platforms <ul style="list-style-type: none"> ALW meeting Lunteren 2002, Nucleic Acids ALW meeting Lunteren 2003, Plant Sciences ALW meeting Lunteren 2004, Plant Sciences ALW meeting Lunteren 2004, Nucleic Acids ALW meeting Lunteren 2005, Plant Sciences ALW meeting Lunteren 2005, Nucleic Acids ALW meeting Lunteren 2006, Plant Sciences ▶ Seminars (series), workshops and symposia <ul style="list-style-type: none"> Flying Seminars (11-10-2002, 22-10-2002, 8-11-2002, 23-09-2003, 11-03-2003, 26-09-2005, 24-10-2005) 1st Dutch Chromatin Meeting 2004-Amsterdam Symposium on Systems Biology, in Honor of Prof.dr.Pierre de Wit 2nd Dutch Chromatin Meeting 2005-Wageningen 3rd Dutch Chromatin Meeting 2005-Kerkrade Frontiers in Plant Science (27-02-2003, 06-03-2003, 22-09-2005, 13-10-2005) Seminar UU. Prof.dr.Gunter Reuter ▶ Seminar plus ▶ International symposia and congresses <ul style="list-style-type: none"> Tubingen Symposia Epigenetics and the Dynamic Genome Conference - Babraham Institute, Cambridge, UK ▶ Presentations <ul style="list-style-type: none"> Theme symposium IV, 2002, Wageningen FEBS Advanced Course, Microspectroscopy: Visualisation of Biochemistry in Living Cells Theme symposium IV, 2005, Wageningen Epigenetics and the Dynamic Genome Conference - Babraham Institute, Cambridge, UK ▶ IAB interview ▶ Excursions 	<div>March 27, 2003</div> <div>June 3, 2004</div> <div>June 2, 2005</div> <div>December 20, 2002</div> <div>December 10, 2003</div> <div>December 9, 2004</div> <div>December 9, 2005</div> <div>December 2-3, 2002</div> <div>April 7-8, 2003</div> <div>April 5-6, 2004</div> <div>December 6-7, 2004</div> <div>April 4-5, 2005</div> <div>November 28-29, 2005</div> <div>April 3-4, 2006</div> <div>2002-2005</div> <div>April 23, 2004</div> <div>November 4, 2004</div> <div>January 21, 2005</div> <div>December 7-8, 2005</div> <div>2003-2005</div> <div>October 13, 2005</div> <div>May 23, 2003</div> <div>June 30 - July 2, 2005</div> <div>December 20, 2002</div> <div>October 3-9, 2004</div> <div>December 9, 2005</div> <div>June 30 - July 2, 2005</div> <div>June 2, 2005</div>
<i>Subtotal Scientific Exposure</i>	<i>13.7 credits*</i>

EPS Statement

3) In-Depth Studies ▶ EPS courses or other PhD courses Advanced Course on Digital Microscopy and Fluorescence Techniques in Cell Biology (heidelberg) FEBS Advanced Course, Microspectroscopy: Monitoring Interactions and Reactions in Living Cells Applied Imaging, Automated FISH Spot Counting Workshop (leiden) Embo Course: Advanced molecular and immuno cytogenetics on chromosomes and nuclei in plants FEBS Advanced Workshop- Nuclear Architecture: Chromatin Structure and Gene Control plant vs. animal vs. yeast FEBS Advanced Course, Microspectroscopy: Visualisation of Biochemistry in Living Cells Mathematics in biology ▶ Journal club ▶ Individual research training	<u>date</u> October 7-11, 2002 Oct. 29 - Nov. 6, 2002 March 5, 2003 October 13-20, 2003 November 14-17, 2003 October 3-9, 2004 19-24 February 2006
<i>Subtotal In-Depth Studies</i>	
4) Personal development ▶ Skill training courses Labmath course (utrecht) Digital Microscopy and Image Analysis (copenhagen) Scientific Publishing: An introductory workshop for PhD students and Young authors The Art of writing ▶ Organisation of PhD students day, course or conference ▶ Membership of Board, Committee or PhD council	<u>date</u> December 11, 2003 January 26-February 6, 2004 October 12, 2004 June, 2005
<i>Subtotal Personal Development</i>	
TOTAL NUMBER OF CREDIT POINTS*	
32	

Herewith the Graduate School declares that the PhD candidate has complied with the educational requirements set by the Educational Committee of EPS which comprises of a minimum total of 30 credits

* A credit represents a normative study load of 28 hours of study

Publication List

Khalid Shah, Eugenia Russinova, Theodorus W.J. Gadella Jr., Joost Willemse and Sacco C. de Vries (2002); “The *Arabidopsis* Kinase Associated Protein Phosphatase controls internalization of the Somatic Embryogenesis Receptor Kinase 1”, *Genes and Development*; July 1 2002; 16(13):1707-1720.

Erik Limpens, Carolien Franken, Patrick Smit, Joost Willemse, Ton Bisseling, Rene Geurts (2003); “LysM Domain Receptor Kinases Regulating Rhizobial Nod Factor–Induced Infection”, *Science*; October 24 2003; 302:630-633

J. Pouwels, T. van der Velden, J. Willemse, J. W. Borst, J. van Lent, T. Bisseling and J. Wellink (2004); “Studies on the origin and structure of tubules made by the movement protein of Cowpea mosaic virus”, *Journal of General Virology*, September 2004 ; 85:3787-3796